UNIVERSITY OF HAWAII
LIBRARY
JAN 3 '62

Geochimica et Cosmochimica Acta

JOURNAL OF THE GEOCHEMICAL SOCIETY

Executive Editors: J. A. S. ADAMS, *Houston, Texas* C. W. CORRENS, *Göttingen* L. R. WAGER, *Oxford.*

Editors: L. H. AHRENS, *Capetown.* S. R. NOCKOLDS, *Cambridge.* H. C. UREY, *La Jolla, Calif.* JOHN VERHOOGEN, *Berkeley, Calif.* E. A. VINCENT, *Oxford* A. P. VINOGRADOV, *Moscow.*

CONTENTS VOLUME 25, No. 4 DECEMBER 1961

YAACOV K. BENTOR: Some geochemical aspects of the Dead Sea and the question of its age 239

F. T. BONNER, E. ROTH, O. A. SCHAEFFER and S. O. THOMPSON: Chlorine-36 and deuterium study of Great Basin lake waters 261

R. F. MUELLER: Analysis of relations among Mg, Fe and Mn in certain metamorphic minerals 267

H. FECHTIG, W. GENTNER und S. KALBITZER: Argonbestimmungen an Kaliummineralien—IX. Messungen zu den verschiedenen Arten der Argondiffusion 297

Book Review 312

Notice 314

PERGAMON PRESS OXFORD • LONDON • NEW YORK • PARIS

GEOCHIMICA ET COSMOCHIMICA ACTA

EXECUTIVE EDITORS

PROF. J. A. S. ADAMS, *Department of Geology, Rice University, Houston* 1, *Texas, U.S.A.*
PROF. C. W. CORRENS, *Sedimentpetrographisches Institut der Universität, Lotzestr.* 13, *Göttingen, Germany*
PROF. L. R. WAGER, F.R.S., *Department of Geology and Mineralogy, The University Museum, Oxford, England*

EDITORS

PROF. L. H. AHRENS, *Department of Chemistry, University of Capetown, Rondebosch, Cape Province, South Africa*
Dr. S. R. NOCKOLDS, *Department of Mineralogy and Petrology, The University, Cambridge, England*
PROF. H. C. UREY, For. Mem. R. S., *University of California, La Jolla, California, U.S.A.*
Dr. JOHN VERHOOGEN, *Department of Geology, University of California, Berkeley, California, U.S.A.*
Dr. E. A. VINCENT, *Department of Geology and Mineralogy, The University Museum, Oxford*
PROF. A. P. VINOGRADOV, *Vernadsky Institute, Moscow, U.S.S.R.*

EDITORIAL ADVISORY BOARD

EUROPE

T. F. W. BARTH, *Oslo*
L. CAPDECOMME, *Toulouse*
E. J. CONWAY, *Dublin*
P. ESKOLA, *Helsinki*
P. GALLITELLI, *Modena*
A. HADDING, *Lund*
O. HAHN, *Göttingen*
H. W. HARVEY, *Plymouth*
F. HEIDE, *Jena*
A. HOLMES, *Edinburgh*
W. Q. KENNEDY, *Leeds*
PH. H. KUENEN, *Gröningen*
S. LANDERGREN, *Stockholm*
F. MASHATSCHKI, *Vienna*
A. MUIR, *Harpenden*
J. ORCEL, *Paris*
E. RAGUIN, *Paris*
E. REINHARD, *Basle*
TH. G. SAHAMA, *Helsinki*
C. E. TILLEY, *Cambridge*
T. VOGT, *Trondheim*

AMERICAN CONTINENT

A. F. BUDDINGTON, *Princeton*
D. GUIMÃRAES, *Belo Horizonte*
G. E. HUTCHINSON, *New Haven*
EARL INGERSON, *Austin*
B. H. MASON, *New York*
F. WHIPPLE, *Cambridge*
R. WILDT, *New Haven*
H. S. YODER, *Washington*

FAR EAST

T. WATANABE, *Tokyo*

AUSTRALIA

D. J. SWAINE, *Sydney*

Publishing Offices: Pergamon Press Ltd., Headington Hill Hall, Oxford

Four issues per volume, three volumes per year

Subscription *per annum* (including postage) (A) £21 (U.S.A. $60.00); (B) For individual subscribers who write directly to the publisher certifying that the Journal is for their private use, £7.7s. (U.S.A. $21.50). Members of the Geochemical Society, or non-members who occasionally publish papers in the Journal, £3. 11s. 6d. (U.S.A. $10.00) *per annum*.

Back numbers, £8 (U.S.A. $24.00) per volume

Single issues, £2. 10s. (U.S.A. $9.00) each

Copyright © 1961 Pergamon Press Ltd.

PERGAMON PRESS LTD.

HEADINGTON HILL HALL, OXFORD 122 EAST 55TH STREET, NEW YORK 22, N.Y.

PRINTED IN NORTHERN IRELAND AT THE UNIVERSITIES PRESS, BELFAST

YOUR ADVERTISING

will have maximum impact in

GEOCHIMICA ET COSMOCHIMICA ACTA

For details write or phone to

R. D. Miller,
Advertisement Manager,
Pergamon Press Limited,
Pergamon House,
4 Fitzroy Square,
London W.1
Phone: EUSton 4455 (Ext. 39)

or

Pergamon Press Inc.,
122 East 55th Street,
New York 22, N.Y.,
U.S.A.
Phone: Plaza 3-9651

THIS IS ONE OF OVER 70 PERGAMON JOURNALS! ASK FOR SPECIMENS OF OTHERS AND REDUCED RATES FOR "COMBINED" ADVERTISING

POTASSIUM - ARGON AGE DETERMINATIONS

We are pleased to offer GEOCHIMICA readers, our Bibliography of Geochronology, available free upon request.

If you might be interested in our laboratory services, send for our pamphlet, *Potassium-Argon Isotope Analysis*

GEOCHRON LABORATORIES, Inc.
Department O
24 Blackstone Street
Cambridge 39
Massachusetts
U.S.A.

A SKILLED TECHNICAL WRITING SERVICE FOR SCIENCE AND INDUSTRY

The technical editing department

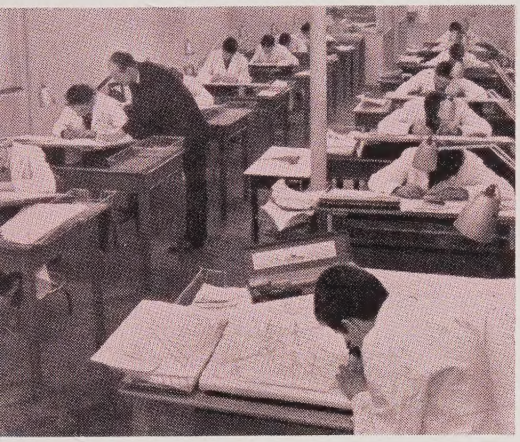

One section of the drawing office

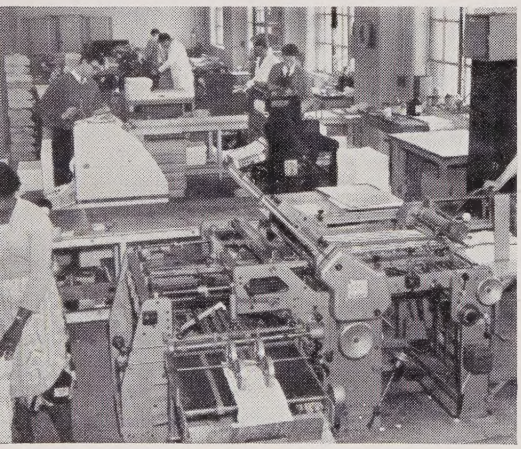

Part of the litho print room

The studio

Do you need a really fast, efficient, 'one source' technical writing, illustrating and printing service? The Pergamon Press Technical Writing Division offers a fully integrated service, capable of undertaking the complete design and production, including translation from and into foreign languages, of all types of technical printed matter, and especially user/operator handbooks, instruction and maintenance manuals, sales brochures, catalogues and company reports.

The Division is staffed by experienced, highly qualified technical writers, draughtsmen and typographic designers, and in addition can consult the several hundred internationally eminent authors and editors who publish with the Press, and obtain their advice and services in every specialized sphere of science, medicine and technology.

We offer keenly competitive prices, high quality and speedy delivery, and shall be pleased to submit quotations for all or any one of our services. We guarantee complete security when handling work of a confidential nature.

For immediate attention to your requirements please write or telephone

JOHN BURLS, B.Sc., *General Manager*

PERGAMON PRESS TECHNICAL WRITING DIVISION

4/5 FITZROY SQUARE,
LONDON W.1
Telephone: EUSton 4455

Editorial and sales offices also at:

Headington Hill Hall, Oxford
122 East 55th Street, New York 22, N.Y., U.S.A.
24 Rue Des Ecoles, Paris V^e^ Kaiserstrasse 75, Frankfurt am Main.

Geochimica et Cosmochimica Acta, 1961, Vol. 25, pp. 239 to 260. Pergamon Press Ltd. Printed in Northern Ireland

Some geochemical aspects of the Dead Sea and the question of its age

Yaacov K. Bentor
Geological Survey of Israel and Hebrew University, Jerusalem

(*Received, in revised form*, 8 *May* 1961)

Abstract—A comparison between the chemical composition of the water of the Dead Sea and its tributaries and that of other lakes and the ocean shows the average salinity of the Dead Sea water (31·50%) to be exceptionally high, concentration of the SO_4''-ion to be very low and that of Br (5920 mg/l) to be probably the highest on record for any surface water. Most of the cationic calcium in the Dead Sea and its tributaries is balanced by chloride. A short summary of the geological history of the area shows that the Dead Sea is not a relict body of sea water; its salt assemblage is the result of accumulation in a closed inland basin under arid conditions. The salts originate from two main sources, about one third from the Jordan River and about two thirds from highly saline springs discharging into the Dead Sea. On this fact a method can be based for calculating the age of the Dead Sea leading to a maximum figure of about 70,000 and a minimum of 12,000 years, the latter being more probable. The annual amount of chemical precipitation in the Southern Dead Sea basin is calculated to 0·306 gr/cm^2 and it is shown that NaCl and $CaSO_4$ are the major and that $CaCO_3$ is a minor component. This result is in good agreement with observations on the present rate of chemical sedimentation in the Dead Sea. Volcanic and organic origins for the vast bromine reserve in the Dead Sea are rejected and the derivation of the bromine from fossil residual brines, formed during the Tertiary, is tentatively accepted.

Introduction

The Dead Sea, situated at the deepest part of the Jordan–Arava graben, which is part of the African Rift system, presents many unusual geochemical features. Its water has an extremely high salinity, and its chemical composition is unique. The area is highly arid, with an average annual rainfall of about 50 mm. Although scientific observations of the Dead Sea have been carried out intermittently since the Lynch expedition first studied the area in 1848–49, a study of its Pleistocene and recent sediments was begun only a short time ago, and its geochemical character is known only in bare outlines. In recent years, however, a considerable amount of data has become known through research in connection with the potash and bromine production from the water of the Dead Sea, through hydrogeological work on the Jordan and its tributaries, through a study of the Pleistocene sediments of the Lisan Lake, the predecessor of the Dead Sea and, finally, as a result of a hydrological survey of the Dead Sea which started in 1959. On the basis of this information, much of which is unpublished, an attempt is made here to re-trace the history of the Dead Sea, to study the main lines of its geochemical development and to determine its age.

Some Hydrogeological Data concerning the Dead Sea

The Dead Sea, the surface of which lies almost 400 m below Mediterranean sea level, covers at the present time an area of 1001 km^2, is 79·5 km long and has a maximum width of 17·5 km. The lake is composed of two parts, very different in character and almost separated from each other by the Lisan Peninsula jutting out from its eastern shore (see Fig. 1). The southern part covers 244 km^2 and is very shallow, rarely exceeding 10 m in depth. The basin north of the Lisan Peninsula covers an area of 757 km^2 and reaches in its eastern section a depth of 401m. The total volume of the Dead Sea is approximately 143 km^3, nine times that of

Great Salt Lake, Utah. Its drainage area (see Fig. 1) has a size of almost 40,000 km^2 and comprises the Hermon mountain massif, the eastern part of the Galilean, Judean and Negev Mountains, a small part of central Sinai, the western mountain belt of Transjordan, the Jebel Druze and, finally, the Jordan Valley and the northern part of the Arava. Within this area a great variety of rock types are present. The more important ones are: Precambrian igneous rocks (mainly granites and siliceous [acid] volcanics) in the south; Paleozoic and Mesozoic (Nubian) sandstones in the southeast; Mesozoic to Eocene marine sediments—mainly limestones and dolomites—in the east, west and north; lacustrine and continental shales and sandstones of Tertiary age, mainly in the northern Negev, the Arava and the Tiberias area; Tertiary to Pleistocene basalts in the north (Tiberias area, Jebel Druze); and, most widespread, the clayey, silty, calcareous and gypsiterous sediments of the Pleistocene Lisan Lake which fill the entire Jordan graben from the Sea of Galilee southward, as well as the northern Arava.

By far the most important tributary of the Dead Sea is the Jordan River. Owing to the arid nature of most of the Jordan Valley, the annual flow of this river is subject to considerable variations. During the period 1932–36, for which figures have been published (IONIDES, 1939), the smallest annual discharge, viz. $387 \cdot 10^6$ m^3, was observed during the 1932–33 season; the highest, $1316 \cdot 10^6$ m^3, during the 1934–35 season. On the basis of all available data the average annual discharge of the Jordan into the Dead Sea can be estimated at approximately $1200 \cdot 10^6$ m^3. Additional amounts of water are supplied by the Arnon River, at a rate of about $30 \cdot 10^6$ m^3/yr, and by numerous springs issuing near the Dead Sea shores. The springs of Wadi Hessi, at the southeastern corner of the lake, have an annual discharge of about $30 \cdot 10^6$ m^3, those of the Zerqa Ma^{c}in $3–5 \cdot 10^6$ m^3; other springs of unknown discharge probably issue at the lake bottom itself. To these must be added the highly irregular amounts of flood-water carried into the Dead Sea by dry rivers, such as Wadi Tsin (Fiqra). A rough estimate puts the amount contributed by the Tsin Valley alone at about 10^6 m^3/yr. The total average annual intake of the Dead Sea is estimated at about $1600 \cdot 10^6$ m^3. This figure agrees well with earlier calculations by NEUMANN (1958) and with the rate of evaporation of 160 cm/yr, measured for the Dead Sea. It follows that slightly more than 1 per cent of the Dead Sea water is renewed annually; but there are definite indications that this hydrological cycle is confined to the uppermost 40 m of the lake water (EMERY and NEEV, 1959, unpublished report).

The large amount of water lost yearly by evaporation—$1600 \cdot 10^6$ m^3—is reflected in the high concentration of deuterium which, in the surface water of the southern Dead Sea basin, is 0·01626 mole per cent in the hydrogen. This figure should be compared with the value of 0·01557 mole per cent in the Red Sea water near Eilat, an area known for its exceptionally high evaporation (personal communication from Centre d'Etudes Nucléaires de Saclay, France).

CHEMICAL COMPOSITION OF THE DEAD SEA AND ITS TRIBUTARIES

The chemical composition (in mg/l) of the Dead Sea water, of some of its tributaries and the springs feeding them, as well as that of some other lakes and the ocean for comparison, are given in Table 1. These analyses have been calculated

Table 1. Chemical composition of water from the Dead Sea, its tributaries, similar lakes and the ocean (in mg/l)*

	1	1a	2	3	4	5	6	7	8	9
Na^+	33,500	34,940	253·40	44	131	292	496	523	978	159
K^+	6,300	7,560	14·85		7	9·7	12·5	5	27	
Rb^+	60	60								
Ca^{2+}	13,000	15,800	80·00	42	49·0	63	151	223	364	132
Mg^{2+}	34,500	41,960	71·42	19	—	6	—	49	105	55
Cl'	180,800	208,020	473·50	55	283·0	599	1,042	1,210	2,231	320
Br'	4,100	5,920	4·338		2·35	3·65	7·1	11·8	20·5	
SO_4''	900	540	174·49	32	34·5	70	128	93	173	130
HCO_3'	248	240	237·90	195	—	200	143	127	240	350
Total	273,408	315,040	1,309·898	387	506·85	1,243·35	1,979·6	2,241·8	4,138·5	1,146

	10	11	12	13	14	15	16	17	18
Na^+	6,915	460	1,210	23,100	24,813	8,115	10,561	67,498	52,250
K^+	295			30,100	15,992	787	380	3,378	4,820
Rb^+							0·2		
Ca^{2+}	3,501	209	700	85,200	37,240	2,986	400	326	tr
Mg^{2+}	584	242	82	21,100	41,670	6,323	1,272	5,616	33,830
Cl'	18,016	1,660	1,930	274,800	247,720	36,660	18,980	112,896	132,730
Br'	246			3,100	2,900	810	64·6		380
SO_4''	734	54	1,490		107	752	2,648·6	13,593	67,830
HCO_3'	162	244	1,035	tr	127	91	139·7	183	670
Total	30,453	2,869	6,447	437,400	370,569	56,524	34,446·1	203,490	292,510

* For legend to Tables 1–5, please see p. 242.

LEGENDS TO TABLES 1–5

1. Dead Sea (surface water) (Analyses by Dead Sea Works Ltd. and Geological Survey of Israel).
1a. Dead Sea (average) (analyses by Dead Sea Works Ltd. and Geological Survey of Israel).
2. Jordan River at Jericho (analysis by Dead Sea Works Ltd.).
3. Yarmuq River near junction with Jordan River (WITZAN, G. R. and WOZAB, 1954).
4. Lake Tiberias (F. YARON, 1952).
5. Beisan Springs (F. YARON and M. HEITNER, 1952).
6. Fuliya Springs (F. YARON, 1952).
7. Tabha Springs (F. YARON, 1952).
8. Tannur Springs (F. YARON, 1952).
9. El Hamme Hot Springs (WITZAN, G. R. and WOZAB, 1954).
10. Tiberias Hot Springs (F. YARON, 1952)
11. Ein Feshha Springs (WITZAN, G. R. and WOZAB, 1954).
12. Zerka Hot Springs (WITZAN, G. R. and WOZAB, 1954).
13. Sdom I (deep drilling) (unpublished analysis by Geological Survey of Israel).
14. Average of 3 salt springs at Mount Sdom (unpublished analyses by Geological Survey of Israel).
15. Zohar Sulphur Springs (analyses by Dead Sea Works Ltd. and Geological Survey of Israel).
16. Ocean (H. U. SVERDRUP, M. W. JOHNSON, R. H. FLEMING, 1957).
17. Great Salt Lake (RANKAMA, R. and SAHAMA, TH. G., 1955).
18. Khara-Bogaz (A. A. BOGDANOFF, Moscow, personal communication).
19. Lake Tahoe, California (CLARKE, F. W., 1924, p. 160, No. A).
20. Humboldt Lake, Nevada (CLARKE, F. W., 1924, p. 161, No. H).
21. Malheur Lake, Oregon (CLARKE, F. W., 1924, p. 163, No. H).
22. Lake Muskiki, Saskatchewan, Canada (CLARKE, F. W., 1924, p. 164, No. Q).
23. Various saline lakes in North-Western Nebraska (CLARKE, F. W., 1924, p. 166, Nos. A–F).
24. Katween Salt Lake, north of Albert Edward Nyanza, Central Africa (CLARKE, F. W., 1924, p. 175, No. C).
25. Borax Lake, California (CLARKE, F. W., 1924, p. 162, No. H).
26. Caspian Sea (CLARKE, F. W., 1924, p. 169, No. A).
27. Aral Lake (CLARKE, F. W., 1924, p. 169, No. F).
28. Red Lake, Perekop, Crimea (CLARKE, F. W., 1924, p. 172, No. B).
29. Koko-Nor, Tibet (CLARKE, F. W., 1924, p. 172, Nos. G/H).
30. Various Siberian Lakes (CLARKE, F. W., 1924, p. 174).
31. Average river water (CORRENS, C. W., 1956).
32. Saratoga Geyser water (CORRENS, C. W., 1956).
33. Mineral water (world average) (SCHOELLER, H., 1956, p. 97).
34. Oil water (world average) (SCHOELLER, H., 1956, p. 97).
35. Igneous rocks (BEHNE, W., 1953).

in Table 2 in weight percentages, the sum of the cations and anions each being brought separately to a total of 100 per cent.

Measurements have shown that the Dead Sea possesses a definite chemical stratification. The average composition of the Dead Sea water, as given in Table 1, under 1a, has been calculated by averaging the chemical composition of the water at 25 m depth intervals, taking into account the known volume of each of these 25 m layers of water.

The average salinity of the Dead Sea water, 31·50 per cent, is higher than that of any other large lake on record but not far above that of the Khara-Bogaz—29·25 per cent—and of the Great Salt Lake—20·35 per cent.* The total amount of salts contained in the Dead Sea is summarized in Table 3.

It is, however, not so much the degree of salinity as the composition of the salts dissolved in the Dead Sea water that is unusual. This water is of the pure chloride type, with a very low percentage of sulphates and only traces of carbonates. While low values of carbonate are also characteristic of other strongly saline lakes (and the ocean), all of these, and particularly the Khara-Bogaz, carry considerable amounts of sulphate. In terms of the total cation content, the amount of calcium is 15·75 per cent, an extraordinarily high value for a water of such high salinity. For other saline lakes this value is only a few tenths of one per cent, and for the ocean slightly more than 3 per cent. Consequently, the major part of the calcium must be balanced by chloride ion in the Dead Sea. This is true not only of the lake itself, but of most of its tributaries. Natural water containing calcium chloride is extremely rare and this feature is not shown in any of the lake water analyses given either by RANKAMA and SAHAMA (1955) or by CLARKE (1924), with the exception of Red Lake, Perekop, Crimea (CLARKE, 1924, p. 172, Analysis B). In this lake, however, the percentage of calcium is considerably smaller than in the Dead Sea.

The two most prominent cations present in the Dead Sea are Na^+ and Mg^{2+}, a feature which it shares with many other lakes in a late stage of development. The Na:K-ratio, however, is rather low; the value 4·6 is three to twenty times lower than that of any of the rivers and springs discharging directly or indirectly into the Dead Sea, and six times as low as that of the ocean. But Na:K-ratios similar to that of the Dead Sea are encountered in many other lakes, as shown in Table 4.

In the proportion of the anions, however, the Dead Sea is unique: not only is Cl′ by far dominant, but the only other anion of any importance is Br′. The Cl:Br-ratio (see Table 5) is 35:1, only about one third that of the tributary springs and rivers, and only one-eighth that of the ocean. Not many pertinent figures of other lakes are on record; but, as far as is known, for most salt lakes this ratio is normally about 1000; for the Khara-Bogaz the figure is 349, while it is 1400 in the average river water (CORRENS, 1956) and 290 in the ocean. The high proportion of Br in the Dead Sea water, in conjunction with the high salinity, leads to a figure of 5920 mg/l Br, the highest one known for any surface water. The extremely low Cl:Br-ratio is not only a feature of the Dead Sea itself, but also—though to a lesser

* This value is not an average, but the result of a single analysis made in 1913. Recorded salinities vary at least from 13·79 to 27·72. The average of 8 values given by CLARKE (1914, p. 157) is 19·77.

Table 2. Chemical composition of water from the Dead Sea, its tributaries, similar lakes and the ocean (in % of cations and anions)

	1	1a	2	3	4	5	6	7	8	9
Na^+	38·29	34·83	60·38	41·91	70·05	78·76	75·20	65·40	66·36	45·96
K^+	7·36	7·53	3·53		3·74	2·62	1·89	0·62	1·82	
Rb^+	0·06	0·06								
Ca^{2+}	14·85	15·75	19·07	39·99	26·21	17·01	22·91	27·87	24·69	38·15
Mg^{2+}	39·44	41·83	17·02	18·10	—	1·61	—	6·11	7·13	15·89
Cl'	97·18	96·88	52·06	19·50	88·50	68·64	78·93	83·88	83·72	40·00
Br'	2·21	2·76	0·51	—	0·71	0·41	0·54	0·81	0·78	—
SO_4''	0·48	0·25	20·06	11·35	10·79	8·02	9·70	6·51	6·49	16·25
HCO_3'	0·13	0·11	27·37	69·15	—	22·93	10·83	8·80	9·01	43·75

	10	11	12	13	14	15	16	17	18	
Na^+	61·20	50·49	60·74	14·48	20·73	44·56	83·75	87·87	57·48	
K^+	2·62			18·87	13·36	4·32	3·00	4·40	5·30	
Rb^+							0·00			
Ca^{2+}	31·00	22·96	35·15	53·43	31·10	16·40	3·17	0·42	tr	
Mg^{2+}	5·18	26·55	4·11	13·22	34·81	34·72	10·08	7·31	37·22	
Cl'	94·04	84·78	43·33	98·88	98·75	95·69	86·92	89·12	65·84	100%
Br'	1·29	—	—	1·12	1·16	2·11	0·30		0·19	
SO_4''	3·83	2·75	33·44	—	0·04	1·96	12·13	10·73	33·64	
HCO_3'	0·84	12·47	23·23	tr	0·05	0·24	0·65	0·15	0·33	
										100%

Table 3. Total salt content of Dead Sea (in 10^6 tons)

$MgCl_2$	23,000
NaCl	12,650
$CaCl_2$	6119
KCl	2050
$MgBr_2$	975
$CaSO_4$	105
$Ca(HCO_3)_2$	46
RbCl	12
Total	44,957 . 10^6 tons

Table 4. Na:K-ratios (in weight %)

1	1a	2	4	5	6	7	8	10	13	14
5·2	4·6	17·1	18·7	30·1	39·8	105·5	36·5	23·4	0·77	1·6
15	16	17	18	19	20	21	22	23	24	
10·3	27·9	20·0	10·8	2·2	4·6	4·3	5·4	1	4·7	

Table 5. Cl:Br-ratios (in weight %)

1	1a	2	4	5	6	7	8	10
44·0	35·1	109·2	124·6	167·3	146·1	103·5	107·2	72·9
13	14	15	16	18	25	26	27	28
88·3	85·4	45·4	289·7	349	807	841	1180	2217
29	30	31	32	33	34	35		
1001	500–1000	1383	50–300	274	329	2–526		

degree—of all its tributaries, which show values between 100 and 170, i.e. two or three times less than the average igneous rock or the ocean.

Geological History of the Dead Sea Area

The origin of the unique salt assemblage in the Dead Sea has been the subject of many speculations. A derivation of the Dead Sea salts from a relict body of ocean water was suggested by older theories. These were certainly incorrect, for geochemical as well as geological reasons, as was already recognized by Lartet (1876). The geological history of the Dead Sea area can be summarized briefly as follows:* Until the end of Mesozoic times the region of the present Jordan–Arava graben was part of the mountain area of Palestine, but separated from the Transjordan block in the east by the very old geosuture, now forming the eastern border-fault of the Rift. The Jordan–Arava graben came into existence during the earlier Tertiary, probably in Oligocene times, through tensional movements which pushed the Transjordan block eastward and led to a downbreak of the western border of the graben along a complicated system of faults.

* A more detailed paleogeographical history of the Dead Sea area is given by Y. K. Bentor and A. Vroman (1960).

Following the period of tectonic disturbances lacustrine deposition took place in the downsunken strip and in the lowlying parts of the adjoining mountain area to the west (Sdom, Foothill, Hatseva and Tiberias Formations). The sediments indicate partly brackish saline conditions, but also a fresh water environment. This can only be explained by the assumption that, notwithstanding the earlier tectonic subsidence, the Rift area drained, at least periodically, toward the west, i.e. in the direction of the Tethys. This view is consistent with the results obtained recently by NEEV (1960) from a study of the Neogene sediments of southern Israel.

It was believed until recently that since the formation of the Dead Sea–Jordan graben in Oligocene(?) times, the sea never gained access to this area. This view must now be revised. The discovery of *Mugil priscus* Ag. (determination by ORVAL, Göteborg) in the Upper Tertiary Sdom Formation of Mount Sdom, as well as the discovery of a marine microfauna of Pliocene age in surface outcrops in the Tiberias area and, buried at great depth, in the Ein Gedi II oil drilling near the western shore of the Dead Sea (Z. REISS, personal communication) make it certain that the Neogene lakes of the Tiberias–Jordan–Arava area communicated at intervals with the open sea in the west, probably through connecting branches along the Yezreel–Beisan depressions (see Fig. 1).

Thus, according to the relative rates of tectonic subsidence and sedimentary accumulation the region of the Jordan–Dead Sea graben formed during the Upper Tertiary, sometimes an area of fresh water lakes draining to the west, at times an extended arm of the Tethys and at other times a closed inland basin in which brackish, saline, fluviatile and aeolian deposition took place alternatively.

In late Pliocene or in early Pleistocene times taphrogenic movements were again accelerated and the subsidence of the area finally overtook the rate of sedimentation. This inland depression was rapidly filled during the early Pleistocene by an extended inland lake, the so-called *Samra Lake*, the first of three lakes which occupied the Jordan–Dead Sea area during the Pleistocene. The Samra Lake stretched at least from the Beisan Valley in the north to Ein Hatseva in the south, a distance of 190 km. (see Fig. 1). The sediments of the Samra Lake are partly sandy and consist commonly of oolitic limestone and chalk, with various amounts of coarse clastics. Fauna found at many places attest to the fresh water character of the Samra Lake. After a short interval the water turned salty and the fresh water Samra Lake was replaced by the brackish *Lisan Lake*. The gradual and oscillatory changes from fresh deposition of the Samra type to brackish deposition of the Lisan type can be studied in excellent exposures in the area north of Ein Hatseva (BENTOR and VROMAN, 1957). At the time of its maximum extension the Lisan Lake filled the entire Jordan–Dead Sea depression, at least from the Tiberias area in the north to a point 34 km south of the present southern end of the Dead Sea, a total length of 235 km. The Lisan sediments are composed of very soft, seasonally varved, thin, alternating layers of white aragonitic powder and dark clayey material; in places gypsum is present, especially in the upper part of the sequence, but salt is absent although minor amounts of salt are shown by X-ray (halite) and by solutions in water. Near the sandy shores of the southern part of the Lisan Lake the sediments consist mainly of silt, while near the rocky shores

farther north coarse clastic sedimentation predominates. The total known thickness of the Lisan sediments varies from 200 to 400 m, but recent oil drillings in the vicinity of the Dead Sea have disclosed similar material interbedded with large amounts of coarse clastics in thicknesses exceeding 1500 m. These sediments are at least in part contemporaneous with those of the Lisan Lake, although frequently they can be distinguished only with difficulty from similar sediments of Pliocene age.

After an existence of several hundred thousand years the Lisan Lake started to shrink. On both steep eastern and western shores of the Dead Sea about 17 regressive shore terraces can be observed, the highest at (—) 175 m below Mediterranean sea level, i.e. about 220 m above the present level of the Dead Sea. The topographic position of the highest of these terraces coincides with the highest occurrences of Lisan sediments (Bentor and Vroman, 1957).

The present *Dead Sea* became established in late Pleistocene times in the lowest part of the area originally occupied by the Lisan Lake. It may well be that before the formation of the Dead Sea the older Lisan Lake had dried up completely. This view, already tentatively suggested by Picard (1943), has gained additional support from the results of a topographical study of the Dead Sea bottom carried out by Emery and Neev (1959). At least down to a depth of 300 m below the present level of the Dead Sea, the topography is so rugged that its formation by subaerial processes is most probable. The possibility, however, cannot be entirely excluded that some relict bodies of Lisan water were still in existence when the present Dead Sea was formed. Its formation coincides with and was probably caused by new fault movements which, among others, uplifted the block of Mount Sdom with its cover of Lisan sediments and young fluviatile scree by at least 100 m.

Origin of the Dead Sea Salts

Turning now to the history of the salts contained in the Dead Sea water, the salient fact emerging from the above sketch of the geological history of the area is that the pre-Pleistocene history of the region has no direct bearing on this problem. Whatever the changes in the interplay of fresh water, saline, marine and aeolian sedimentation during the Tertiary, this period was followed by the establishment of the fresh water Samra Lake which must have blanketed all earlier sediments. The case of the Pleistocene Lisan Lake is different. Although this lake too may have disappeared before the establishment of the Dead Sea, it is not impossible that a small amount of the salt now contained in it is inherited directly from the Lisan Lake. The exact composition of this lake, is, of course, unknown, but it was doubtlessly very much less saline than the present water of the Dead Sea. This view is based on two facts:

(1) the character of the sediments of the Lisan Lake which are composed mainly of carbonates with only very subordinate amounts of gypsum and practically no halite;

(2) the recent discovery of well preserved fish remains in the Lisan sediments.

It may be concluded that the total amount of salts derived directly from the Lisan Lake, if such a connexion exists altogether, must be small in comparison to the amount of salt in the present-day Dead Sea. Some indications that certain

Dead Sea salts may in fact be inherited from the Lisan Lake are discussed below (see p. 258).

The salts must, therefore, have been carried into the Lake mainly by rivers, floods and springs. Of these the Jordan River is by far the most important contributor. Not only does this river account for about 75 per cent of all the surface water at present carried into the Dead Sea, but its water is considerably more saline than that of the other rivers discharging into it. The total amount of salts discharged annually into the Dead Sea by the Jordan River is about twice the quantity of new salts brought by the various rivers into Great Salt Lake (EARDLY *et al.*, 1957).

At a first glance it does not seem impossible that the Dead Sea salts derive from those contained in the Jordan River, although the salt composition of the two waters is basically different. It is, however, obvious that some of the more insoluble compounds must be thrown out of the highly concentrated salt solution of the Dead Sea. The Jordan River carries into the Dead Sea annually about $240 \cdot 10^3$ tons of $CaCO_3$. This compound must be deposited immediately, most probably in the form of aragonite. Precipitation is not necessarily confined to the vicinity of the Jordan delta owing to the currents known to exist in the Dead Sea and particularly in its northern part. In addition, a state of supersaturation in respect to $CaCO_3$ seems to exist frequently for a considerable time (EMERY and NEEV, 1959). The actual deposition of $CaCO_3$ by the Dead Sea is in fact occasionally observed in the form of a sudden whitening of its whole surface. Water taken during these periods contained crystals of calcium carbonate in suspension. If the amount of calcium carbonate brought annually by the Jordan River into the Dead Sea is spread uniformly over its bottom, the thickness of the resulting sediment layer, calculated on a water-free basis, amounts to 0·1 mm, i.e. only a fraction of the thickness of the annual deposit of the Lisan Lake, as deduced from a measurement of its annual varves, and only a fraction of the total sedimentary thickness deposited annually at present in the Dead Sea, as shown by preliminary measurements (NEEV, personal communication).

Although considerable amounts of calcium are contained in the present Dead Sea water, the quantity of HCO_3' is very low, but much bicarbonate must have been present at an earlier stage of its development, when the total salinity was lower. In this connection it may be noted that a terrace of aragonitic travertine is found all along the western shore of the Dead Sea, approximately 30 m above its present level. This terrace was most probably formed as a chemical precipitate at an earlier stage in the development of the Dead Sea, when its water became first supersaturated in respect to $CaCO_3$.

Another discrepancy between the Jordan and the Dead Sea water is the different Na:K-ratio, which is 4·6 for the Dead Sea and 17·1 for the Jordan River near its delta (see Table 4). The most obvious explanation is that part of the sodium has been removed from the Dead Sea water by precipitation of NaCl. At present no part of the Dead Sea seems to be saturated in respect of this compound.*

* It is, therefore, surprising that crystals of NaCl have been dredged from recent sediments in the deep northern basin of the Dead Sea. The mechanism of NaCl precipitation from under saturated water is at present under investigation.

The amount of NaCl brought into the Dead Sea annually by the Jordan River is about 750.10^3 tons, while the total amount of NaCl in the Dead Sea water is slightly in excess of $12 . 10^9$ tons. This quantity would thus have been brought into the Dead Sea by the Jordan River in only 16,000 years—a much shorter period than the minimum possible age for the accumulation of the other salts in the lake through the Jordan River (see below). A borehole drilled recently in the central part of the southern Dead Sea basin to a depth of 100 m has disclosed, beneath a 40 cm thick surface layer of silt, a continuous sequence of porous crystalline rock salt with some gypsum extending to the bottom of the hole and only interrupted by occasional thin layers of shales. This is the first direct proof that NaCl was in fact precipitated in considerable quantities by the Dead Sea in sub-Recent time. The

Table 6. Changes in Dead Sea level

Year	Elevation below Mediterranean Sea level in m
1865	393·8
1879	395·7
1910	390·6
1929	388·8
1938	392·6
1958	395·0

Figures contained in this table are partly taken from the Report of Dead Sea Committee, Jerusalem (1956)

precipitation may be limited to certain parts of the lake, and the southern basin is a particularly favourable one. Between the point of the Lisan Peninsula and the western shore of the Dead Sea the lake is at present only a few metres deep, and a low, but well defined, sublacustrine swell has been found here separating the northern from the southern basin. A small drop in the level of the Dead Sea would effectively separate the southern basin from the northern one. During the subsequent strong evaporation of the shallow southern body of water NaCl must precipitate, and this process would continue until the southern basin is again connected with the northern one by a temporary rise of the lake level. Those periods are probably marked in the drilled section mentioned above by the intercalated shale horizons. Fluctuations of the Dead Sea level of sufficient magnitude even during the past century alone have been proven by measurements as shown by the figures of Table 6.

The fact that NaCl was deposited in the Dead Sea, at least locally and temporarily, is thus well established. It also helps to explain, at least partially, another chemical discrepancy between the Jordan and the Dead Sea waters, i.e. the different Cl:Br-ratio which, as shown in Table 5, is 35·1 for the Dead Sea and 109·2 for the Jordan River. The NaCl precipitating in the evaporation pans of the Dead Sea contains only negligible amounts of bromine. The Cl:Br-ratio of this precipitate is approximately 2500 (Bloch and Schnerb, 1953). The precipitation of large amounts of $CaCO_3$ and NaCl from the Dead Sea explains immediately the high

proportion of magnesium which, in percentage of total solids, is 5·4 times as high in the Dead Sea water than in the Jordan River. Although slight amounts of magnesium may precipitate as carbonate, this amount must be very small, since $CaCO_3$ crystallizes from the Dead Sea water as aragonite.

It is, however, impossible to explain quantitatively the present salt assemblage of the Dead Sea water as derived from those contained in the Jordan River alone for the following reasons:

(1) The amount of Ca^{2+} contained in the Jordan River is sufficient only to precipitate almost exactly half the amount of the CO_3''-ion of the Jordan water. No Ca^{2+} is available for the elimination of the remaining half of the CO_3''-ion.

(2) No Ca^{2+} is available in the Jordan River for the almost quantitative precipitation of sulphate as anhydrite or gypsum. The SO_4''-ion in fact amounts to 20·06 per cent of the total anions in the Jordan River, but only to 0·25 per cent of those in the Dead Sea.

Table 7. Comparison of major ions in Jordan River and Dead Sea

Ion	Content in Jordan River at mouth in g/l	Annual supply to Dead Sea by Jordan River in 10^3 tons	Amounts present in Dead Sea in 10^6 tons	Number of years needed for accumulation in Dead Sea
Na^+	253·40	304·08	4,996·4	16,431
K^+	14·85	17·82	1,081·1	60,668
Ca^{2+}	80·00	96·00	2,259·4	23,535
Mg^{2+}	71·42	85·70	6,000·3	70,015
Cl'	473·50	568·20	29,746·9	52,353
Br'	4·338	5·21	846·6	162,495
SO_4''	174·49	209·38	77·2	369
HCO_3'	237·90	285·48	43·2	151
Total	1,309·898	1,571·87	45,051·1	

(3) Even on the assumption that considerable quantities of NaCl, containing only negligible amounts of Br, have been thrown out of the Dead Sea, the Cl:Br-ratio of 35·1 of the Dead Sea is still too low as compared with the Cl:Br-ratio of 109·2 of the Jordan River.

In order to arrive at a quantitative treatment of the problem the figures of Table 7 have been calculated. This table shows the amount of the various ions contained in the Jordan River; the amount of each ion supplied annually to the Dead Sea by the Jordan River; the amount of the various ions at present contained in the Dead Sea water; and the number of years required to supply these amounts by the Jordan River, at its present rate of flow, on the assumption that no salts were removed from the Dead Sea.

Of all the ions present in the Dead Sea and the Jordan River waters this last assumption should most nearly be fulfilled for K^+ and Mg^{2+}. These two cations form, under the conditions of the Dead Sea, only such highly soluble salts that their solubility product is still considerably above that of the Dead Sea water. It

is, therefore, interesting to note that the time needed for the accumulation of these two ions is very similar: 60,000 years for K^+, and 70,000 years for Mg^{2+}. It may thus be concluded that the maximum age of the Dead Sea is 60,000 to 70,000 years.

It is necessary to consider the possible errors contained in the above conclusion. The following factors would tend to reduce the age of the Dead Sea;

(1) Salts inherited from relict water bodies of the Lisan Lake.

(2) Supply of salts from rivers other than the Jordan, or from springs.

(3) Higher salinity of the Jordan water in its earlier stages, owing to initial stronger leaching of the Lisan deposits and their salty connate water which up to the present form the major source of the salts in the Jordan River.

(4) A higher rate of flow of the Jordan River at some earlier stage. This factor should not be overrated. Even if—which is not proven—the Jordan River was ever larger during the past 70,000 years than it is today, observations of the changing amounts of salts during the very large fluctuations in the annual flow of this river at present show that an increased flow is accompanied by diminishing salinity; the annual amounts of salt carried by the Jordan River are thus at present nearly independent of its rate of flow.

(5) Contribution of air-borne salt through fall-out from the atmosphere. The precipitation of air-borne salt carried by the prevailing western winds from the Mediterranean was studied recently by S. Löwengart (in press). This author reached the conclusion that in the Dead Sea area the annual fall-out of air-borne Cl′, both dry and contained in rain water, is approximately 25 kg/acre, corresponding to 0·625 mg/cm^2. It follows that the Dead Sea receives directly from the air 6250 tons Cl′ per year, an entirely negligible amount. It is, however, interesting to note that air-borne salts form a not inconsiderable contribution to the salt content of the Jordan River (see also Table 7). If it is assumed that the rate of Cl′ fall-out over the entire drainage basin of the Jordan River, which is 16,360 km^2 in size, is equal to the figure stated above, slightly more than 100,000 tons of Cl′ are added annually to this area by atmospheric fall-out. On the assumption that this amount is quantitatively taken up by the Jordan River—although with a certain time lag—it follows that about 18 per cent of the total Cl′ carried by the Jordan River must be attributed to this source, and a similar proportion may be assumed for most of the other ions.

The following factors would tend to increase the age of the Dead Sea:

(1) The loss of K^+ through absorption on the clayey bottom deposit or through its entrance into clay structures. Preliminary X-ray investigations have, in fact, shown a high proportion of illites in the Recent sediments of the Dead Sea.

(2) Loss of magnesium through co-precipitation with $CaCO_3$.

(3) Loss of both K^+ and Mg^{2+} through Dead Sea water being trapped as connate water in the Dead Sea sediments.

(4) Removal of salt through wind ablation.

This mechanism is frequently considered a major factor in the salt cycle of arid regions. Thus, Eardly *et al.* (1957) conclude that no less than 87 per cent of the salts brought into the Great Salt Lake basin during the past 30,000 years were lost through ablation. The rate of salt ablation is not amenable to quantitative treatment. It is, however, highly unlikely that this factor plays any considerable role

in the Dead Sea basin. In contrast with the Great Salt Lake, the Dead Sea is situated in a deep rift valley with steep walls on both sides, morphological conditions which make removal of salt by wind action extremely difficult. Moreover, the area of the salt marshes, the main contributor to air-borne salt, is very limited in the Dead Sea area.

A quantitative analysis of these factors is impossible, but it is obvious that those tending to reduce the age of the Dead Sea largely outweigh the retarding factors. The age of 60,000 to 70,000 years must, therefore, be considered the maximum possible age of the Dead Sea.

Compared with this figure those contained in the last column of Table 7 are most revealing: they show not only that $CaCO_3$ and $CaSO_4$ are at present almost quantitatively thrown out of the Dead Sea, but also that during the last 60,000 to 70,000 years about three-quarters of the sodium and almost two-thirds of the calcium brought by the Jordan River into the Dead Sea were removed through precipitation. On the other hand, additional sources must have been available, particularly in respect to the supply of Br′.

The present composition of salts contained in the Dead Sea can thus only be explained on the assumption that in addition to the Jordan River another quantitatively important source of salts was available. This source must have contained a high proportion of Ca^{2+} and Br′ and, at the same time, very low values of SO_4'' and CO_3''. Although water of such composition is highly unusual, two kinds of springs are known in the vicinity of the Dead Sea whose waters fulfill these requirements. They are the so-called Zohar Sulphur Springs (see Table 1, No. 15) and the artesian water discovered recently in the oil-drilling of Sdom I (Table 1, No. 13).

The sulphur springs issue at the western shore of the Dead Sea, 17 km north of Sdom (see Fig. 1). They contain abundant H_2S and a salt composition which is intriguingly similar to that of the present Dead Sea, although the total salinity is only one-sixth of it. It may, therefore, be concluded that these springs are fed by Dead Sea water, trapped near the shore, following annual, or secular, fluctuations in its level and diluted by fresh water draining underground into the Rift Valley from the mountain formations in the west. This is all the more probable as the similarity between the sulphur springs and the Dead Sea water extends also to the trace elements. The Au content, for instance, of both waters is $X \cdot 10^{-3}$ p.p.m. a value corresponding to that of the average igneous rock, but exceeding that of the ocean by a factor of 10^3.

The water discovered in the oil-well drilling of Sdom I is entirely different. This well is situated on the western flank of Mount Sdom, 1 km distant from the western Dead Sea shore. At a depth of some hundreds of metres the drill struck water which, originally confined beneath an impervious shale layer, stood under high pressure and rose to the surface. The chemical composition of this water (Table 1, No. 13) is most unusual: salinity is as high as 43·74%, the major cations are Ca^{2+} and—to a lesser degree—Mg^{2+}, K^+ and Na^+. But the only anions present are Cl′ and Br′. The Na:K-ratio of 0·77 is lower than in any other water in the vicinity. Water of similar composition has since been found seeping out at various places at Mount Sdom, near the Dead Sea shore. The average chemical composition of the water of these springs and seepages is given in Table 1, No. 14. The salt

assemblage of this water corresponds perfectly to the requirements outlined above.

The assumption may thus be made that the salts of the Dead Sea are derived essentially from two sources: the Jordan River and springs discharging on the Dead Sea shore or at the sea bottom, carrying a salt assemblage corresponding or similar to that of Sdom I. This assumption can be checked by a calculation: the amount of Ca^{2+} which must be added annually, from sources other than the Jordan River, so as to precipitate the excess of SO_4'' and HCO_3' contained in the Jordan River, is calculated as $178{\cdot}8 \cdot 10^3$ tons. An additional amount of Ca^{2+} is needed to supply the $2259{\cdot}4 \cdot 10^6$ tons of Ca^{2+} at present dissolved in the Dead Sea water (Table 7). If this amount of Ca^{2+} is supplied by springs of the Sdom I type, the amount of Mg^{2+} which would simultaneously be supplied can be found from Table 1, No. 14. This amount of Mg^{2+}, added to that carried annually by the Jordan River, gives the total of the annual Mg^{2+} supply. The amount of Mg^{2+} present in the Dead Sea viz. $6000 \cdot 10^6$ tons, divided by the total annual supply of Mg^{2+}, gives the time needed to arrive at the present composition of the Dead Sea salts. A slight correction is needed to eliminate the very small amounts of HCO_3' and SO_4' contained in the spring waters. Once the number of years is known, the quantity of Sdom I water to be supplied annually can be calculated. The two equations in question are as follows:

$$a = \frac{Mg_{DS}}{\frac{\left(Ca_{exc} + \frac{Ca_{DS}}{a}\right) \cdot Mg_S}{Ca_S} + Mg_J} \tag{1}$$

$$a \cdot Mg_J + d \cdot a \cdot Mg_S \cdot 10^{-6} = Mg_{DS} \tag{2}$$

where:

Mg_{DS} = amount of Mg^{2+} in Dead Sea in tons = $6000{\cdot}3 \cdot 10^6$
Ca_{exc} = amount of Ca^{2+} needed to precipitate the excess SO_4'' and HCO_3' of Jordan River in tons = $178{\cdot}84 \cdot 10^3$
Ca_{DS} = amount of Ca^{2+} in Dead Sea in tons = $2259{\cdot}4 \cdot 10^6$
a = number of years
Mg_S = amount of Mg^{2+} in springs in mg/l. = 41,670
Ca_S = amount of Ca^{2+} in springs in mg/l. corrected for HCO_3' and SO_4'' content of springs = 37,112
Mg_J = amount of Mg^{2+} supplied annually by Jordan River in tons = $85{\cdot}7 \cdot 10^3$
d = annual discharge of springs in m^3

The solution of these equations is:

$$a = 12{,}089$$

$$d = 9{\cdot}854 \cdot 10^6$$

It may be significant that this figure of 12,000 years is very close to the 11,000 years deduced for the end of the Pleistocene and the onset of a sudden climatic change, on the basis of C^{14} analyses of ocean cores (Broecker *et al.*, 1959). It corresponds also with the Gilbert stage and the time of rapid increase in the salinity

of the Great Salt Lake, as deduced by EARDLY *et al.* (1957), and the time of disappearance of the upper Searle's Lake (FLINT and GALE, 1958). As to the Dead Sea, it means that the age of 60,000 to 70,000 years, arrived at on the assumption that all its salts are derived from the Jordan River, is reduced to about one-fifth if the influx of salt water from springs is taken into account. The annual spring flow needed turns out to be very small; the value of $d = 9{\cdot}85 \cdot 10^6$ m^3/yr corresponds to a flow of 1125 m^3/hr, i.e. about 0·9 per cent of the amount of water carried by the Jordan River. Such small quantities may even at present be discharged underground into the Dead Sea.

Table 8. Salts supplied to Dead Sea by saline springs and Jordan River during last 12,089 years in 10^6 tons

Ions	Saline springs	Jordan River	Total	Precipitated in Dead Sea	Present in Dead Sea (calculated)	Present in Dead Sea (observed)
Na^+	2,955·9	3,676·0	6,631·9	1,635·5	4,996·4	4,996·4
K^+	1,905·1	215·4	2,120·5	—	2,120·5	1,081·1
Ca^{2+}	4,436·3	1,160·5	5,596·8	3,276·9	2,319·9	2,259·4
Mg^{2+}	4,964·0	1,036·1	6,000·1	—	6,000·1	6,000·3
Cl'	29,503·8	6,868·9	36,372·7	2,521·5	33,851·2	29,746·9
Br'	390·7	62·9	453·6	—	453·6	846·6
SO_4''	12·7	2,531·2	2,543·9	2,466·7	77·2	77·2
HCO_3'	15·1	3,451·1	3,466·2	3,423·0	43·2	43·2
Total	44,183·6	19,002·1	63,185·7	13,323·6	49,862·1	45,051·1

Notwithstanding the small volume of spring water, its influence on the chemical composition of the Dead Sea water is very considerable, owing to its extremely high salinity. The figures of the various ions supplied by these springs with a discharge of $9{\cdot}85 \cdot 10^6$ m^3/yr, and by the Jordan River at its present annual flow of 1200 10^6 m^3 during a period of $a = 12{,}089$ years, are tabulated in the first columns of Table 8. The total amount of salts supplied by the springs is more than double that of the Jordan River and there are considerable differences in composition. Part of the total salts thus brought into the Dead Sea (Table 8, column 3) are removed by precipitation. The amounts of salt precipitated during this period of 12,089 years are given in Table 8, column 4. The amount of the various salts which should, according to these assumptions, be present in the Dead Sea are given in Table 8, column 5. Comparison with the quantities of salt actually present in the Dead Sea (Table 8, column 6) shows very satisfactory agreement and provides an additional check for the correctness of the basic assumption. The only major difference between calculation and observation concerns the figure for KCl which on calculation, is almost twice as high as the observed value ($4044 \cdot 10^6$ tons against $2065 \cdot 10^6$). This means that either vast quantities of sylvite were precipitated from the Dead Sea during the past 12,000 years and lie buried somewhere beneath the Dead Sea bottom, or that the saline spring-water on which the calculation is based carries too high a proportion of K^+. The first alternative is much less probable, for

it is hard to see how during the last 12,000 years the Dead Sea water could ever have been sufficiently concentrated for the deposition of KCl. The second alternative is more likely, as the Na:K-ratio of the saline springs is abnormally low. In view of the high salinity of this water, only a slight change in this ratio is needed to remove the discrepancy.

It is interesting to note that of the $63{,}000 \cdot 10^6$ tons of salt brought into the Dead Sea during the past 12,000 years, less than one-third was carried by the Jordan River and more than two-thirds by springs and seepages, although these account for less than 0·9 per cent of the volume of water carried by the Jordan. Of the total amount of salts brought into the Dead Sea roughly one-fifth was precipitated, and four-fifths are still in solution.

The composition and amount of chemical sediments deposited in the Dead Sea can be calculated on the basis of the figures in Table 8. It may be assumed that $CaCO_3$ was precipitated more or less uniformly over the entire Dead Sea bottom,

Table 9. Chemical sedimentation in Dead Sea

	Total amount precipitated in 12,089 years in 10^6 tons (total Dead Sea)	Annual precipitation in gr/cm^2 (Southern Basin)	% of total chemical precipitate (Southern Basin)
$CaCO_3$	5,671·0	0·0469	15·3
$CaSO_4$	3,495·6	0·1185	38·7
NaCl	4,157·0	0·1409	46·0
Total	13,323·6	0·3063	100·0

while sedimentation of $CaSO_4$ and NaCl took place mainly in the more closed southern basin. Under these assumptions the figures of Table 9 have been calculated. They show that the average annual rate of chemical sedimentation in the southern Dead Sea basin over the last 12,000 years was approximately 0·3 g/cm^2. This figure agrees well with preliminary results of the present sedimentation rate as measured by sedimentation traps (personal communication, Neev). The chemically precipitated part of the sediment consists of about 46 per cent NaCl, 39 per cent $CaSO_4$ and 15 per cent $CaCO_3$. These figures refer to the chemical precipitate only and do not include sedimentation of clay material. The sedimentation rate of the latter in the present Dead Sea is not known, but seems to be smaller than that of the chemical sediments.

On the basis of these figures the total thickness of the Dead Sea sediments, excluding the halite masses, may be estimated at about 15 m. At depths of 3·5–4·0 and 10·2–10·8 m respectively, samples were taken in the southern Dead Sea basin (hole Ca 27) for C^{14} analysis. These determinations, based on organic carbon, carried out by T. A. Rester of the Department of Scientific and Industrial Research, Division of Nuclear Science, New Zealand, gave an age of 4410 ± 320 years for the upper, and of 9580 ± 150 years for the lower sample. Not much reliance should be placed on two determinations, the exact positions of which in the total column of the Dead Sea sediments are, moreover, not yet known; but it can safely be said

that they do not contradict the age of 12,000 years derived from geochemical considerations.

Origin of Bromine

One of the most characteristic geochemical features of the Jordan Valley and the Dead Sea is the high concentration of bromine in the lake, springs and underground waters. The relevant figures are summarized in Table 1.

The total amount of bromine now present in the Dead Sea is $846{\cdot}6 \cdot 10^6$ tons. If this amount has accumulated during the past 12,000 years, it necessitates an annual intake of 70,000 tons. From all known and inferred sources at present active, only about 34,000 tons can be derived annually (see Table 10).

Table 10. Sources of Br carried into the Dead Sea in tons/yr

Jordan River	Via Lake of Galilee	1,175	Northern Jordan	tr
	Beisan Springs	560	Tannur Springs	400
	Yarmuk River, Zerka Hot Springs and other sources (?)	3,465	Tabha Springs	35
			Fuliya Springs	60
			Tiberias Hot Springs	246
			Springs at Lake Bottom	434 (?)
	Total	5,200		
Saline springs discharging directly into Dead Sea		28,578		
Total		33,778		

Only about 5200 tons/yr, i.e. 15 per cent of the total, are brought by the Jordan River, while more than 28,000 tons must be attributed to springs and seepages discharging directly into the Dead Sea at a rate of $9{\cdot}85 \cdot 10^6$ m^3/yr (see Table 1, No. 14). The 5200 tons carried by the Jordan River can in part be followed to their source: a small contributor is the Tiberias Hot Springs—which have frequently been considered to be the major source—with an annual discharge of about 1.10^6 m^3. Since these springs carry on the average 246 p.p.m. Br, their contribution is 246 ton/yr, i.e. only 4·7 per cent of the total Br brought into the Dead Sea by the Jordan River. Quantitatively the springs of the Beisan area draining into the Jordan are more important owing to their much higher discharge ($\sim 140 \cdot 10^6$ m^3), although their Br content is only a fraction of that of the Tiberias Hot Springs (see Table 1, No. 5). The total amount of bromine discharged annually from the Beisan springs can be calculated at 560 tons. A major source of the Br contained in the Jordan River is the Sea of Galilee. On the basis of the figures cited in Table 1 it is calculated that at its outflow from the Sea of Galilee the Jordan River carries 1175 ton/yr Br, i.e. slightly less than one-quarter of its total Br discharge into the Dead Sea. The origin of the Br contained in the Sea of Galilee is only partly known: very small amounts are brought by the Jordan into the lake; 400 tons per year are delivered by the Tannur Springs north of Tiberias, 35 tons

come from the nearby Tabha group, 60 tons are attributed to the Fuliya group of springs, and 246 tons to the Tiberias Hot Springs—all discharging into the Sea of Galilee.

From these two sources—the Sea of Galilee and the Beisan springs—the Jordan River receives altogether 1735 tons of bromine, corresponding to 33 per cent of its total bromine content, at the point where its enters the Dead Sea. Although precise data are not available, it can be assumed that the difference is made up in major part by the Yarmuq River—mainly from the El Hamme Hot Springs which have an annual discharge of $1{\cdot}18 \cdot 10^6$ m^3—and by the Zerka River, probably mainly from the Zerka Hot Springs.

From this short description it is clear that the entire Jordan–Dead Sea basin is characterized by a high concentration of Br and represents probably the largest Br province in the world. It might be mentioned in passing that some of the springs, such as those of Fuliya and of the Tannur group, seem to contain Br in excess of the equivalent amount of Mg. Another characteristic of most of these springs is their large content of $CaCl_2$. This is true in particular of the brines of the Sdom I type, the Zohar sulphur springs, those of the Tabha and Tannur groups, and of the Tiberias Hot Springs. In the latter, 88 per cent of the total Ca must be calculated as $CaCl_2$.

The origin of these Br occurrences is a matter for speculation. Their distribution over a large area and their almost constant association with $CaCl_2$ make a common origin almost certain. Three theories as to the origin of these salts may briefly be considered:

The northern part of the area under discussion, i.e. Lower Galilee and the surroundings of Tiberias, is an area of sub-Recent *volcanic activity*. Magmatic emanations at depth may carry hydrochloric acid. On their way up it would react with the limestone layers which form a large part of the geological section on both sides of the Jordan Valley, and as a result $CaCl_2$ would be formed. However, most of the springs, as they reach the surface, have a pH of 7 or slightly higher; nevertheless they contain only moderate amounts of H_2CO_3. Volcanic rocks of Tertiary to Quaternary age are widespread in the Tiberias area but absent in the Sdom region, where, however, the water richest in $CaCl_2$ is found. In addition, it is very doubtful whether magmatic emanations are ever rich in Br.

The Cl:Br-ratio of igneous rocks (Table 5, No. 35) is in fact low and varies for basic and intermediate rock types from 17 to 79 (Behne, 1953), values very similar to that of the Dead Sea water. No determinations of Br in volcanic exhalations seem ever to have been published, but the average Br content of a large number of mineral waters collected by Schoeller (1956) is only 90 p.p.m., i.e. slightly higher than that of the ocean. Moreover, the Cl:Br-ratio of mineral waters (Table 5, No. 33) is 274, equal to that of the ocean.

Another geochemical environment leading to Br enrichment is the *organic* one. Most oil waters carry considerable amounts of Br, although—as pointed out by Schoeller (1956)—this is more a consequence of the higher total salinity of oil waters than of a specific enrichment of Br in relation, for instance, to Cl. The average value of this ratio for 128 samples quoted by Schoeller is 329, i.e. very similar to that of the ocean. Still, these oil waters contain on the average 149 p.p.m.

Br and much higher values, up to 6500 p.p.m., i.e. $1\frac{1}{2}$ times the concentration of Br in the Dead Sea water have occasionally been recorded (Krejci–Graf and Leipert, 1936). However, oil waters high in Br are invariably also high in I. While Schoeller points out that high amounts of I are a likely rather than a necessary characteristic of oil waters, the Br:I-ratio of oil waters is surprisingly constant. Iodine content of oil waters vary from 0 to 236 p.p.m., and the average of 151 determinations quoted by Schoeller is 18 p.p.m., as against values of 0·011–0·07 p.p.m. in ocean water. High values of I also characterize almost all bituminous and fossiliferous sediments. The Br:I-ratio varies much less. Relevant figures are summarized in Table 11. Although this ratio is subject to regional variations, the range of the

Table 11. Br:I–ratio of oil waters

Locality	Range of ratio	Average ratio	No. of analyses
California	0·3– 6·7	3·4	5
Hungary	1·2–17·0	4·1	11
Poland (Borislav)	0·5–27·7	9·6	13
Rumania	0·5–31·5	5·9	11
Russia (Polasna-Krasnokamsk Anticline)	30·0–41·5	36·2	6
World	0·3–41·5	10·2	46

Figures in this table are based on data quoted by H. Schoeller (1936) pp. 109–111.

average ratio for various oil-fields in the world is only 3·4–36·2, with a world average of 10·2, as against a value of 7000 for the ocean. In the Dead Sea water I is present only in very small quantities; no reliable determinations are available, but its concentration is less than 0·1 p.p.m. Notwithstanding the frequent occurrences of asphalt and oil seepages in and near the Dead Sea, the Br:I-ratio of more than 10^5 in the Dead Sea water almost certainly excludes an organic origin of the Br.

The most likely assumption for the origin of the Br in the Dead Sea is its concentration in *fossil residual salt brines*. Large lakes are known to have existed in the Jordan–Dead Sea area since Oligocene times. These lakes were at certain periods highly saline, even more than the present Dead Sea, as shown *inter alia* by the huge rock-salt masses of the Sdom Formation. That residual brines resulting from strong evaporation of water of the Dead Sea type can be very rich in Br, is shown by the experience in the evaporation pans of the Dead Sea Works. While Dead Sea water of a specific gravity of 1·192 contains about 4000 p.p.m. Br, the residual brine, resulting from the precipitation of halite and carnallite, with a specific gravity of 1·341, contains 8750 p.p.m. Br, and this notwithstanding the fact that the crystallizing salts are isomorphous with the corresponding bromine compounds. It is conceivable that the most soluble salts contained in these lakes never crystallized, and that these solutions were trapped at depth. The highly saline water discovered in the Sdom I oil drilling was confined and released only after the drill pierced a sequence of impermeable shales. Prolonged evaporation of lakes in a desert environment and the trapping of their residual brines through the

long continued subsidence of the Rift Valley and the rapid infilling of the graben, seem to be the best explanation for the high Br concentration in the Dead Sea basin.

Acknowledgments—Thanks are due to the Dead Sea Works Ltd. and Water Planning of Israel Ltd., which supplied part of the hydrographical and chemical data. I wish further to express my sincere appreciation to my colleagues of the Geological Survey of Israel, who have been working with me on the geological problems of the Dead Sea, and especially to W. Bodenheimer, D. Neev and Z. Shiftan. I am particularly indebted to K. O. Emery of the University of Southern California, with whom I had many stimulating discussions during our joint work on the Dead Sea, and to Engineer M. A. Novomeysky, the pioneer in the development of the Dead Sea region.

References

Behne, W. (1953) Untersuchungen zur Geochimie des Chlor und Brom. *Geochim. et Cosmochim. Acta*, *3*, 186–215.

Bentor, Y. K. and Vroman, A. (1957) *The Geological Map of Israel*, 1:100,000, *Sheet* 19: *Arava Valley*. Geological Survey of Israel, Jerusalem.

Bentor, Y. K. and Vroman, A. (1960) *The Geological Map of Israel*, 1:100,000, *Sheet* 16: *Mount Sdom, with explanatory text*. Geological Survey of Israel, Jerusalem, 2nd. (revised) edition.

Blake, G. S. and Goldschmidt, M. J. (1941) *Geology and Water Resources of Palestine*. Dept. of Land Settlement and Water Commissioner, Govt. of Palestine, Jerusalem.

Bloch, R., Littman, H. Z. and Volcani, B. E. (1944) Occasional whiteness of the Dead Sea. *Nature, Lond.* **154,** 402–403.

Bloch, M. R. and Schnerb, J. (1953) On the Cl:Br-ratio and the distribution of Br-ions in liquids and solids during evaporation of bromine-containing chloride solutions. *Bull. Res. Counc. of Israel*, Vol. III 3, 151–158.

Broecker, W. C., Ewing, M. and Heezen, B. C. (1959) Evidence for a Sudden Climate Change 11,000 years ago. *Int. Oceanic. Congr. New York*, preprint p. 87.

Clarke, F. W. (1924) Data on Geochemistry *U.S.G.S., Bull.* 770.

Correns, C. W., (1956) The Geochemistry of the Halogens. *Physics and Chemistry of the Earth*, **1,** 181–223. Edited by Ahrens, L. H., Rankama, K. and Runcorn, S. K., McGraw-Hill, New York and Pergamon Press, London.

Dead Sea Committee, (1956) Unpublished Report, Dead Sea Works, Jerusalem.

Eardly, A. J. and Gvodetsky, V. (1960) Analysis of Pleistocene Core from Great Salt Lake, Utah. *Bull. Geol. Soc. Am.*, **71,** 1323–1344.

Eardly, A. J., Gvodetsky, V. and Marcell, R. E. (1957) Hydrology of Lake Bonneville and Sediments and Soils of its Basin. *Bull. Geol. Soc. Amer.*, **68,** 9, 1141–1201.

Emery, K. O. and Neev, D. (1959) Preliminary Report on Surveys of the Dead Sea. Unpublished Report, Geological Survey of Israel, Jerusalem.

Flint, R. F. and Gale, W. A. (1958) Stratigraphy and radio-carbon dates at Searles Lake, California. *Amer. J. Sci.*, **256,** 689–714.

Goldschmidt, M. J. (1955) Precipitation over and run-off from Jordan and Litani Catchments. *State of Israel*, Ministry of Agriculture, *Hydrological Survey*, *Hydrological paper* No. 1, Jerusalem.

Goldschmidt, V. M. (1954) (Edit. A. Muir,) *Geochemistry*. Oxford University Press.

Government of Israel (1958) *Hydrology Yearbook of Israel*, Ministry of Agriculture, Jerusalem.

Ionides, M. G. (1939) *Report on the Water Resources of Transjordan and their Development*. Publ. on behalf of Transjordan by Crown Agents for Colonies, London.

Irwin, W. (1925) The origin of the salts in the Jordan. *Geogr. J. Lond.* Vol. LXVI, 527–533.

Krejci-Graf, K. and Leipert, T. (1936) Bromgehalte in mineralogischen, kohligen und bituminoesen Ablagerungen. *Z. Prakt. Geol.* ,*44*, p. 117.

Lartet, L. (1876) Exploration Géologique de la Mer Morte de la Palestine et de l'Idumée. Bertrand, Paris.

LÖWENGART, S. (in press) Air-borne salts—the major source of the salinity of waters in Israel. *Bull. Res. Counc. Israel.*

LYNCH, W. F. (1852) *Official Report of the U.S. Expedition to Explore the Dead Sea and the River Jordan.* Publ. by authority of the Hon. Wm. A. Graham, Secretary of the Navy at the National Observatory, Lieut. M. F. Maury, U.S.N. Superintendent, John Murphy and Co. Baltimore.

NEEV, D. (1960) A pre-Neogene erosion channel in the southern coastal plain of Israel. *Geological Survey of Israel, Bull.* 25.

NEUMANN, J. (1958) Tentative energy and water balances for the Dead Sea. *Bull. Res. Counc. of Israel.* **75,** 137–163.

NOLAN, T. B. (1928) Potash Brines in the Great Salt Lake Desert, Utah. *U.S.G.S. Bull.* **795,** 25–44.

NOVOMEYSKY, M. A. (1936) The Dead Sea: A Storehouse of Chemicals. *Trans. Inst. Chem. Eng. London,* **14,** 60–81.

PICARD, L. (1943) Structure and Evolution of Palestine. *Bull. Geol. Dept. Hebrew University,* Jerusalem, Vol. 2, No. 224.

RANKAMA, K. and SAHAMA, Th. G. (1955) *Geochemistry.* The University of Chicago Press, Chicago.

SCHOELLER, H. (1956) Géochimie des eaux souterraines. *Revue de l'Institut François du Pétrole et Annales des combustibles liquides.* Paris.

SHIFTAN, Z. L. (1958) An Artesian Aquifier of the Dead Sea Basin. *Geological Survey of Israel, Bull.* 13*A*, Jerusalem.

SVERDRUP, H. C., JOHNSON, M. W., FLEMING, R. H. (1957) *The Oceans.* Prentice-Hall Inc. Englewood Cliffs, N.J.

WITZAN, G. R. and WOZAB, D. H. (1954) Chemical quality of waters occurring in the Jordan Valley area. *Ass. Int. Hydrol. Soc. Assemblée Gén. Rome.* pp. 170–178.

YARON, F. (1952) The Springs of Lake Kinnereth and their relationship to the Dead Sea. *Bull. Res. Counc. of Israel,* **2,** 121–128.

YARON, F. and HEITNER, M. (1952) The Chloride-Bromide Ratio of the Water Sources of Eastern Emek Yezreel and of the Beisan Valley. *Bull. Res. Counc. of Israel,* **2,** 118–120.

Geochimica et Cosmochimica Acta, 1961, Vol. 25, pp. 261 to 266. Pergamon Press Ltd. Printed in Northern Ireland

Chlorine-36 and deuterium study of Great Basin lake waters*

F. T. Bonner†, E. Roth‡, O. A. Schaeffer§ and S. O. Thompson§

(*Received* 13 *January* 1961; *in revised form* 17 *April* 1961)

Abstract—Chloride samples from the waters of Mono Lake, Pyramid Lake and the lower Truckee River have been examined by low-level counting techniques for chlorine-36 content. Chlorine-36 in the lake samples was found to be below the limit of detectability of the method, indicating a cosmic ray exposure age of less than 300,000 years for the chloride examined. No detectable chlorine-36 was found in surface chloride samples from three separate salt-flat locations in Utah and Nevada. Significantly detectable chlorine-36 was found in the lower Truckee River sample and it is suggested that this activity has its origin in recent thermonuclear tests.

Hydrogen–deuterium ratios were determined for Mono Lake, Pyramid Lake, Lake Tahoe and associated streams. It is indicated that all three lakes lose water largely by evaporation, and that Lake Tahoe water has substantial residence time despite its outflow into the Truckee River. It is also indicated that the Truckee River is subject to strong dilution by fresh runoff water.

Introduction

The prehistoric lakes Bonneville and Lahontan were the subjects of careful geological investigations in the late nineteenth century by, respectively, Gilbert (1890) and Russell (1885). Bonneville, in Gilbert's reconstruction, stood at a level some 1000 ft above that of its present remnant, Great Salt Lake, and covered 19,750 miles^2 in area. The lake level fluctuated with glaciation associated climatic changes, and at a relatively late stage Bonneville found a northward outlet to the Snake River, dropping in level some 375 ft to the Provo shoreline. Russell concluded that the more westerly Lake Lahontan had covered 8422 miles^2 in area and that its level was 886 ft above that of its principal remnant, Pyramid Lake. He also concluded that Lahontan did not overflow at any time in its history. The geological evidence indicates that both lakes had two high-water stages separated by a period of aridity, and that the fluctuations in the two basins are correlated.

The Great Basin area includes other, smaller, independent closed basins whose histories seem to have been similar, in broad outline, to those of Bonneville and Lahontan. In particular Mono Lake, in California, shows evidence of two high-water stages, one of them some 900 ft in depth, and associated with an essentially contemporaneous Sierra Nevada Glacier (Russell, 1889).

The Great Salt Lake is the most saline of the present-day lakes mentioned above, Mono Lake much less so but relatively strongly saline, and Pyramid Lake relatively fresh. Recent analyses of chloride ion concentrations of these three lakes reported by Broecker and Walton (1959) indicate 187,000 p.p.m. for Great Salt Lake, 14,000 p.p.m. for Mono Lake, and 1685 p.p.m. for Pyramid. In the case of Great Salt Lake much of the chloride must be of relatively recent accumulation, since overflow provides a mechanism for substantial freshening.

Broecker and Orr (1958) have investigated the absolute chronology of Lakes

* Research performed under the auspices of the U.S. Atomic Energy Commission.

† Department of Chemistry, State University of New York, Long Island Center, Oyster Bay, New York.

‡ Centre d'Etudes Nucléaires de Saclay, Gif-sur-Yvette (Seine-et-Oise), France.

§ Department of Chemistry, Brookhaven National Laboratory, Upton, New York.

Lahontan and Bonneville by radiocarbon analysis of calcareous tufa deposits in the two areas. In this study the correlations of level fluctuation between Lahontan and Bonneville, adduced by Gilbert and Russell, have been confirmed. Broecker and Orr conclude that there was a period of relatively low water level from 25,000 to at least 34,000 years ago, a high water period between 25,000 and 14,000 years ago, recession to low water at about 13,000 years ago, followed by rise to maximum levels at about 11,700 years ago. The decline to low level was apparently rapid at about 11,000 years ago, and there is some evidence that a final rise took place about 10,000 years ago, followed by decline to low level at at least 9000 years ago. Broecker and Orr conclude that the climatic changes required to cause such fluctuations are not extreme.

Broecker and Walton (1959) have carried out a study of the salt chronology of Great Salt, Mono, Pyramid and Walker Lakes, based entirely on chloride ion, and employing the assumption that Cl^- in these waters is due almost entirely to the addition of oceanic salt from rain. Their calculations employ estimates of the rate of addition of Cl^- to the basins by rainfall, rather than analyses of chloride content of rivers within the basin, and attempt to correct for chloride loss through wind entrainment at lake surfaces. In order to calculate chloride accumulation times, further assumptions concerning the physical characteristics of the lakes during the past are made, based in part on the radiocarbon results of Broecker and Orr. The results of this study indicate accumulation times for the salt in these lakes substantially greater than previous estimates based upon present rates of addition by rivers. For Great Salt Lake and Mono Lake it is concluded that accumulation times are in excess of 73,000 years and that there has been no desiccation since the last interpluvial period. A similar conclusion, although a less certain one, is reached with respect to Pyramid Lake. On the basis of a highly simplified model which leaves climatic change out of account, the total amount of Cl^- presently found in Mono Lake divided by the present rate of addition of Cl^- to the Mono Lake Basin yields an accumulation time of 460,000 years.

Davis and Schaeffer (1955) called attention to the possibility of detection of chlorine-36 in the chloride of inland closed-basin waters. For a given lake, knowing its chloride concentration, the cosmic-ray neutron flux at its particular altitude and latitude, and its mean depth, it is possible to calculate a value for the specific activity of its chlorine-36 content at saturation (ca. 1 million years) and shorter periods of exposure. For Mono Lake, if in the unlikely event that it had existed at approximately its present mean depth and general level of chlorine content for the past million years, calculation shows that it should have a chlorine-36 specific activity of about 0·025 dis/min per g, a value that is well within the limits of detection by low-level counting techniques.

Davis and Schaeffer reported no detectable chlorine-36 in the chloride of Great Salt Lake. The case of this lake is complicated, however, by the fact of its relatively recent outflow, and also by the existence of evidence (Feth, 1959) that littoral springs may be contributing substantial quantities of salt to the basin. In the present investigation attempts were made to detect chlorine-36 in the chloride of Mono Lake and of Pyramid Lake, with a view of testing the geochronological usefulness of the nuclide. Age information concerning the longer-range history of

the Great Basin is lacking, and it was believed that despite the well-established level fluctuations of relatively recent date and their implications for periodic chloride redistribution, possible circumstances exist under which the chlorine of a given basin could have received cosmic-ray exposure sufficient to result in detectable chlorine-36 content. Mono Lake Basin, for example, is presumed to have had a long, more or less continuous existence. If its history should include prolonged periods of very low level, a major portion of the salt of greatest cosmic-ray exposure age could have been retained by the processes of re-solution and of recycling within the basin.

In addition to lake water chloride, samples of chlorine from the lower Truckee River and from three separate salt flat locations were examined for chlorine-36 content in the present investigation. Finally, water samples from three Great Basin lakes and two of their associated drainage streams were analysed for deuterium content.

Experimental

Samples of lake and river chlorides were obtained by collection on anion-exchange resin. A sample of chloride from a saline region near Dugway, Utah was obtained by leaching of the soil-salt mixture typical of the area. A sample from the Utah Salt Flats near Danger Cave consisted of salt crystals removed from the surface. Finally, a chloride sample was obtained from the Forty Mile Desert by removal of the thin salt layer found deposited on clay in the typically playa-like region.

Purification of the chlorine in the samples included the steps of silver chloride precipitation, removal of silver from concentrated ammonia solution by sulphide precipitation, and evolution of hydrogen chloride gas. Counting of chlorine-36 was carried out in a screen-wall counter arrangement with appropriate shielding and anti-coincidence circuitry, with sample and reference deposited uniformly, as dry ammonium chloride, on the inside surfaces of steel liners. All samples were re-purified by HCl evolution until constant specific activity was obtained. As a non-radioactive reference sample, for background counting, chloride from a deeply buried salt dome formation was employed. This chloride had been compared with Atlantic Ocean chloride for radioactivity, and no statistically meaningful difference was found.

Water samples of the lakes and rivers were also collected. The water samples were introduced into a mass spectrometer gas line and converted to hydrogen *in situ* in a uranium furnace. The technique employed was that developed by Nief and Botter (1959).

Results and Discussion

Chlorine-36

The ^{36}Cl counting results for three water samples and three solid surface samples are shown in Table 1. All values shown are reported relative to salt dome chloride as background reference. In the case of Pyramid Lake the apparent result is somewhat greater than the activity calculated for saturation exposure, which in turn is small because of the small chloride content and considerable depth of the lake. However, since the reported specific activity is only twice the standard deviation

in the measurement, no significance is attached to this fact. For Mono Lake we can say from the measurement shown that the cosmic ray exposure age of the chlorine presently found is less than 300,000 years. This complements the salt chronology of Broecker and Walton (1959) by the addition of an upper limit, but provides no new insights.

Table 1. Chlorine-36 counting results

Sample	Weight as NH_4Cl (g)	Measured specific activity (dis min^{-1} g^{-1} of Cl)	Calculated specific activity at saturation* (dis min^{-1} g^{-1} of Cl)
Mono Lake (Water)	30·0	$-0{\cdot}011 \pm 0{\cdot}005$	0·025
Pyramid Lake (Water)	30·8	$+0{\cdot}013 \pm 0{\cdot}006$	0·0044
Lower Truckee River (Water)	4·0	$+0{\cdot}13 \pm 0{\cdot}02$	—
Dugway, Utah (Solid)	43·2	$-0{\cdot}006 \pm 0{\cdot}003$	0·019
Utah Salt Flat (Solid)	37·6	$-0{\cdot}015 \pm 0{\cdot}004$	0·019
Forty Mile Desert (Solid)	38·4	$-0{\cdot}008 \pm 0{\cdot}003$	0·019
Atlantic Ocean*	26·6	$-0{\cdot}01 \pm 0{\cdot}01$	$2{\cdot}6 \times 10^{-5}$
Great Salt Lake*	41·4	$0{\cdot}00 \pm 0{\cdot}01$	0·028

* Davis and Schaeffer (1955).

The Truckee River runs between Lake Tahoe and Pyramid Lake. Since the water sample from the lower portion of the Truckee River (collected during August 1958) showed substantial chlorine-36 it seemed likely that this activity might be due to fallout. As a result the samples were subjected to purification with respect to several potential fission–fallout activities by carrier precipitation. In the final counting result for this sample, as shown, we are confronted with the phenomenon of a lake whose chloride does not contain detectable chlorine-36 being fed by river waters which contain a substantial proportion of the nuclide.

It has been reported by Schaeffer *et al.* (1960) that rain water collected in 1957, 1959 and 1960 contains significantly detectable chlorine-36, ranging from $0{\cdot}4 \pm 0{\cdot}1$ to $8{\cdot}0 \pm 0{\cdot}1$ dis min^{-1} g^{-1} in separate samples. These investigators have reported lesser but unmistakable quantities in the water of the Long Island water table and in a Vermont stream. The general level of activity detected is of the order of 3000 times that of the chlorine-36 production rate estimated from cosmic-ray sources alone; hence it was proposed that the source of this activity is neutron activation of ocean chloride in the high neutron fluxes of recent thermonuclear tests. The results reported here, concerning the relative chlorine-36 levels of Pyramid Lake and one of its principal sources, confirm this hypothesis.

Broecker and Walton (1959) report a chloride concentration for the Truckee River of 55·2 p.p.m. at Nixon, Nevada, near the site of acquisition of the sample described in this paper. A value of 1·5 p.p.m. for the upper reaches of this river, at Truckee, is given by the U.S. Geological Survey (1957). The large increase in concentration can be taken as a probable indication of recycling of salt within the basin. Assuming that all of the chloride added between the two points on the river is of pre-bomb test origin, one can estimate a value for the specific activity of relatively fresh water in the upper Truckee. The resulting value is 4·8 dis min^{-1} g^{-1},

undoubtedly high due to unwarranted simplicity of the underlying assumption, yet well within the limits detected by SCHAEFFER *et al.* in rain water.

The three surface, solid salt samples examined, as shown in Table 1, contain no detectable chlorine-36, which would indicate that the salt had been exposed to cosmic rays on the surface for less than about 350,000 years. This number should be considered more as a measure of the limitation of the method rather than as adding significantly to the chronology.

Deuterium

Results of the deuterium analyses of several Great Basin water samples are shown in Table 2.

Table 2. Deuterium analyses

Water sample	Deuterium–hydrogen ratio (atoms D per 10^6 atoms H)
Mono Lake	152·8
Leevining Creek	143·5
Lake Tahoe	152·4
Lower Truckee River	147·5
Pyramid Lake	157·1

Leevining Creek drains into Mono Lake, which in turn has no apparent outlet. The higher deuterium content of the lake water may be taken to reflect the effects of evaporation on water of initial composition similar to that of Leevining Creek. The effect of a single stage of evaporation on the deuterium content of water is determined by the ratio of the vapour pressures of H_2O and HDO (for water that is dilute in deuterium). WESTON and BIGELEISEN (1952) have calculated for this ratio, employing the equation of MILES and MENZIES (1936), the value $P_{H_2O}/P_{HDO} = 1{\cdot}074$ at 25°C. From the data of Table 2 the ratio of deuterium content in Mono Lake to that in Leevining Creek is computed to be 1·065. This result is consistent with the hypothesis that Mono Lake loses water largely by evaporation. For a semiquantitative estimate of the extent of such evaporation loss we employ the following argument: Let a represent the quantity of water entering Mono Lake, b the quantity leaving the lake by evaporation, and c the quantity leaving by all other means (wind entrainment, etc.), all in equivalent periods of time. Let x, y and z represent the deuterium–hydrogen ratios in, respectively, input water, vapour and the lake water itself which has the same H/D ratio as the water lost by all means other than vaporization. Then for total mass balance

$$a = b + c \tag{1}$$

and for deuterium balance

$$xa = by + cz \tag{2}$$

Then the fraction lost by evaporation, b/a, is:

$$b/a = z - x/z - y \tag{3}$$

Substituting the values $z = 152{\cdot}8$ (observed, Mono Lake), $x = 143{\cdot}5$ (observed,

Leevining Creek) and $y = 152{\cdot}8/1{\cdot}074$ (the expected composition of vapour in equilibrium with water of observed Mono Lake concentration at 25°C), the value for the ratio b/a is found to be 0·89. Accordingly, nearly 90 per cent of Mono Lake water loss would appear to occur through evaporation.

The Truckee River constitutes the principal outlet of Lake Tahoe, and flows into Pyramid Lake, which in turn has no evident outlet other than its occasional overflow into Lake Winnemucca. The ratio of deuterium content in Pyramid Lake, relative to that in the lower Truckee, is computed from the data to be 1·0650, and analysis similar to that shown for Mono Lake indicates approximately 90 per cent water loss by evaporation in the case of this lake. For Lake Tahoe, assuming an isotopic composition for input water similar to that of Leevining Creek, analysis of the data again indicates loss by evaporation to the extent of about 90 per cent. This result is consistent with the hypothesis that the water of Lake Tahoe is subject to substantial residence time.

The fact that the lower Truckee River water has a deuterium content considerably lower than that of Lake Tahoe indicates that this river is strongly diluted by rain runoff water prior to its entry to Pyramid Lake. This is reasonable in view of the large area it drains. Assuming the Truckee River to be diluted by water of isotopic composition similar to that of Leevining Creek, an analysis similar to that employed in determining evaporation losses above leads to the conclusion that the original Lake Tahoe water has become diluted by an approximately equal quantity of runoff water by the time of its arrival at the lower reaches of the Truckee River. The approximate nature of the assumptions employed in our quantitative arguments concerning this point and the question of evaporation, above, must be stressed.

References

Broecker W. S. and Orr P. C. (1958) Radiocarbon chronology of Lake Lahontan and Lake Bonneville. *Bull. Geol. Soc. Amer.* **69,** 1009.

Broecker W. S. and Walton A. P. (1959) Re-evaluation of the salt chronology of several Great Basin Lakes. *Bull. Geol. Soc. Amer.* **70,** 601.

Davis R., Jr. and Schaeffer O. A. (1955) Chlorine-36 in nature. *Ann. N.Y. Acad. Sci.* **62,** 105.

Feth J. H. (1959) Re-evaluation of the salt chronology of several Great Basin Lakes—A discussion. *Bull. Geol. Soc. Amer.* **70,** 637.

Gilbert G. K. (1890) *Lake Bonneville.* U.S. Geological Survey Monograph, Vol. 1.

Miles F. T. and Menzies A. W. C. (1936) Vapour pressure of deuterium water from 20 to 230°C. *J. Amer. Chem. Soc.* **58,** 1068.

Nief G. and Botter R. (1959) Mass spectrometric analysis of simple hydrogen compounds. *Advances in Mass Spectrometry* (Edited by Waldron J. D.) pp. 515–525. Pergamon Press, London.

Russell I. C. (1885) *Geological History of Lake Lahontan.* U.S. Geological Survey monograph, Vol. XI.

Russell I. C. (1889) *Quaternary History of Mono Valley, California.* U.S. Geological Survey, 8th Annual Report, Pt. 1, 261.

Schaeffer O. A., Thompson S. O. and Lark N. (1960) Chlorine-36 in rain. *J. Geophys. Res.* **65,**

U.S. Geological Survey (1957) *Quality of Surface Waters of U.S., 1952,* Pt. 9–14. *Colorado River Basin to Pacific Slope Basins in Oregon and the Lower Columbia River Basin.* U.S. Geological Water-supply paper 1253, p. 225.

Weston R. E., Jr. and Bigeleisen J. (1952) Equilibrium in the exchange of hydrogen between phosphine and water. *J. Chem. Phys.* **20,** 1400.

Geochimica et Cosmochimica Acta, 1961, Vol. 25, pp. 267 to 296. Pergamon Press Ltd. Printed in Northern Ireland

Analysis of relations among Mg, Fe and Mn in certain metamorphic minerals

R. F. Mueller

(*Received* 25 *March* 1961)

Abstract—Existing data on the distribution of Mg, Fe and Mn among coexisting metamorphic actinolites, cummingtonites, Ca-pyroxenes, and orthopyroxenes, are examined in terms of theoretical solution models applicable to binary and ternary solid solutions.

Analysis indicates that the data on the distribution of the major components Mg and Fe may be satisfactorily approximated by functions derived on the assumption that actinolite, Ca-pyroxene and orthopyroxene are ideal binary solutions of their Mg and Fe end members and that cummingtonite is of the general type of regular solution, at least with respect to composition.

Although the distribution of Mg and Fe may be regarded as governed by the laws of binary solutions, thus disregarding the minor element Mn, the distribution of Mn can be explained only with reference to the ternary system. One predictable ternary effect is the increase in the atomic fraction $Mn/(Mg + Fe^{2+} + Mn)$ of cummingtonite and orthopyroxene relative to the same fraction of actinolite and Ca-pyroxene as these minerals increase in Mg relative to Fe content.

Certain observed invariant relations of the distribution functions are also interpreted in terms of the multicomponent systems.

The data are also examined with a view of detecting the elemental source of certain deviations in the atomic fractions which might be attributed to errors in the chemical analyses or to failure of a given element to attain equilibrium.

In addition, the structural–energetic basis for the thermodynamic functions is discussed in terms of the crystal structure of cummingtonite.

Introduction

One of the central problems of petrology and geochemistry is concerned with the interrelations of variables in multicomponent–multiphase systems. One facet of this larger problem involves the interactions of atoms or ions within several complex coexisting solid solutions which comprise most of the natural mineral assemblages.

This problem may be approached according to two distinct but related methods of investigation. One of these methods centres around the theory of thermodynamics and is concerned with deducing the interrelations of the temperature, pressure and composition variables, making use of the law of mass action and certain thermal and volumetric data when these are available. The second method of approach makes use of known or inferred properties of atoms and ions such as the atomic or ionic radii, polarizability, and other parameters as well as the structure of minerals as revealed by X-rays. Some of this wide variety of data is useful in elucidation of the thermodynamic properties of the mineral assemblages. This is especially true of the detailed X-ray data on the mineral structures now becoming available.

The thermodynamic approach to problems of the complex coexisting solid solutions of metamorphic mineral assemblages was extensively stressed by Ramberg (1944) and Ramberg and DeVore (1951) in several ground-breaking publications. The approach to complex silicates by way of ionic properties and crystal structure has a long history with its most extensive applications in the works of Goldschmidt (1937, 1944), Ahrens (1952), Ramberg (1952), DeVore

(1955a, b, 1957) and Ringwood (1955). The works of Neumann (1949) and Fyfe (1951) are also of interest.

The first detailed application of thermodynamic methods to multi-componental effects in coexisting complex minerals is found in the important paper by Kretz (1959) in which he demonstrated how the distribution coefficient of a given element may be influenced by the variations in the concentrations of other elements. His conclusions are of the greatest relevance to the present study.

The general scheme of treatment is as follows: since all the minerals discussed in the paper may, to a first approximation, be considered as binary solutions of their pure iron and magnesium end members, they will be treated as such in the first section which deals with the distribution of Fe and Mg. Later these same minerals will be regarded as ternary solutions of their iron, magnesium and manganese end members.

All of the data upon which this study is based are taken from the literature. Some of the observed relations and their theoretical implications were previously discussed (Mueller, 1960); however, most of the present theoretical discussion is new and represents conclusions drawn from a re-examination of the data in terms of the models of solutions and the ternary system. For information regarding the geological background of the data the reader is referred to the original papers.

The data are presented in Table 1 as atomic fractions which have been calculated from the published chemical analyses. These fractions may also be regarded as mole fractions of the corresponding end members. Some of the atomic fractions of Table 1 and the subsequent text are "partial" atomic fractions, as for examples $Mn/(Fe^{2+} + Mn)$ and $Mn/(Mg + Mn)$ as distinguished from "total" atomic fractions such as $Mn/(Mg + Fe^{2+} + Mn)$ for the same minerals. Strictly the fractions $Mg/(Mg + Fe^{2+})$ and $Fe^{2+}/(Mg + Fe^{2+})$ are also partial; however, this may usually be disregarded since the manganese content of most minerals is quite small.

Figs. 1 to 17 are graphical presentations of the data of Table 1. The figures give a good comparison of the results of different investigators. From them it is apparent that the general agreement between the diverse sources is good, considering the complexities of the minerals and variety of analysts. For example, the curve of Fig. 4, previously derived (Mueller, 1960) from the data of Howie (1955) is an equally good representation of the data of Clavan *et al.* (1954), and Norton and Clavan (1959) and a fair approximation for those of Kranck (1959). The data of Figs. 12, 13 and 14 are in equally good agreement, and those of Figs. 16 and 17, although apparently showing some grouping according to source, still show considerable uniformity.

The form of the data so presented is such that they may under certain conditions reflect the pressure and temperature of the environment at the time of crystallization. They may also, as was shown by Kretz, reflect complications in the compositional environment, as when ions other than those under consideration affect the distributions. The question of the effects of temperature and pressure, although an interesting one, must be deferred until more information becomes available. However, it seems almost certain that any temperature or pressure effects in the assemblages treated here are completely obscured by analytical errors and compositional effects.

Table 1

Reference number		1	2	3	4	5	6	7
Specimen number		B–15	DH3–172	DH9–324	DH10–169	2B	B–13	B–16
	$\frac{Mg}{Mg + Fe}$	0·197	0·332	0·270	0·259	0·115	0·217	0·169
Cummingtonite	$\frac{Mn}{Mg + Fe + Mn}$	0·0150	0·0323	0·0369	0·0210	0·0146	0·0108	0·0146
	$\frac{Mn}{Fe + Mn}$	0·0187	0·0477	0·0499	0·0282	0·0164	0·0137	0·0176
	$\frac{Mn}{Mg + Mn}$	0·0717	0·0914	0·125	0·0766	0·114	0·478	0·0808
	$\frac{Mg}{Mg + Fe}$		0·440				0·286	
Actinolite	$\frac{Mn}{Mg + Fe + Mn}$		0·0198				0·00532	
	$\frac{Mn}{Fe + Mn}$		0·0348				0·00744	
	$\frac{Mn}{Mg + Mn}$		0·0438				0·0183	
	$\frac{Mg}{Mg + Fe}$	0·261	0·425	0·334	0·304	0·114	0·313	0·222
Ca-pyroxene	$\frac{Mn}{Mg + Fe + Mn}$	0·0134	0·0292	0·0347	0·0208	0·0155	0·00785	0·0125
	$\frac{Mn}{Fe + Mn}$	0·0180	0·0498	0·0512	0·0297	0·0175	0·0114	0·0159
	$\frac{Mn}{Mg + Mn}$	0·0494	0·0663	0·0972	0·0653	0·0122	0·0247	0·0536
	$\frac{Mg}{Mg + Fe}$							
Ortho-pyroxene	$\frac{Mn}{Mg + Fe + Mn}$							
	$\frac{Mn}{Fe + Mn}$							
	$\frac{Mn}{Mg + Mn}$							

Table 1—(*contd.*)

Reference number		8	9	10	11	12	13	14
Specimen number		DH3–149	CL–1	6B	B–14	DH5–77	DH10–158	B–22
Cummingtonite	$\frac{Mg}{Mg + Fe}$	0·280	0·252	0·292	0·160	0·274	0·420	0·543
	$\frac{Mn}{Mg + Fe + Mn}$	0·0422	0·0160	0·0122	0·0143	0·0408	0·0174	0·0112
	$\frac{Mn}{Fe + Mn}$	0·0578	0·0213	0·0171	0·0170	0·0554	0·0296	0·0241
	$\frac{Mn}{Mg + Mn}$	0·136	0·0607	0·0404	0·0833	0·135	0·0404	0·0204
Actinolite	$\frac{Mg}{Mg + Fe}$						0·573	0·693
	$\frac{Mn}{Mg + Fe + Mn}$						0·00695	0·00675
	$\frac{Mn}{Fe + Mn}$						0·0161	0·0216
	$\frac{Mn}{Mg + Mn}$						0·0121	0·00971
Ca-pyroxene	$\frac{Mg}{Mg + Fe}$	0·364	0·342	0·324	0·218	0·360		
	$\frac{Mn}{Mg + Fe + Mn}$	0·0399	0·0147	0·0109	0·0132	0·0407		
	$\frac{Mn}{Fe + Mn}$	0·0614	0·0221	0·0160	0·0167	0·0623		
	$\frac{Mn}{Mg + Mn}$	0·103	0·0417	0·0327	0·0577	0·105		
Ortho-pyroxene	$\frac{Mg}{Mg + Fe}$							
	$\frac{Mn}{Mg + Fe + Mn}$							
	$\frac{Mn}{Fe + Mn}$							
	$\frac{Mn}{Mg + Mn}$							

Table 1—(*contd.*)

Reference number		15	16	17	18	19	20	21
Specimen number		B–20	DH7–445	12BA	10G	DH13-607	35–5	35–6
Cummingtonite	$\frac{Mg}{Mg+Fe}$				0·770			
	$\frac{Mn}{Mg+Fe+Mn}$				0·0150			
	$\frac{Mn}{Fe+Mn}$				0·0620			
	$\frac{Mn}{Mg+Mn}$				0·0194			
Actinolite	$\frac{Mg}{Mg+Fe}$	0·608	0·653	0·521	0·871	0·862		
	$\frac{Mn}{Mg+Fe+Mn}$	0·00638	0·0172	0·00774	0·00558	0·0111		
	$\frac{Mn}{Fe+Mn}$	0·0161	0·0481	0·0161	0·0418	0·0750		
	$\frac{Mn}{Mg+Mn}$	0·0105	0·0262	0·0148	0·00641	0·0128		
Ca-pyroxene	$\frac{Mg}{Mg+Fe}$	0·581	0·650	0·485		0·841	0·722	0·706
	$\frac{Mn}{Mg+Fe+Mn}$	0·00934	0·0237	0·0106		0·0164	0·0108	0·0142
	$\frac{Mn}{Fe+Mn}$	0·0220	0·0650	0·0204		0·0951	0·0379	0·0467
	$\frac{Mn}{Mg+Mn}$	0·0160	0·0361	0·0216		0·0195	0·0150	0·0200
Ortho-pyroxene	$\frac{Mg}{Mg+Fe}$						0·585	0·572
	$\frac{Mn}{Mg+Fe+Mn}$						0·0122	0·0156
	$\frac{Mn}{Fe+Mn}$						0·0289	0·0357
	$\frac{Mn}{Mg+Mn}$						0·0207	0·0270

Table 1—(*contd.*)

Reference number		22	23	24	25	26	27	28
Specimen number		35–8	35–9	35–13	35–19	35–32	B1–3	B1–6
Cummingtonite	$\frac{Mg}{Mg + Fe}$							
	$\frac{Mn}{Mg + Fe + Mn}$							
	$\frac{Mn}{Fe + Mn}$							
	$\frac{Mn}{Mg + Mn}$							
Actinolite	$\frac{Mg}{Mg + Fe}$							
	$\frac{Mn}{Mg + Fe + Mn}$							
	$\frac{Mn}{Fe + Mn}$							
	$\frac{Mn}{Mg + Mn}$							
Ca-pyroxene	$\frac{Mg}{Mg + Fe}$	0·746	0·771	0·696	0·817	0·826	0·529	0·445
	$\frac{Mn}{Mg + Fe + Mn}$	0·0108	0·00736	0·00612	0·00592	0·00539	0·00561	0·0184
	$\frac{Mn}{Fe + Mn}$	0·0411	0·0324	0·0198	0·0315	0·0301	0·0118	0·0326
	$\frac{Mn}{Mg + Mn}$	0·0144	0·00988	0·00878	0·00724	0·00653	0·0106	0·0403
Ortho-pyroxene	$\frac{Mg}{Mg + Fe}$	0·610	0·632	0·561	0·704	0·727	0·423	0·305
	$\frac{Mn}{Mg + Fe + Mn}$	0·0121	0·00936	0·00668	0·00686	0·00655	0·00676	0·0215
	$\frac{Mn}{Fe + Mn}$	0·0305	0·0251	0·0151	0·0228	0·0236	0·0117	0·0307
	$\frac{Mn}{Mg + Mn}$	0·0197	0·0147	0·0119	0·00971	0·00900	0·0158	0·0674

Table 1—(*contd.*)

Reference number		29	30	31	32	33	34	35
Specimen number		B1–21	B–9	H–3	H–4	H–9	B–18	A–12
	$\frac{Mg}{Mg + Fe}$		0·382	0·432		0·288	0·342	
Cummingtonite	$\frac{Mn}{Mg + Fe + Mn}$		0·00501	0·0897		0·0250	0·00489	
	$\frac{Mn}{Fe + Mn}$		0·00809	0·148		0·0347	0·00742	
	$\frac{Mn}{Mg + Mn}$		0·0130	0·186		0·0817	0·0142	
	$\frac{Mg}{Mg + Fe}$							
	$\frac{Mn}{Mg + Fe + Mn}$							
Actinolite	$\frac{Mn}{Fe + Mn}$							
	$\frac{Mn}{Mg + Mn}$							
	$\frac{Mg}{Mg + Fe}$	0·441	0·464	0·540	0·350	0·377	0·458	0·888
Ca-pyroxene	$\frac{Mn}{Mg + Fe + Mn}$	0·00195	0·0112	0·0805	0·00854	0·0239	0·00479	0·00330
	$\frac{Mn}{Fe + Mn}$	0·00349	0·0107	0·160	0·0131	0·0378	0·00879	0·0285
	$\frac{Mn}{Mg + Mn}$	0·00441	0·0238	0·139	0·0241	0·0608	0·0104	0·00371
	$\frac{Mg}{Mg + Fe}$	0·327			0·228	0·258		0·778
	$\frac{Mn}{Mg + Fe + Mn}$	0·00265			0·00997	0·0303		0·00376
Ortho-pyroxene	$\frac{Mn}{Fe + Mn}$	0·00393			0·0129	0·0404		0·0167
	$\frac{Mn}{Mg + Mn}$	0·00806			0·0424	0·108		0·00484

Atomic fractions of coexisting minerals. Reference numbers 1–19 refer to data taken from MUELLER (1960). Reference numbers 20–26 refer to data taken from CLAVAN *et al.* (1954) and NORTON and CLAVAN (1959). Reference numbers 27–35 refer to data taken from KRANCK (1959).

Relations among Coexisting Binary Solutions involving Mg and Fe^{2+}

Approximate binary solutions in quaternary systems

Although the mineral solutions may be considered to be essentially binary it is desirable to stress that the system of several coexisting mineral phases consists of the four components $CaSiO_3$, $MgSiO_3$, $FeSiO_3$, and SiO_3H_2. These components are sufficient to represent element distribution equilibria between the minerals actinolite, cummingtonite, orthopyroxene, and Ca-pyroxene when Mn is disregarded. However, they are not adequate to represent equilibria involving such mineral phases as quartz, calcite, etc., which would require additional components such as SiO_2, CO_2 and H_2O. The latter type of equilibria are not discussed here.

In the theoretical treatment of multicomponent mineral equilibria it is advantageous to make use of the concept of absolute activities (Guggenheim, 1950), since this concept makes possible a convenient separation of variables. The expression for the absolute activity of the component; in terms of temperature pressure and composition variables is as follows:

$$\lambda_i = \lambda_i^0 X_i f_i$$

where

$$\mu_i = RT \ln \lambda_i$$

Here λ_i is the absolute activity of the component i in a solution of any number of components and μ_i is the corresponding chemical potential. In low pressure chemistry of solids λ_i^0 is usually regarded as a function of the temperature only. However, because of the high pressures of the geologic environment this quantity must here be considered as a function of the pressure as well. The quantity f_i is the activity coefficient of the component i and is in general a function of the temperature, pressure, and composition, whereas X_i is the concentration of the component i expressed as its mole fraction in the solution. In treating mineral solid solutions the components are the end members of the solid solution series. For example, cummingtonite is a solid solution of the end members $\frac{1}{7}Mg_7Si_8O_{22}(OH)_2$ (kupfferite) and $\frac{1}{7}Fe_7Si_8O_{22}(OH)_2$ (grunerite). As may be seen from the mineral formulae the mole fraction in the binary solution is also equal to the atomic fraction $Mg/(Mg + Fe^{2+})$. The pure end members are the standard states to which the λ^0's refer. These λ^0's are then combined to form equilibrium constants which are then of course solely functions of the temperature and pressure.

In order to apply these concepts to the distribution of Mg and Fe, the pertinent ion exchange reactions are written as follows:

hedenbergite tremolite

$$CaFeSi_2O_6 + \tfrac{1}{5}Ca_2Mg_5Si_8O_{22}(OH)_2 \rightarrow$$

diopside ferroactinolite

$$CaMgSi_2O_6 + \tfrac{1}{5}Ca_2Fe_5Si_8O_{22}(OH)_2 \qquad (a)$$

ferroactinolite kupfferite

$$\tfrac{1}{5}Ca_2Fe_5Si_8O_{22}(OH)_2 + \tfrac{1}{7}Mg_7Si_8O_{88}(OH)_2 \rightarrow$$

tremolite grunerite

$$\tfrac{1}{5}Ca_2Mg_5Si_8O_{22}(OH)_2 + \tfrac{1}{7}Fe_7Si_8O_{22}(OH)_2 \qquad (b)$$

hedenbergite + kupfferite → diopside + grunerite

$$CaFeSi_2O_6 + \tfrac{1}{7}Mg_7Si_8O_{22}(OH)_2 \rightarrow CaMgSi_2O_6 + \tfrac{1}{7}Fe_7Si_8O_{22}(OH)_2 \qquad (c)$$

hedenbergite + enstatite → diopside + ferrosilite

$$CaFeSi_2O_6 + MgSiO_3 \rightarrow CaMgSi_2O_6 + FeSiO_3 \qquad (d)$$

ferrosilite + kupfferite → enstatite + grunerite

$$FeSiO_3 + \tfrac{1}{7}Mg_7Si_8O_{22}(OH)_2 \rightarrow MgSiO_3 + \tfrac{1}{7}Fe_7Si_8O_{22}(OH)_2 \qquad (e)$$

Here each reaction is written in terms of 1 mole of Mg and 1 mole of Fe. This is desirable because the solid solutions are formed by mixing of individual ions.

The following designations for atomic fractions will be used:

$$X_{\text{ca-px}} = \text{Mg}/(\text{Mg} + \text{Fe}^{2+}) \text{ in Ca-pyroxene}$$
$$X_{\text{or-px}} = \text{Mg}/(\text{Mg} + \text{Fe}^{2+}) \text{ in orthopyroxene}$$
$$X_{\text{act}} = \text{Mg}/(\text{Mg} + \text{Fe}^{2+}) \text{ in actinolite}$$
$$X_{\text{cum}} = \text{Mg}/(\text{Mg} + \text{Fe}^{2+}) \text{ in cummingtonite}$$

The activity coefficients corresponding to these mole fractions are identified by subscripts which refer to the mineral and superscripts which refer to the end member, as for example $f^{\text{Fe}}_{\text{Ca-px}}$ refers to the component $CaFeSi_2O_6$ in Ca-pyroxene.

In interpreting the data of the Quebec iron formation it is necessary to identify the fraction Mg/(Mg + Fe) where Fe represents total iron, with the fraction Mg/(Mg + Fe^{2+}) which refers only to divalent iron. However, the difference is not great since the preponderance of iron in all the minerals is in the ferrous state.

For conditions of constant and uniform temperature and pressure throughout the region in which the minerals crystallized, it is possible to write expressions for equilibrium constants corresponding to reactions (a), (b), (c), (d), and (e).

$$K_a = \frac{(1 - X_{\text{act}})X_{\text{Ca-px}} f^{\text{Fe}}_{\text{act}} f^{\text{Mg}}_{\text{Ca-px}}}{(1 - X_{\text{Ca-px}})X_{\text{act}} f^{\text{Fe}}_{\text{Ca-px}} f^{\text{Mg}}_{\text{act}}} \qquad (1)$$

$$K_b = \frac{(1 - X_{\text{cum}})X_{\text{act}} f^{\text{Fe}}_{\text{cum}} f^{\text{Mg}}_{\text{act}}}{(1 - X_{\text{act}})X_{\text{cum}} f^{\text{Fe}}_{\text{act}} f^{\text{Mg}}_{\text{cum}}} \qquad (2)$$

$$K_c = \frac{(1 - X_{\text{cum}})X_{\text{Ca-px}} f^{\text{Fe}}_{\text{cum}} f^{\text{Mg}}_{\text{Ca-px}}}{(1 - X_{\text{Ca-px}})X_{\text{cum}} f^{\text{Fe}}_{\text{Ca-px}} f^{\text{Mg}}_{\text{cum}}} \qquad (3)$$

$$K_d = \frac{(1 - X_{\text{or-px}})X_{\text{Ca-px}} f^{\text{Fe}}_{\text{or-px}} f^{\text{Mg}}_{\text{Ca-px}}}{(1 - X_{\text{Ca-px}})X_{\text{or-px}} f^{\text{Fe}}_{\text{Ca-px}} f^{\text{Mg}}_{\text{or-px}}} \qquad (4)$$

$$K_e = \frac{(1 - X_{\text{cum}})X_{\text{or-px}} f^{\text{Fe}}_{\text{cum}} f^{\text{Mg}}_{\text{or-px}}}{(1 - X_{\text{or-px}})X_{\text{cum}} f^{\text{Fe}}_{\text{or-px}} f^{\text{Mg}}_{\text{cum}}} \qquad (5)$$

where $K_a = \exp(-\Delta G_a^0/RT)$, $K_b = \exp(-\Delta G_b^0/RT)$, $K_c = \exp(-\Delta G_c^0/RT)$, $K_d = \exp(-\Delta G_d^0/RT)$, and $K_e = \exp(-\Delta G_e^0/RT)$. The ΔG^0's are the Gibbs free

energies of the ion exchange reactions between the pure end members at the temperature and pressure of crystallization and correspond to combinations of the λ^0's of the same end members.

Each of the equations (1) through (5) gives a solution for the atomic fraction of one mineral in terms of the corresponding atomic fraction of another mineral provided that expressions for the activity coefficients can be found.

In attempting to solve this problem it is necessary to refer to the observed

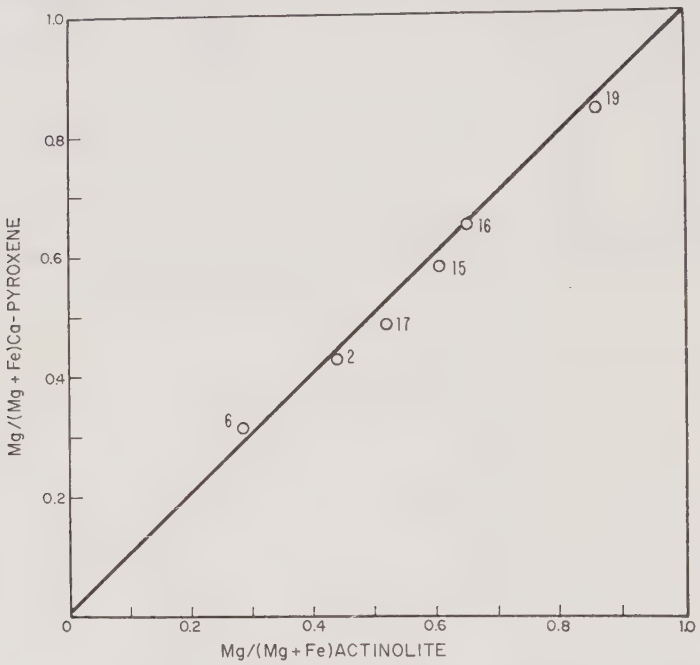

Fig. 1. Relation between the atomic fractions of magnesium in coexisting Ca-pyroxenes and actinolites. The curve is arbitrarily drawn at 45°.

values of the distributions as given by Table 1 and Figs. 1 to 5. In Fig. 1, a line has been arbitrarily drawn at 45°, and this seems to approximate the data fairly well. This corresponds to a solution $X_{\text{Ca-px}} = X_{\text{act}}$, which implies that

$$K_a = \frac{f_{\text{act}}^{\text{Fe}} f_{\text{Ca-px}}^{\text{Mg}}}{f_{\text{act}}^{\text{Mg}} f_{\text{Ca-px}}^{\text{Fe}}} \tag{6}$$

To get some idea of the values of these activity coefficients it is necessary to refer to equation (4) and the corresponding curve plotted in Fig. 4. This curve is a solution to the equation

$$\frac{(1 - X_{\text{or-px}}) X_{\text{Ca-px}}}{(1 - X_{\text{Ca-px}}) X_{\text{or-px}}} = K \tag{7}$$

where K is a constant. Reference to equation (4) shows that this also implies that

$$\frac{f_{\text{or-px}}^{\text{Fe}} f_{\text{Ca-px}}^{\text{Mg}}}{f_{\text{Ca-px}}^{\text{Fe}} f_{\text{or-px}}^{\text{Mg}}} = K' \tag{8}$$

where K' is another constant. Consequently $KK' = K_a$.

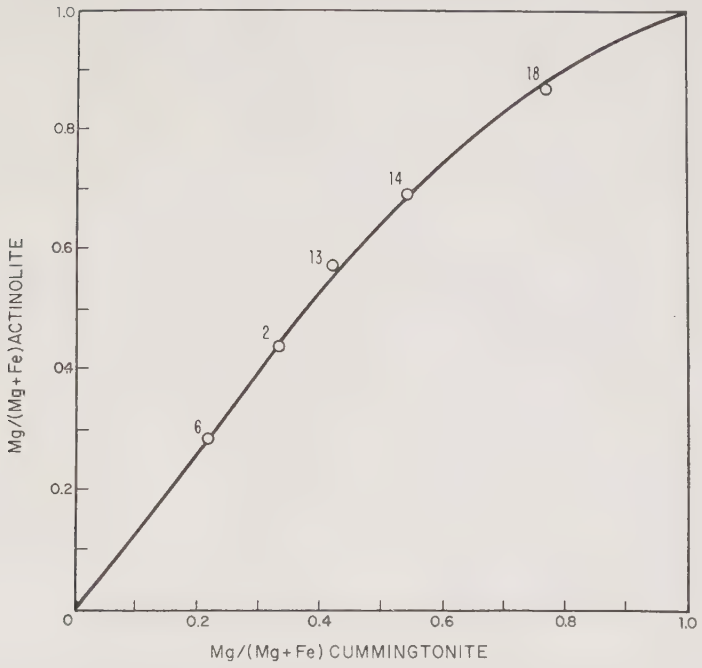

Fig. 2. Relation between the atomic fractions of magnesium in coexisting cummingtonites and actinolites. The curve is based on the theoretical regular solution model.

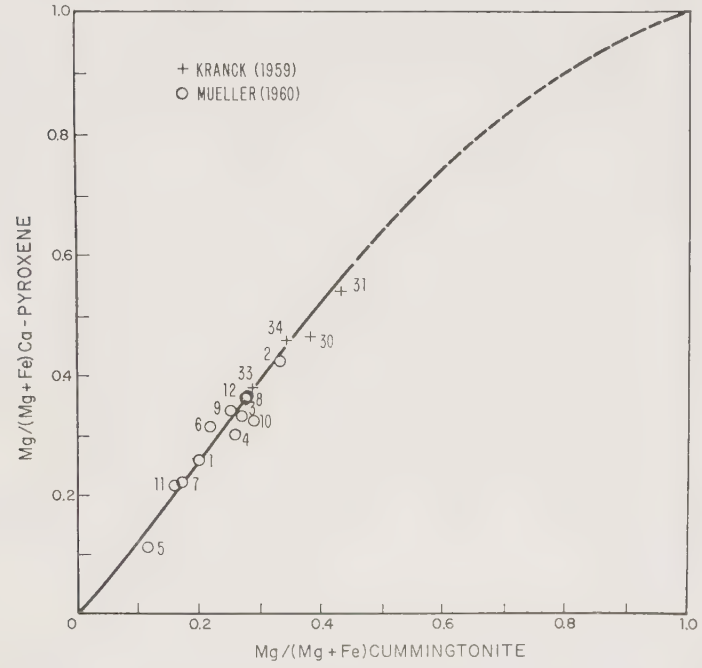

Fig. 3. Relation between the atomic fractions of magnesium in coexisting cummingtonites and Ca-pyroxenes. The curve is identical to that of Fig. 2. The data of KRANCK are based on Fe^{2+}. The data of MUELLER are based on total Fe.

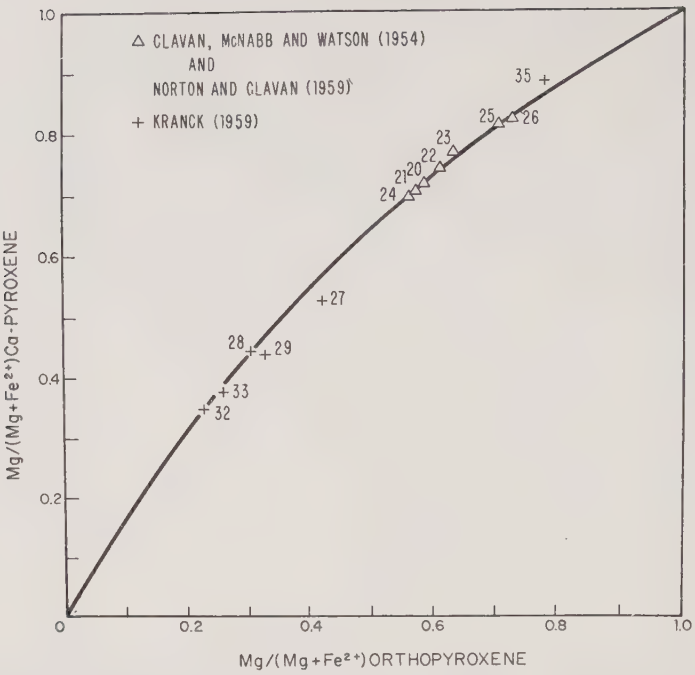

Fig. 4. Relation between the atomic fraction of magnesium in coexisting orthopyroxenes and Ca-pyroxenes. The curve is based on the theoretical ideal solution model for both minerals.

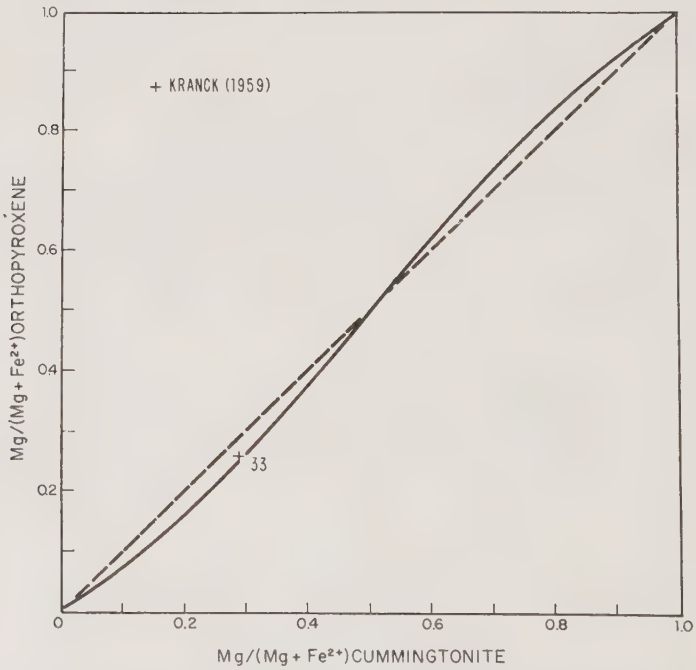

Fig. 5. Relation between the atomic fraction of magnesium in coexisting cummingtonites and orthopyroxenes. The solid curve is based on the theoretical regular solution model. The dashed curve shows the equal distribution for comparison.

Although the activity coefficients of (6) and (8) are indeterminate, those of any binary solution are related to each other by a corollary to the Gibbs–Duhem relation. Thus, for example at constant T and P

$$(1 - X_{\text{Ca-px}}) \frac{\partial \ln f^{\text{Fe}}_{\text{Ca-px}}}{\partial X_{\text{Ca-px}}} + X_{\text{Ca-px}} \frac{\partial \ln f^{\text{Mg}}_{\text{Ca-px}}}{\partial X_{\text{Ca-px}}} = 0 \qquad (9)$$

and similarly for the other mineral phases considered to be binary solutions.

From the nature of activity coefficients it seems highly unlikely that (8) could hold under any condition other than that in which all its activity coefficients are equal to 1. This may be seen by considering ratios such as $f^{\text{Mg}}_{\text{Ca-px}}/f^{\text{Fe}}_{\text{Ca-px}}$ in relation to (9). For if $f^{\text{Mg}}_{\text{Ca-px}}$ decreases, $f^{\text{Fe}}_{\text{Ca-px}}$ must increase for the same change in $X_{\text{Ca-px}}$. Only the very improbable identical changes in the ratio $f^{\text{Mg}}_{\text{or-px}}/f^{\text{Fe}}_{\text{or-px}}$ could compensate this to keep K' a constant. The simplest alternative to these improbable compensations is that both Ca-pyroxene and orthopyroxene are essentially ideal solutions, making all the activity coefficients equal to 1. This is also in agreement with the work of Sahama and Torgeson (1949) on the orthopyroxene solid solutions. If the conclusion as to the ideality of Ca-pyroxene is admitted, it follows from the same reasoning and relation (6) that actinolite is also essentially ideal, making its activity coefficients equal to one.

The fact that Mg and Fe are equally distributed among actinolite and Ca-pyroxene indicates that these minerals have equal standard affinities for these elements.

Turning now to Fig 2, it is seen that X_{act} appears to be a somewhat more complex function of X_{cum} than of $X_{\text{Ca-px}}$. Since actinolite is inferred to be an essentially ideal solution this complexity can only be attributed to cummingtonite. In attempting to account for the shape of the curve of Fig. 2, it seems reasonable to consider a solution model of cummingtonite which is next in degree of complexity to the ideal solution. In one such model the activity coefficient of each component has an exponential form in which the exponent of e is the product of the square of the mole fraction of the other component and a temperature–pressure coefficient. The best known solution model of this type is the regular solution defined by Hildebrand (1929). Assuming that cummingtonite is a solution of this general type, the activity coefficients of its end members become

$$f^{\text{Mg}}_{\text{cum}} = \exp \alpha(1 - X_{\text{cum}})^2 \quad \text{and} \quad f^{\text{Fe}}_{\text{cum}} = \exp \alpha X^2_{\text{cum}}$$

If the solution is strictly regular $\alpha = W/RT$ and $W(1 - X_{\text{cum}})^2$ and WX^2_{cum} become the partial molar heats of solution of the end members, where W is a constant independent of temperature.

Using these expressions for the activity coefficients equation (2) becomes

$$K_b = \frac{(1 - X_{\text{cum}}) X_{\text{act}} \exp \alpha(2X_{\text{cum}} - 1)}{(1 - X_{\text{act}}) X_{\text{cum}}} \qquad (10)$$

The curve plotted in Fig. 2 is a solution to this equation with $K_b = 1{\cdot}80$ and $\alpha = -0{\cdot}40$, and it apparently approximates the data quite well. Also, since the exponential factor in (10) is near unity over most of the range, the departure from ideality is not great. If cummingtonite were an ideal solution, the curve of Fig. 2 would resemble that of Fig. 4 and obey a function of the form of equation (7).

Although α appears to be essentially constant with respect to changes in composition, it is impossible from the data at hand to determine whether or not it is an inverse function of the temperature as required for strictly regular solutions. Thus, it is possible that cummingtonite is an essentially regular solution with respect to composition but not with respect to temperature. The liquid solutions of thallium and tin studied by Hildebrand and Sharma (1929) are of the latter type.

Once solutions for equations (1) and (2) are obtained, it follows that a solution for equation (3) is also possible since the latter contains no new quantities. If the relation $X_{\text{act}} = X_{\text{Ca-px}}$ holds, $K_b = K_c$. Of course, this conclusion also depends on the essential invariance of the distribution functions with respect to the presence or absence of other phases in the assemblage. For example, it is assumed that the distribution of Mg and Fe among actinolite and Ca-pyroxene is independent of the presence of cummingtonite or any other phase.* That this situation is closely approximated is indicated by Fig. 3 which shows the observed distribution with the curve of Fig. 2 superimposed.

As was previously concluded the curve of Fig. 4 shows the relation

$$K_d = \frac{(1 - X_{\text{or-px}})X_{\text{Ca-px}}}{(1 - X_{\text{Ca-px}})X_{\text{or-px}}} \tag{11}$$

This curve, based originally on the data of Howie (1955), is a reasonable approximation of most of the data. The curve shown in Fig. 4 gives $K_d = 1.82$.

It is interesting that this curve bears considerable resemblance to those of Figs. 2 and 3, K_b, K_c and K_d being nearly identical. The only difference is the slight asymmetry of the curves of Figs. 2 and 3 due to the non-ideality of cummingtonite. Since the equilibrium constants contain as exponents the Gibbs free energies of the ion exchange reactions, the implication is that, relative to Ca-pyroxene, orthopyroxene has about the same standard affinity for Mg and Fe as has cummingtonite, except that there is a slight excess of free energy of solution which favours the solution of the Mg component in Fe-rich cummingtonite, and the Fe component in Mg-rich cummingtonites, as indicated by the symmetrical type of activity coefficient used to fit the data.

The curve of Fig. 5 expresses the following relation based on equation (5):

$$K_e = \frac{(1 - X_{\text{cum}})X_{\text{or-px}} \exp \alpha(2X_{\text{cum}} - 1)}{(1 - X_{\text{or-px}})X_{\text{cum}}} \tag{12}$$

The constant α here also has the value $-0{\cdot}40$ since it refers to cummingtonite.

* For tabulations of coexisting phases, the original papers should be consulted.

The equilibrium constant K_e has the value 0·989 as a consequence of the derivation of (12) from (10) and (11). Since there is only one example of coexisting orthopyroxene and cummingtonite tabulated (pair 33) and since this pair also falls close to the curves of Figs. 3 and 4, it of necessity falls close to the curve of Fig. 5. The dashed line of Fig. 5 is the 45° (equal distribution) line presented for comparison.

Explanation of certain invariant relations of the distribution of Mg *and* Fe *among* Ca*-pyroxene and orthopyroxene*

Examination of Fig. 4 shows that the distribution points in the range Mg/(Mg + Fe^{2+}) = 0·5 to 0·8 are remarkable in their conformity to the curve although they and the data from which the curve was derived (Howie, 1955) represent widely different rock types, especially with respect to mineral compositions. For example, a comparison of the mineral analyses presented by the various investigators shows that orthopyroxenes and clinopyroxenes of the charnockites of Madras, India are markedly higher in Al_2O_3 than those from the iron formation and the gneisses of the Pennsylvania and Delaware Piedmont. Also TiO_2 is high in the charnockite minerals and Na_2O and K_2O are highly variable. How then can the distributed constant of Fe and Mg fail to reflect these variations, especially insomuch as Kretz (1959) has demonstrated that the effect may be very large in some minerals?

One explanation suggested by the forms of the distribution functions is as follows: If a mineral solid solution such as Ca(Mg, Fe)Si_2O_6 contains an additional component, as for example, jadeite ($NaAlSi_2O_6$), the concentration of the diopside and hedenbergite components will be reduced. However, it is significant that their concentrations will be reduced in the same proportion. Thus, $X^{Mg}_{Ca\text{-}px}/X^{Fe}_{Ca\text{-}px}$ is invariant. If in addition all constituents $CaMgSi_2O_6$, $CaFeSi_2O_6$ and $NaAlSi_2O_6$ mix in an ideal way, equation (11) remains unchanged. Under these circumstances the partial atomic fractions $X^{Mg}_{Ca\text{-}px}$ and $X^{Fe}_{Ca\text{-}px}$ give uniform plots regardless of the presence of other components. This property will be utilized later when manganese is considered.

If $NaAlSi_2O_6$ or any other component does not form an ideal solution with Ca(Mg, Fe)Si_2O_6, the activity coefficients appearing in equation (4) will not be equal to unity and this will change the shape of the distribution curve in the general case. However, it is still possible that the activity coefficients of numerator and denominator might be equally affected since the affecting constituent is the same in each mineral. This is all the more probable in this case since an affecting constituent such as $NaAlSi_2O_6$ would be expected to behave similarly toward both of the constituents $CaMgSi_2O_6$ and $CaFeSi_2O_6$ since these have been inferred to form ideal solutions with each other.

Coexisting Ternary Solutions Involving Mg, Fe and Mn

Actinolite and Ca-Pyroxene

The distribution of manganese among actinolite and Ca-pyroxene is shown as a function of the total mole fractions of the end members in Fig. 6. Following the

method of the previous treatment, the equilibrium may be expressed in terms of reactions between end members:

$$\begin{matrix}\text{hedenbergite} & \text{manganactinolite} \\ CaFeSi_2O_6 + \tfrac{1}{5}Ca_2Mn_5Si_8O_{22}(OH)_2 \rightarrow \\ \text{Johannsenite} & \text{ferroactinolite} \\ CaMnSi_2O_6 + \tfrac{1}{5}Ca_2Fe_5Si_8O_{22}(OH)_2\end{matrix} \qquad (f)$$

$$\begin{matrix}\text{diopside} & \text{manganactinolite} \\ CaMgSi_2O_6 + \tfrac{1}{5}Ca_2Mn_5Si_8O_{22}(OH)_2 \rightarrow \\ \text{Johannsenite} & \text{tremolite} \\ CaMnSi_2O_6 + \tfrac{1}{5}Ca_2Mg_5Si_8O_{22}(OH)_2\end{matrix} \qquad (g)$$

Corresponding to these reactions are the equilibrium equations

$$K_f = \frac{X^{Mn}_{Ca\text{-}px}\, X^{Fe}_{act}\, f^{Mn}_{Ca\text{-}px}}{X^{Mn}_{act}\, X^{Fe}_{Ca\text{-}px}\, f^{Mn}_{act}} \qquad (13)$$

and

$$K_g = \frac{X^{Mn}_{Ca\text{-}px}\, X^{Mg}_{act}\, f^{Mn}_{Ca\text{-}px}}{X^{Mn}_{act}\, X^{Mg}_{Ca\text{-}px}\, f^{Mn}_{act}} \qquad (14)$$

where the following definitions apply:

$$\begin{aligned} X^{Mn}_{Ca\text{-}px} &= Mn/(Mg + Fe^{2+} + Mn) \text{ in Ca-pyroxene} \\ X^{Fe}_{Ca\text{-}px} &= Fe^{2+}/(Mg + Fe^{2+} + Mn) \text{ in Ca-pyroxene} \\ X^{Mg}_{Ca\text{-}px} &= Mg/(Mg + Fe^{2+} + Mn) \text{ in Ca-pyroxene} \\ X^{Mn}_{act} &= Mn/(Mg + Fe^{2+} + Mn) \text{ in actinolite} \\ X^{Fe}_{act} &= Fe^{2+}/(Mg + Fe^{2+} + Mn) \text{ in actinolite} \\ X^{Mg}_{act} &= Mg/(Mg + Fe^{2+} + Mn) \text{ in actinolite} \end{aligned}$$

The activity coefficients f^{Fe}_{act}, f^{Mg}_{act}, $f^{Fe}_{Ca\text{-}px}$ and $f^{Mg}_{Ca\text{-}px}$ have not been written in expressions (13) and (14) because they are regarded as equal to unity as was deduced in the last section.

Reactions (f), (g) and (a) form a natural triad as do the corresponding equations of equilibrium (13), (14) and (1). These reactions and equations link the two ternary solid solutions in the systems composed of the components $CaSiO_3$, $MgSiO_3$, $FeSiO_3$, $MnSiO_3$ and SiO_3H_2.

A simplification of some utility may be introduced into equations (13) and (14) by regarding the activity coefficients of the manganese components as constant. That these activity coefficients should in fact approach constants for low concentrations of manganese may be seen by considering the solution properties of actinolite and Ca-pyroxene. Since these minerals seem to be ideal solutions with respect to Mg and Fe^{2+} the interactions (heats of solution) of the Mn component and the Fe component should be very similar to the interactions of the Mn component and the Mg component, whereas the Fe and Mg components show no interactions. This should result in functional relations of the type

$$f^{Mn}_{act} = f\,(X^{Mg}_{act} + X^{Fe}_{act})$$

and

$$f^{Mn}_{Ca\text{-}px} = f\,(X^{Mg}_{Ca\text{-}px} + X^{Fe}_{Ca\text{-}px}),$$

in which the sum of the atomic fractions of the magnesium and iron end members enter into the activity coefficients. This is well illustrated by the ternary regular solution model (PRIGOGINE and DEFAY, 1951). Since the sums $(X^{Mg}_{act} + X^{Fe}_{act})$ and $(X^{Mg}_{Ca\text{-}px} + X^{Fe}_{Ca\text{-}px})$ are essentially constant for all low concentrations of Mn, the activity coefficients should also be constant for this range.

Thus equations (13) and (14) may be rearranged as

$$K_f' = \frac{X^{Mn}_{Ca\text{-}px}\, X^{Fe}_{act}}{X^{Mn}_{act}\, X^{Fe}_{Ca\text{-}px}} \tag{15}$$

and

$$K_g' = \frac{X^{Mn}_{Ca\text{-}px}\, X^{Mg}_{act}}{X^{Mn}_{act}\, X^{Mg}_{Ca\text{-}px}} \tag{16}$$

where $K_f' = K_f \dfrac{f^{Mn}_{act}}{f^{Mn}_{Ca\text{-}px}}$ and $K_g' = K_g \dfrac{f^{Mn}_{act}}{f^{Mn}_{Ca\text{-}px}}$

Also $K_a = K_f'/K_g' = 1$; consequently $K_f' = K_g'$ and $K_f = K_g$. Thus the ratio $X^{Mn}_{Ca\text{-}px}/X^{Mn}_{act}$ is invariant with respect to variations in X^{Fe}_{act}, $X^{Fe}_{Ca\text{-}px}$, X^{Mg}_{act} and $X^{Mg}_{Ca\text{-}px}$. From Fig. 6 it is seen that $K_f' \approx K_g' \approx 1{\cdot}42$.

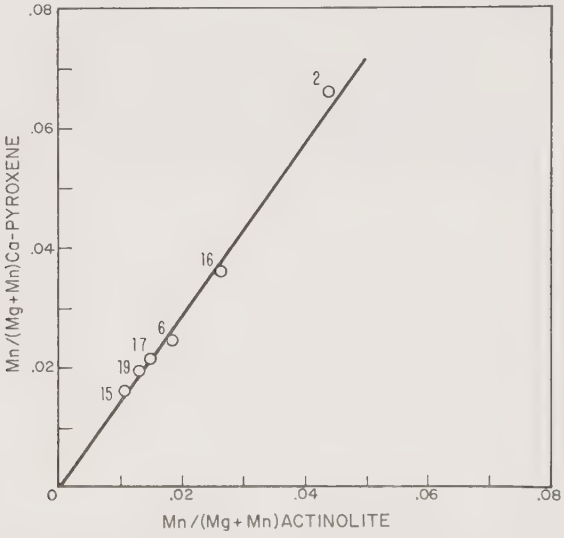

Fig. 6. Relation between the total atomic fraction of manganese in coexisting actinolites and Ca-pyroxenes.

Figs. 7 and 8 show the data of Fig 6 plotted in terms of the partial atomic or mole fractions. The pertinent partial atomic fractions are defined as follows:

$$Y_{act} = \text{Mn}/(\text{Fe}^{2+} + \text{Mn}) \text{ in actinolite}$$

$$Y_{Ca\text{-}px} = \text{Mn}/(\text{Fe}^{2+} + \text{Mn}) \text{ in Ca-pyroxene}$$

$$Z_{act} = \text{Mn}/(\text{Mg} + \text{Mn}) \text{ in actinolite}$$

$$Z_{Ca\text{-}px} = \text{Mn}/(\text{Mg} + \text{Mn}) \text{ in Ca-pyroxene}$$

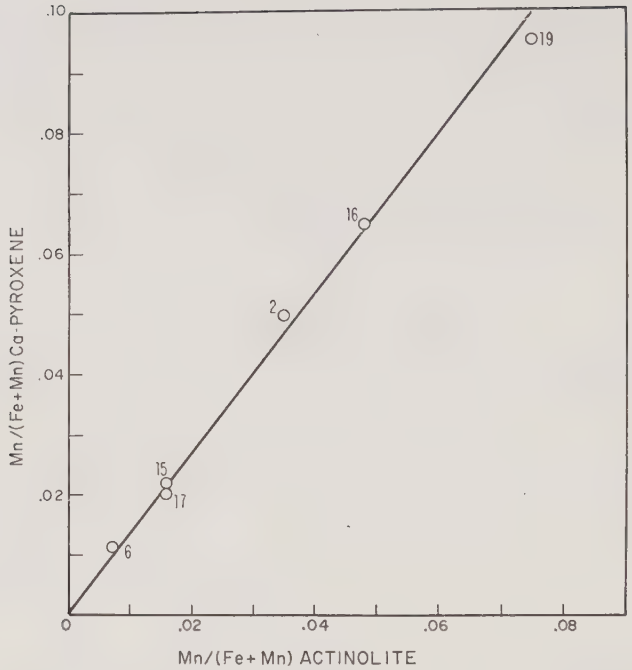

Fig. 7. Relation between the partial atomic fraction of manganese in coexisting actonilites and Ca-pyroxenes.

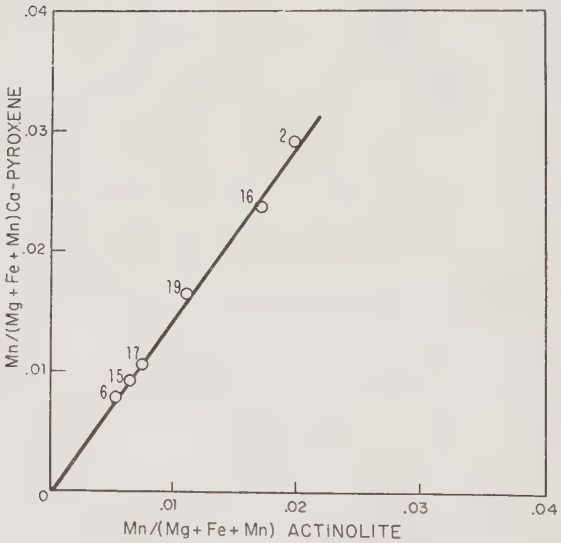

Fig. 8. Relation between the partial atomic fractions of manganese in coexisting actinolites and Ca-pyroxenes.

Using this notation equations (15) and (16) may be written as follows:

$$K_f' = \frac{Y_{\text{Ca-px}}(1 - Y_{\text{act}})}{Y_{\text{act}}(1 - Y_{\text{Ca-px}})} \tag{17}$$

and

$$K_g' = \frac{Z_{\text{Ca-px}}(1 - Z_{\text{act}})}{Z_{\text{act}}(1 - Z_{\text{Ca-px}})} \tag{18}$$

It is evident from the equality of K_f' and K_g' that (17) and (18) are identical functions. This similarity should prevent all scatter due to changes of Mg and Fe in Fig. 6.

It should be noted that here again, as in the case of the distribution of Fe and Mg among Ca-pyroxene and orthopyroxene, the equilibrium constants may be written in terms of the partial atomic fraction since the only effect of the third component is one of dilution and this dilution affects equally the numerator and the denominator of the expression for the equilibrium constant.

Actinolite and cummingtonite

Although the ion exchange equilibrium between actinolite and Ca-pyroxene represents a relatively simple case, the equilibrium between actinolite and cummingtonite is considerably more complicated. Part of this complication is due to the fact that iron and magnesium are not equally distributed among the two minerals, and this difficulty would be present even if both minerals were ideal solutions. However, the non-ideality of cummingtonite greatly increases the complexity.

The pertinent reactions in addition to reaction (b) are as follows:

manganactinolite grunerite

$$\tfrac{1}{5}Ca_2Mn_5Si_8O_{22}(OH)_2 + \tfrac{1}{7}Fe_7Si_8O_{22}(OH)_2 \rightarrow$$

ferroactinolite mangancummingtonite

$$\tfrac{1}{5}Ca_2Fe_5Si_8O_{22}(OH)_2 + \tfrac{1}{7}Mn_7Si_8O_{22}(OH)_2 \tag{h}$$

manganactinolite kupfferite

$$\tfrac{1}{5}Ca_2Mn_5Si_8O_{22}(OH)_2 + \tfrac{1}{7}Mg_7Si_8O_{22}(OH)_2 \rightarrow$$

tremolite mangancummingtonite

$$\tfrac{1}{5}Ca_2Mg_5Si_8O_{22}(OH)_2 + \tfrac{1}{7}Mn_7Si_8O_{22}(OH)_2 \tag{i}$$

The corresponding equations of equilibrium are

$$K_h = \frac{X_{\text{act}}^{\text{Fe}} X_{\text{cum}}^{\text{Mn}} f_{\text{cum}}^{\text{Mn}}}{X_{\text{act}}^{\text{Mn}} X_{\text{cum}}^{\text{Fe}} f_{\text{act}}^{\text{Mn}}} \cdot \exp 0{\cdot}40\ (X_{\text{cum}}^{\text{Mg}})^2 \tag{19}$$

and

$$K_i = \frac{X_{\text{act}}^{\text{Mg}} X_{\text{cum}}^{\text{Mn}} f_{\text{cum}}^{\text{Mn}}}{X_{\text{act}}^{\text{Mn}} X_{\text{cum}}^{\text{Mg}} f_{\text{act}}^{\text{Mn}}} \cdot \exp 0{\cdot}40\ (X_{\text{cum}}^{\text{Fe}})^2 \tag{20}$$

where

$$X_{\text{cum}}^{\text{Mn}} = \text{Mn}/(\text{Mg} + \text{Fe}^{2+} + \text{Mn})$$

$$X_{\text{cum}}^{\text{Fe}} = \text{Fe}^{2+}/(\text{Mg} + \text{Fe}^{2+} + \text{Mn})$$

$$X_{\text{cum}}^{\text{Mg}} = \text{Mg}/(\text{Mg} + \text{Fe}^{2+} + \text{Mn})$$

The exponential factors which appear in both of these equations are the activity coefficients of the iron and magnesium end members of cummingtonite as previously deduced from Fig. 2.

In order to simplify (19) and (20) the assumption will be made that the activity coefficient of the manganese component in cummingtonite is a constant, as was previously done for the activity coefficients of this component in actinolite and Ca-pyroxene. In the case of cummingtonite this assumption is probably not a very good one since the activity coefficient of any given component of a completely non-ideal ternary solution depends on the relative concentrations of the other components in a complex way in the general case. Thus the functional relation

$$f_{\text{cum}}^{\text{Mn}} = f\,(X_{\text{cum}}^{\text{Mg}} + X_{\text{cum}}^{\text{Fe}}) \tag{21}$$

probably does not hold except in a rough way. However, it will be assumed, as a first approximation that (21) does hold. Then

$$K_h' = K_h \frac{f_{\text{act}}^{\text{Mn}}}{f_{\text{cum}}^{\text{Mn}}} \quad \text{and} \quad K_i' = K_i \frac{f_{\text{act}}^{\text{Mn}}}{f_{\text{cum}}^{\text{Mn}}}$$

where K_h' and K_i' are constants. The equations (19) and (20) then become

$$K_h' = \frac{X_{\text{act}}^{\text{Fe}}\, X_{\text{cum}}^{\text{Mn}}}{X_{\text{act}}^{\text{Mn}}\, X_{\text{cum}}^{\text{Fe}}} \cdot \exp 0{\cdot}40\ (X_{\text{cum}}^{\text{Mg}})^2 \tag{22}$$

and

$$K_i' = \frac{X_{\text{act}}^{\text{Mg}}\, X_{\text{cum}}^{\text{Mn}}}{X_{\text{act}}^{\text{Mn}}\, X_{\text{cum}}^{\text{Mg}}} \cdot \exp 0{\cdot}40\ (X_{\text{cum}}^{\text{Fe}})^2 \tag{23}$$

It is apparent that the ratios $X_{\text{act}}^{\text{Fe}}/X_{\text{cum}}^{\text{Fe}}$ and $X_{\text{act}}^{\text{Mg}}/X_{\text{cum}}^{\text{Mg}}$, here no longer constant as in the case of coexisting actinolite and Ca-pyroxene, will affect the ratios $X_{\text{cum}}^{\text{Mn}}/X_{\text{act}}^{\text{Mn}}$. Thus both $X_{\text{act}}^{\text{Fe}}/X_{\text{cum}}^{\text{Fe}}$ and $X_{\text{act}}^{\text{Mg}}/X_{\text{cum}}^{\text{Mg}}$ decrease in the Mg end of Fig. 2. Unfortunately only the mineral pair 18 falls in this range. However, if the exponential factors are taken into consideration these also introduce considerable variation. In the case of (23) $X_{\text{act}}^{\text{Mg}}/X_{\text{cum}}^{\text{Mg}}$ and $\exp 0{\cdot}40\ (X_{\text{cum}}^{\text{Fe}})^2$ both decrease with increasing Mg. The result is that $X_{\text{cum}}^{\text{Mn}}/X_{\text{act}}^{\text{Mn}}$ must show a compensating increase to keep K_i' constant. A consequence of this variation is an introduction of scatter into Fig. 9. The scatter due to these sources must of course be isolated from that due to analytical errors, possible failure to attain equilibrium, and variations in $f_{\text{cum}}^{\text{Mn}}$. However, it is apparent that the pair 18 representing high magnesium minerals shows the largest value of $X_{\text{cum}}^{\text{Mn}}/X_{\text{act}}^{\text{Mn}}$, in conformity with the theory outlined.

Equations (22) and (23) can be made to yield some additional information when their total atomic fractions are converted into partial atomic fractions. In terms of the latter they become

$$K_h' = \frac{(1 - Y_{\text{act}})Y_{\text{cum}}}{(1 - Y_{\text{cum}})Y_{\text{act}}} \exp 0{\cdot}40\ (X_{\text{cum}}^{\text{Mg}})^2 \tag{24}$$

and

$$K_i' = \frac{(1 - Z_{\text{act}})Z_{\text{cum}}}{(1 - Z_{\text{cum}})Z_{\text{act}}} \exp 0{\cdot}40\ (X_{\text{cum}}^{\text{Fe}})^2 \tag{25}$$

Figs. 10 and 11 show as open circles the plots of the observed partial atomic

fractions. It is possible to obtain from this data by the method of averages values for K_h' and K_i'. The result is $K_h' = 1{\cdot}70$ and $K_i' = 3{\cdot}08$. From these values of the equilibrium constants equations (24) and (25) may then be used to obtain Y_{act}

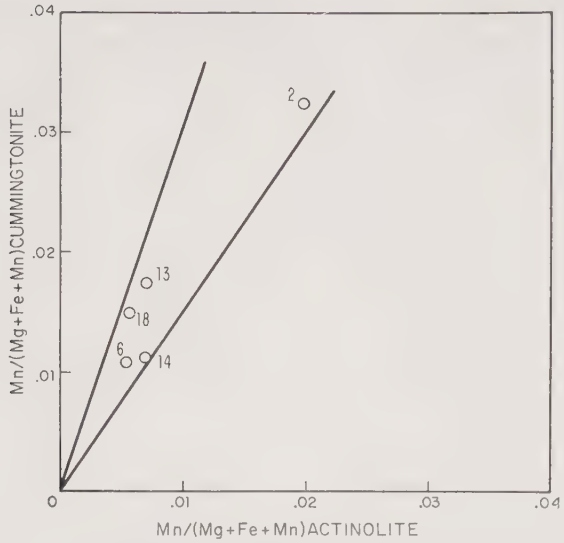

Fig. 9. Relation between the total atomic fraction of manganese in coexisting actinolites and cummingtonites.

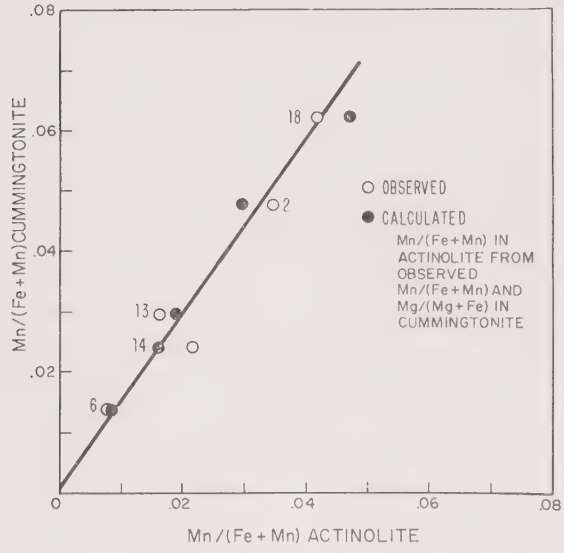

Fig. 10. Relation between the partial atomic fractions of manganese in coexisting actinolites and cummingtonites.

and Z_{act} in terms of the observed values of Y_{cum} and Z_{cum}, $X_{\text{cum}}^{\text{Mg}}$, and $X_{\text{cum}}^{\text{Fe}}$. The corresponding points appear as blackened circles in Figs. 10 and 11. These plots are interesting because they eliminate all scatter except that imposed by the exponential term. It is apparent that the calculated distribution trends are of the

same general types as those observed. The plots show well the increase of Z_{cum}/Z_{act} and the corresponding decrease of Y_{cum}/Y_{act} through the sequence of increasingly Mg-rich mineral pairs 6, 2, 13, 14 and 18. The scatter of the calculated points of Figs. 10 and 11 is thus only apparent. The points represent the projections of points lying in a spiral surface in space formed from the two axes Z_{cum} and Z_{act} (or Y_{cum} and Y_{act}) and the additional axis X^{Mg}_{Cum} (or X^{Fe}_{Cum}). Thus the curves drawn on Figs. 10 and 11 have no real existence as functions but show only the trends of the projections.

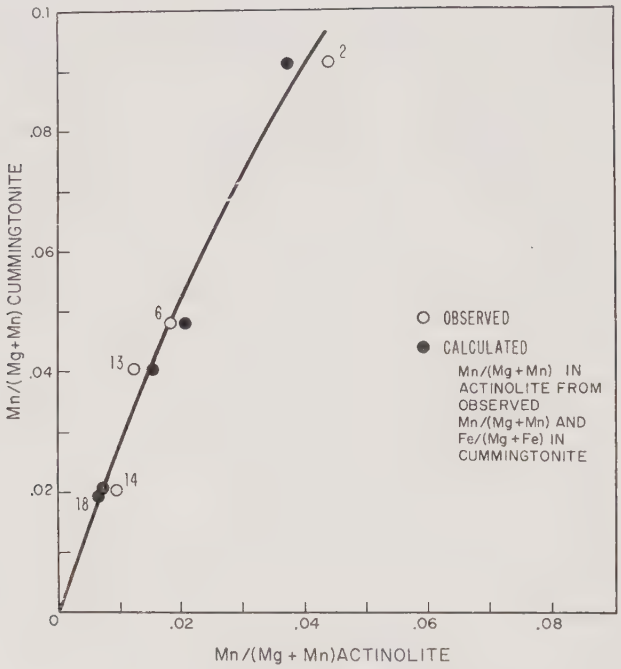

Fig. 11. Relation between the partial atomic fraction of manganese in coexisting actinolites and cummingtonites.

Ca-*pyroxene and cummingtonite*

The observed distributions of manganese among coexisting Ca-pyroxene and cummingtonite are presented in Figs. 12, 13 and 14. Fig 12 is a plot of the total atomic fraction and Figs. 13 and 14 of the partial atomic fractions.

All the reasoning applied to the pair actinolite–cummingtonite may again be applied here if Ca-pyroxene is substituted for actinolite. Omitting the reactions, the equations of equilibrium expressed as partial atomic fractions are

$$K_j' = \frac{(1 - Y_{Ca\text{-}px})Y_{cum}}{(1 - Y_{cum})Y_{Ca\text{-}px}} \cdot \exp 0{\cdot}40\ (X^{Mg}_{cum})^2 \qquad (26)$$

and

$$K_k' = \frac{(1 - Z_{Ca\text{-}px})Z_{cum}}{(1 - Z_{cum})Z_{Ca\text{-}px}} \cdot \exp 0{\cdot}40\ (X^{Fe}_{cum})^2 \qquad (27)$$

Rather than attempt to determine K_j' and K_k' from the data of Figs. 13 and 14, it

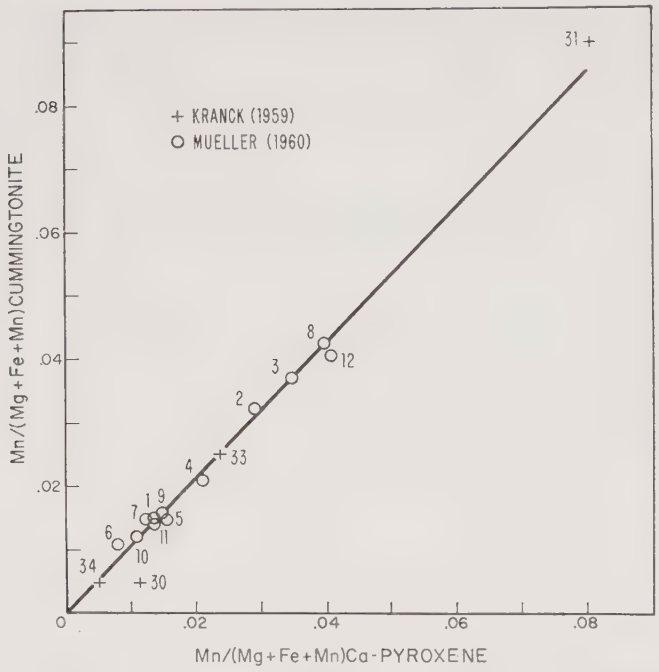

Fig. 12. Relation between total atomic fractions of manganese in coexisting Ca-pyroxenes and cummingtonites. The data of KRANCK are based on Fe^{2+}. The data of MUELLER are based on total Fe.

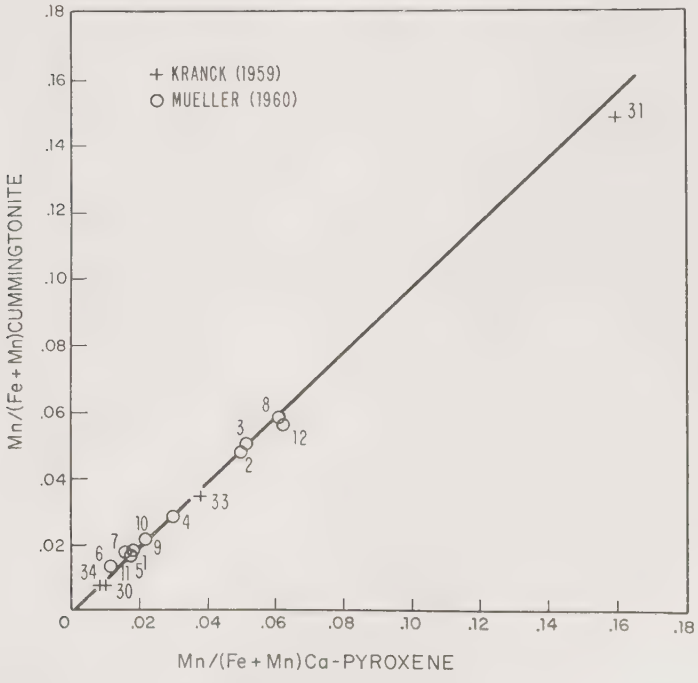

Fig. 13. Relation between partial atomic fractions of manganese in coexisting Ca-pyroxene and cummingtonites. The data of KRANCK are based on Fe^{2+}. The data of MUELLER are based on total Fe.

is more interesting to calculate them from the data on the previously discussed mineral pairs. This may be done by referring to equations (17), (18), (24) and (25). Thus

$$K_j' = \frac{K_h'}{K_f'} = 1{\cdot}20$$

and

$$K_k' = \frac{K_i'}{K_g'} = 2{\cdot}17$$

These values of K_j' and K_k' may then be used to calculate distributions from equations (26) and (27). Table 2 shows the calculations for certain of the data of

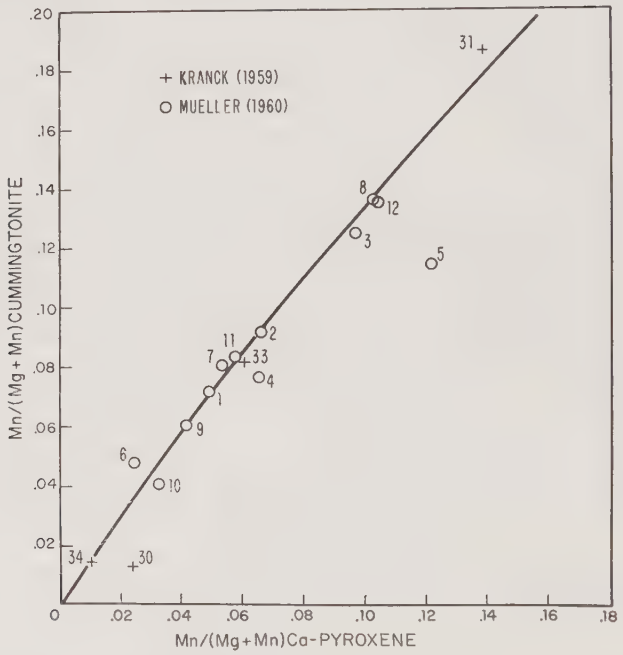

Fig. 14. Relation between partial atomic fraction of manganese in coexisting Ca-pyroxenes and cummingtonites. The data of Kranck are based on Fe^{2+}. The data of Mueller are based on total Fe.

Fig. 13. The mineral pairs of this table are tabulated in order of increasing Mg content. The calculated values have not been plotted but it is apparent that such a plot would be somewhat displaced toward cummingtonite as compared with the observed values as shown by the curve of Fig. 13.

Table 3 is a similar tabulation for data corresponding to Fig. 14. It is apparent that here also there is a similar displacement of calculated from observed values. The discrepancy is greatest for the pair (5). Later it will be shown that this is almost certainly due to analytical errors. The general agreement is, however, quite good considering the indirect methods used to calculate K_j' and K_k' and the assumptions made as to the invariance of the distribution functions in different

mineral assemblages. It should, however, be emphasized that the curves drawn in Figs. 12, 13 and 14 again have no functional basis and merely indicate trends of projections of three dimensional distribution functions.

Ca-*pyroxene and orthopyroxene*

The distribution of manganese among these minerals is shown in Figs. 15, 16 and 17 in terms of the total and partial atomic fractions. Two sets of data distinguished by considerable differences in Mg and Fe content of the minerals are

Table 2

Mineral pair	Y_{cum} (obs.)	exp 0·40 $(X^{Mg}_{cum})^2$	$Y_{Ca\text{-}px}$ (calc.)	$Y_{Ca\text{-}px}$ (obs.)
(5)	0·0164	1·005	0·0138	0·0175
(11)	0·0170	1·010	0·0144	0·0167
(6)	0·0137	1·020	0·0117	0·0114
(33)	0·0347	1·034	0·0300	0·0378
(2)	0·0477	1·045	0·0414	0·0498
(31)	0·148	1·077	0·135	0·160

Table 3

Mineral pair	Z_{cum} (obs.)	exp 0·40 $(X^{Fe}_{cum})^2$	$Z_{Ca\text{-}px}$ (calc.)	$Z_{Ca\text{-}px}$ (obs.)
(5)	0·114	1·381	0·0756	0·122
(11)	0·0833	1·326	0·0524	0·0577
(6)	0·0478	1·280	0·0287	0·0247
(33)	0·0817	1·225	0·0478	0·0608
(2)	0·0914	1·195	0·0524	0·0663
(31)	0·186	1·138	0·107	0·139

represented in these figures as may be seen by comparison with Fig. 4. The data of Clavan *et al.* (1954) and Norton and Clavan (1959) comprise the Mg-rich set whereas those of Kranck (1959) comprise the Fe-rich set.

In Figs. 16 and 17 these two sets of data may be distinguished by two separate trends of the plots of the partial atomic fractions. The reason for this separation into two groups is not known. It is possible that systematic differences in the analyses of Mn by the different investigators are responsible. Another possibility is that there is a considerable change in the activity coefficient of the Mn components with changing Mg content. However, it should be noted that the distributions within each group are uniform and are thus in conformity with the previous deduction that the Mg and Fe components form approximately ideal solutions (no activity coefficient effect).

The comparatively large deviation of the pair 35 is apparent. This will be explained in the following section.

Reference to Fig. 15 shows that the two groups distinguished in the plots of the partial atomic fractions vanish in the plot of the total atomic fraction. This feature may be explained in terms of the ternary compositional effects previously

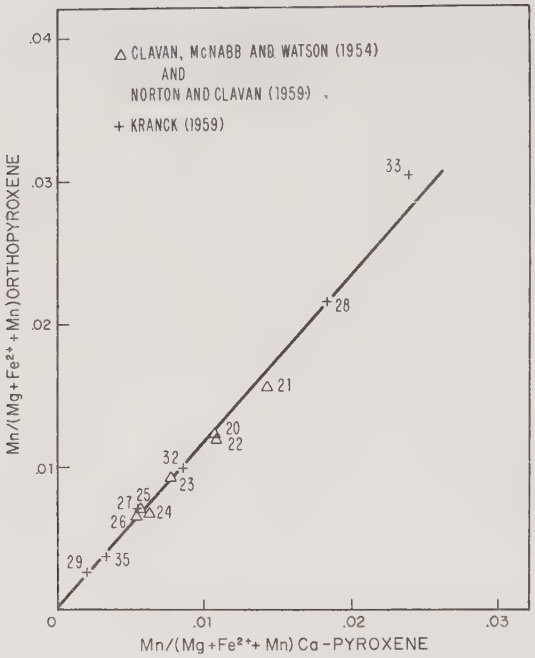

Fig. 15. Relation between the total atomic fraction of manganese in coexisting Ca-pyroxenes and orthopyroxenes.

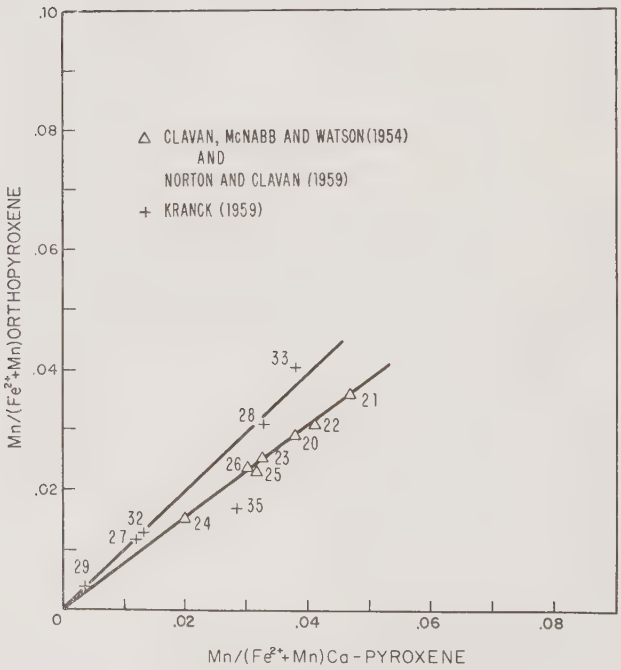

Fig. 16. Relation between the partial atomic fraction of manganese in coexisting Ca-pyroxenes and orthopyroxenes.

discussed. As in the case of the pair cummingtonite–actinolite the effect is one of increasing the ratio of the total atomic fractions $X^{Mn}_{or\text{-}px}/X^{Mn}_{Ca\text{-}px}$ with increasing Mg content. The effect in the case of the pair orthopyroxene-Ca-pyroxene is especially marked because of the form of the distribution curve of Fig. 4. The result on Fig. 15 is to cause a merging of the two groups distinguished in Figs. 16 and 17, since the points representing Mg-rich minerals are shifted upward (toward cummingtonite) relative to the points representing Fe-rich minerals.

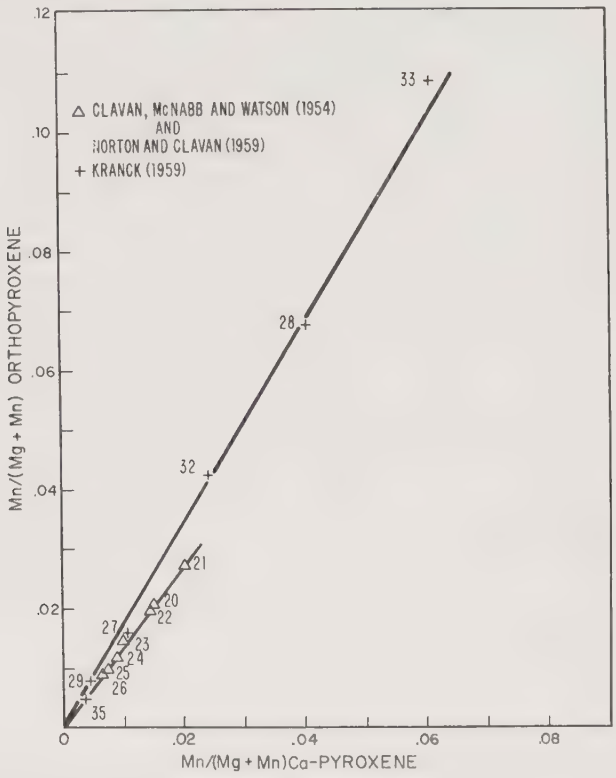

Fig. 17. Relation between the partial atomic fraction of manganese in coexisting Ca-pyroxenes and orthopyroxenes.

Detection of scatter due to analytical errors or failure to attain equilibrium

It is apparent from the figures that some points deviate considerably from the normal distribution trends. As was demonstrated in the foregoing sections some of these deviations may be attributed to complications arising in the ternary systems. However, it is highly probable that much of the scatter is attributable to other causes with analytical errors playing a leading role.

Unfortunately most of the analytical data are not good enough to detect errors by reference to ideal formulae or summation to 100 per cent. However, the trends defined by the plots of the partial atomic fractions provide a means for assigning approximately the source of scatter as to the elements concerned. As one example, the point 5 appearing in Figs. 3, 12, 13 and 14 may be chosen. At first sight it

might appear that the large deviation shown by this point in Fig. 14 might be due to errors in either Mn, Mg or Fe. Actually, however, point 5 is seen to deviate not at all in Figs. 12 and 13. Now point 5 of Fig 3 does not appear to deviate much from the distribution curve. However, this is deceptive since in the range of Mg/(Mg + Fe) in which the point lies, relatively large errors in the weight per cents of oxides show up as only small errors in the atomic fractions. This is true because the maximum scatter in the atomic fraction is proportional to the function X–X^2 (Mueller, 1960) which equals zero at $X = 0$ and $X = 1$, where X is the total atomic fraction. The relatively small amount of deviation of point 5 in Figs. 12 and 13 which involve chiefly the elements Fe and Mn makes it seem likely that the deviation in Fig 14 may be largely attributed to errors in Mg. Accordingly it should be possible to correct point 5 of Fig. 14 by moving this point of Fig. 3 to the curve, attributing the error entirely to Mg in either Ca-pyroxene or cummingonite or both. When this calculation is done point 5 of Fig. 14 is seen to be moved close to the curve, the correction applied in Fig. 3 affecting the suitable direction and amount of correction in Fig. 14. Unfortunately, however, it is impossible to determine to which mineral the greater part of correction should be applied.

A similar analysis may be applied to several other mineral pairs, notably the pairs 35 of Figs. 4, 15, 16 and 17 and pairs 4, 6 and 10 of Figs. 3, 12, 13 and 14.

Correlation of Solution Properties with Crystal Structure as Revealed by X-rays

All of the effects which have been observed and which have been interpreted in terms of thermodynamic theory in the foregoing discussion have as their basis the interactions of ions or atoms which give rise to the crystal structures. The detailed study of these structures by means of X-rays thus provides valuable data which may eventually be used to estimate certain parameters such as bond energies and entropies.

A study of this kind, which is at the same time pertinent to the present work and its conclusions, was made by Ghose and Hellner (1959) on the crystal structure of grunerite. These investigators found that grunerite is isostructural with other monoclinic amphiboles and that Fe is concentrated relative to Mg in the metal position which corresponds to Ca in tremolite. This observation is pertinent because its consequences should be reflected in the thermodynamical solution properties of the cummingtonite solid solutions. For example, if as in the distribution functions 2, 3, and 5, cummingtonite is regarded as a mixture of $\frac{1}{7}Fe_7Si_8O_{22}(OH)_2$ and $\frac{1}{7}Mg_7Si_8O_{22}(OH)_2$ units, no distinction is made between the various metal positions occupied by Mg and Fe. If there were no energetic distinction between these positions the solid solution might behave ideally. However, it was deduced from Figs. 2 and 3 that cummingtonite, at the time of its crystallization, apparently behaved in a slightly non-ideal manner resembling the regular solution model. However, an ordering process such as that detected by Ghose and Hellner should involve entropy as well as heat effects, and it is only the latter that are taken account of in the strictly regular solution.

Another factor to be considered in interpreting the results of the structural

investigation is the amount of ordering which may have occurred subsequent to the period of crystallization in which the element distributions between phases was established. For example the element distribution may reflect the solution (and structural) properties at the time of crystallization, but X-ray investigation of order–disorder phenomena and element distribution within the lattice of a given mineral may reflect some subsequent lower temperature.

Acknowledgements—The contents of this paper were in part conceived during a period of a research assistantship, financed by an American Petroleum Institute Project. The writer is grateful for the many courtesies extended by Dr. Tj. Van Andel, project director.

The writer is particularly grateful to Hans Ramberg and Ralph Kretz for their critical discussions and comments relative to this paper.

References

Ahrens L. H. (1952) The use of ionization potentials, Part 2. Anion affinity and geochemistry. *Geochim. et Cosmochim. Acta* **3,** 1–29.

Clavan W. S., McNabb W. M. and Watson E. H. (1954) Some hypersthenes from S.E. Pennsylvania and Delaware. *Amer. Min.* **39,** 566–580.

DeVore G. W. (1955a) The role of adsorption in the fractionation and distribution of elements *J. Geol.* **63,** 159–190.

DeVore G. W. (1955b) Crystal growth and the distribution of elements. *J. Geol.* **63,** 471–494.

DeVore G. W. (1957). The association of strongly polarizing cations with weakly polarizing cations as a major influence in element distribution, mineral composition, and crystal growth. *J. Geol.* **65,** 178–195.

Fyfe W. S. (1951) Isomorphism and bond type. *Amer. Min.* **36,** 538–542.

Ghose S. and Hellner E. (1959) The crystal structure of grunerite and observations on the Mg–Fe distribution. *J. Geol.* **67,** 691–701.

Goldschmidt V. M. (1937) The principles of distribution of chemical elements in minerals and rocks. *J. Chem. Soc.* 655–673.

Goldschmidt V. M. (1944) Crystal chemistry and geochemistry. Applications for recovery of rare elements in science and industry. *Chemical Products* March–April, 1944.

Guggenheim E. A. (1950) *Thermodynamics.* North Holland, Amsterdam.

Hildebrand J. H. (1929) Solubility—XII. Regular solutions. *J. Amer. Chem. Soc.* **51,** 66.

Hildebrand J. H. and Sharma J. N. (1929) The activities of molten alloys of thallium with tin and with lead. *J. Amer. Chem. Soc.* **51,** 462–471.

Howie R. A. (1955) The geochemistry of the charnockite Series of Madras, India. *Trans. R. Soc. Edinb.* **62,** 725–768.

Kranck S. (1959) Chemical petrology of metamorphosed iron formations and associated rocks in the Mount Reed area in Northern Quebec. Ph.D. Thesis, Massachusetts Institute of Technology.

Kretz R. (1959) Chemical study of garnet, biotite, and hornblende from gneisses of Southwestern Quebec with emphasis on distribution of elements in coexisting minerals. *J. Geol.* **67,** 371–402.

Mueller R. F. (1960) Compositional characteristics and equilibrium relations in mineral assemblages of a metamorphosed iron formation. *Amer. J. Sci.* **258,** 449–497.

Neumann H. (1949) Notes on the mineralogy and geochemistry of zinc. *Min. Mag.* **29,** 575–581.

Norton D. A. and Clavan W. S. (1959) The optical mineralogy, chemistry and X-ray crystallography of ten clinopyroxenes from the Pennsylvania and Delaware Piedmont Province. *Amer. Min.* **44,** 844–874.

Prigogine I. and Defay R. (1951) *Chemical Thermodynamics* (English translation by Everett D. H., 1954). Longmans Green, London.

Ramberg H. (1944) Petrologic significance of subsolidus phase transitions in mixed crystals. *Norsk Geol. tidsskr.* **24,** 42–74.

Ramberg H. and DeVore G. W. (1951) The distribution of Fe^{++} and Mg^{++} in coexisting olivines and pyroxenes. *J. Geol.* **59,** 193–210.

Ramberg H. (1952) Chemical bonds and the distribution of cations in silicates. *J. Geol.* **60,** 331–355.

Ringwood A. E. (1955) The principles governing trace element distribution during magnetic crystallization—I. The influence of electronegativity. *Geochim. et Cosmochim. Acta* **7,** 189–202.

Sahama Th. G. and Torgeson D. R. (1949) Some examples of the application of thermochemistry to petrology. *J. Geol.* **57,** 255–262.

Geochimica et Cosmochimica Acta, 1961, Vol. 25, pp. 297 to 311. Pergamon Press Ltd. Printed in Northern Ireland

Argonbestimmungen an Kaliummineralien—IX

Messungen zu den verschiedenen Arten der Argondiffusion

H. Fechtig, W. Gentner und S. Kalbitzer
Max-Planck-Institut für Kernphysik, Heidelberg

(*Received* 24 *April* 1961)

Abstract—By using the radioactive isotopes Ar^{37} and Ar^{39} it was possible to measure the diffusion of argon in natural samples of sanidine, phonolithe and augite, as well as in a Bohemian tectite (moldavite) and in synthetic sylvine. The measurements of moldavite and sanidine resulted in a straight line when log D/a^2 was plotted against $1/T$; the results of the other material in the same graph were two straight lines cutting each other. The boundary layer theory applied by Wrage to solve this problem made it possible to show that the straight line resulting from the moldavite and sanidine measurements and one of the two straight lines resulting from the other material examined represent the volume diffusion. The second straight line in the results of phonolithe and augite however, does not obey these laws of volume diffusion. In this case another mechanism has to be assumed, probably based on diffusion from lattice imperfections.

For all substances studied the values of D/a^2 for the volume diffusion at room temperature are $<5 \cdot 10^{-24}$ (sec^{-1}). Thus the argon loss caused by volume diffusion is so small that the potassium–argon ages on these materials need not be corrected. For the diffusion from lattice imperfections however, the values for D/a^2 at room temperature would be between $6 \cdot 10^{-18}$ and $2 \cdot 10^{-28}$ (sec^{-1}). This means that argon losses which are not based on volume diffusion may have considerable losses. The investigations proved again that for potassium–argon dating sanidine and mica are the best suitable material, whereas other feldspars and rocks are less suited and salts may be used in exceptional cases only.

1. Einleitung

In einer früheren Arbeit (Fechtig *et al.*, 1960) wurde über Ergebnisse von Argonverlusten an einigen Mineralien im Rahmen der Altersbestimmung berichtet. Mit Hilfe des radioaktiven Isotops Ar^{37} konnten für die Minerale Flusspat Anorthit, Augit und Margarit die Diffusionskonstanten für Temperaturen von 1000°C bis herab zur Zimmertemperatur gemessen werden. Es zeigte sich dabei dass die Aktivierungsenergie in diesem Temperaturbereich variiert, d.h. die Ergebniskurve vermöge der Beziehung

$$D = D_0 \cdot \exp\left(-\frac{Q}{RT}\right) \tag{1}$$

mit D = Diffusionskonstante (cm^2/sec);
D_0 = Konstante mit der Dim. (cm^2/sec).
Q = Aktivierungsenergie (cal./mole).
R = 1,9869(cal/°K mole) = Gaskonstante;
T = absolute Temperatur (°K).

im ln D–1/T-Diagramm ist keine Gerade, sondern weist einige Knicke auf.

Aus den damals gewonnenen Daten konnte jedoch nicht auf den Bewegungsmechanismus des Argons in den betreffenden Mineralien geschlossen werden. Es wurden dort zwar aus ähnlichen Ergebnissen bei der Abgabe von Emanation aus Eisenhydroxyd von Cook (1939) und von Flügge und Ziemens (1939) entwickelte Vorstellungen zitiert, die jedoch, wie unsere weiteren Messungen zeigen, für vorliegende Verhältnisse wohl nicht ganz zutreffen. Zudem haben sich auch die Vorstellungen in der Physik der Festkörper so erweitert und präzisiert, dass die in

diesen Arbeiten gewonnenen Ergebnisse unter anderen Aspekten gesehen werden müssen.

Um durch geeignete Proben und geeignete Versuche den Diffusionsmechanismus aufzuklären, haben wir in der letzten Zeit weitere Messungen an verschiedenen Materialien durchgeführt. Als Proben erwiesen sich dafür besonders günstig ein Tektit aus Böhmen (Moldavit), der als reine Glasmasse keine ausgeprägte Gitterstruktur besitzt, ein Sanidin aus der Eifel mit der chemischen Summenformel $K(AlSi_3O_8)$, sowie synthetische Sylvine (KCl-Einkristalle). Des weiteren untersuchten wir noch die Argonabgabe an einem Phonolith vom Kaiserstuhl und an einem Augit aus der Eifel.

Die Messtechnik war dieselbe wie sie in unserer früheren Arbeit schon beschrieben wurde (Fechtig *et al.*, 1960). Proben geeigneter Korngrösse wurden im Forschungsreaktor Garching bei München bestrahlt. Vermöge der Reaktionen

$$K^{39}\ (n,p)\ Ar^{39} \text{ und } Ca^{40}\ (n,\alpha)\ Ar^{37}$$

entstehen die radioaktiven Argonisotope Ar^{37} und Ar^{39} mit 35d und 325a Halbwertszeit.

2. Volumendiffusion

2.1. *Schwierigkeiten bei früheren Messungen*

Schon bei der Auswertung der Messergebnisse bei unseren früheren Messungen erhob sich die Frage, wie aus dem gemessenen Argon die Diffusionskonstanten berechnet werden können. Folgende Beziehungen standen zu diesen Berechnungen zur Verfügung:

Jost (1952) gibt die Formel:

$$\frac{C_0 - C}{C_0} = 1 - \frac{6}{\pi^2} \sum_{n=1}^{\infty} \frac{1}{n^2} \cdot \exp\left(-\frac{n^2 \pi^2\, Dt}{a^2}\right) \tag{2}$$

wobei C_0 = Gaskonzentration vor der Diffusion;
C = Gaskonzentration nach der Diffusion;
D = Diffusionskonstante;
a = Radius der Kristalle;
t = Diffusionszeit bedeutet.

Für grosse Konzentrationsabnahmen genügt in Formel(2) das erste Glied der Summe womit sich ergibt:

$$\frac{C_0 - C}{C_0} = 1 - \frac{6}{\pi^2} \cdot \exp\left(-\frac{\pi^2\, Dt}{a^2}\right) \tag{3}$$

Für sehr kleine Konzentrationsänderungen, wie sie bei unseren Untersuchungen des öfteren vorliegen, konvergiert die Summe in Gleichung (2) sehr langsam. Deshalb benützt man besser die von Carslaw und Jaeger (1959) angegebene Näherungsformel:

$$\frac{C_0 - C}{C_0} = \frac{6}{\pi^{1/2}} \cdot \left(\frac{Dt}{a^2}\right)^{1/2} - 3\,\frac{Dt}{a^2} \tag{4}$$

Eine Tabellierung der Werte $\pi^2\, Dt/a^2$ in Abhängigkeit der Variablen $(C_0 - C)/C^0$

wurde von REICHENBERG (1953) gegeben. Er benutzte dazu für Konzentrationsverluste von 0 bis 85% die Beziehung (4), von 85 bis 100% die Beziehung (3).

Das Modell, das den Formeln (2) bis (4) zugrunde liegt, verlangt folgende Bedingungen:

(a) Isotrope Diffusion aus einem kugelförmigen Kristall mit dem Radius a.

(b) Eine gleiche Anfangskonzentration C_0 über das ganze Volumen.

(c) Verschwindende Konzentration auf der Kristalloberfläche zu allen Zeiten t.

Die Abb. 1 zeigt die Ergebnisse für Moldavit und Sanidin. D/a^2 wurde nach

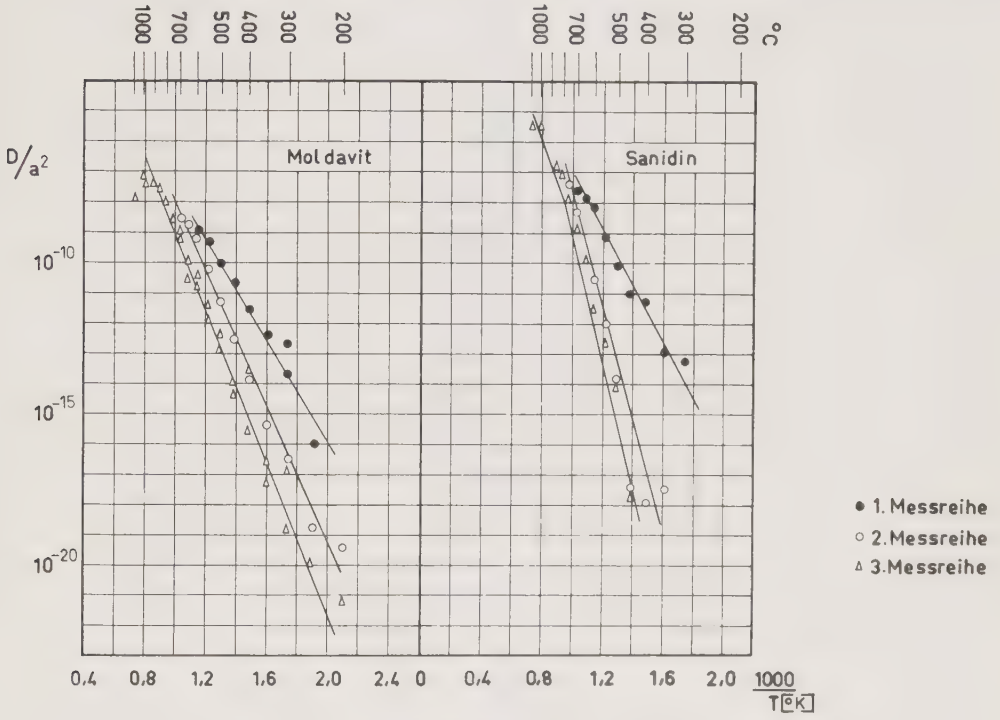

Abb. 1. Argonverluste (D/a^2) in Abhängigkeit von der reziproken Temperatur ($1000/T$) für Moldavit und Sanidin. Die drei Messreihen wurden hintereinander immer mit der tiefsten Temperatur beginnend durchlaufen.

Formel (4) ausgerechnet und in Abhängigkeit von $1/T$ aufgetragen. Die Messungen wurden mehrere Male in Richtung von tiefer zu hoher Temperatur wiederholt. Als Ergebnis erhalten wir Geraden, die in ihrer Steigung zunehmen, während die einzelnen Messwerte für gleiche Temperaturen zu kleineren Werten hin abnehmen.

2,2. *Prüfung der mathematischen und physikalischen Voraussetzungen*

Zur Aufklärung der Tatsache, dass die Messreihen überraschenderweise nicht reproduzierbar sind, sollen alle bisher gemachten Voraussetzungen und Annahmen überprüft werden.

Für den Fall von Volumendiffusion sind unter Berücksichtigung möglicher Störeffekte folgende Voraussetzungen zu überprüfen:

(1) Unabhängigkeit der Diffusionskonstanten von der Argonkonzentration.

(2) Unabhängigkeit der Diffusionskonstanten von der Grösse der Kristalle.

(3) Homogenität der im Reaktor erzeugten Argonkonzentration im Kristall (rechteckiges Konzentrationsprofil).

(4) Unabhängigkeit der Diffusionskonstanten von der Neutronendosis und dem damit verbundenen Strahlenschaden.

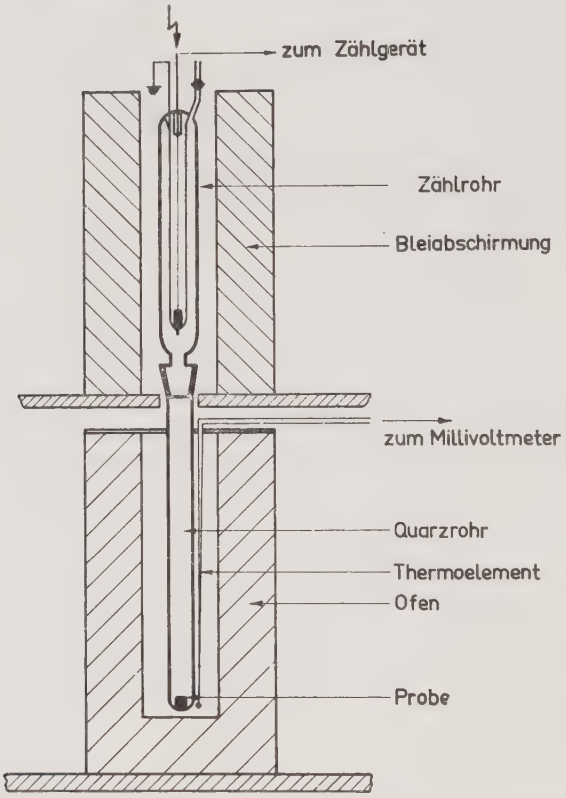

Abb. 2. Schematische Darstellung der Versuchsanordnung zur Prüfung der Zeitabhängigkeit der Gasabgabe.

(5) Vernachlässigbarkeit der Diffusionsverluste während der Bestrahlung und der Verluste in Oberflächennähe durch den Rückstoss des Argonkerns.

Erweisen sich die Gleichungen (2) bis (4) in ihrem Gültigkeitsbereich als anwendbar, so kann umgekehrt auf die Richtigkeit der Annahmen 1, 3, 5 geschlossen werden. Durch Variation der Bestrahlungsdauer und der Korngrösse lassen sich die Annahmen 1, 2, 4 überprüfen.

Die Zeitabhängigkeit der Gasabgabe gemäss den Gleichungen (2) bis (4) wurde durch folgende Experimente geprüft (Abb. 2 und 3): Kommerzielle KCl-Einkristalle (Firma Korth, Kiel) wurden mit einer Rasierklinge zu Kuben bzw. Quadern verschiedener Kantenlänge gespalten. Die Bestrahlung im Münchener Reaktor

erzeugte durch den Prozess K^{39} (n,p) Ar^{39} das gewünschte aktive Argon. Die Bestrahlungen mit einer Dosis von $5 \cdot 10^{18}$–$1 \cdot 10^{19}$ Neutronen oberhalb der Brennelemente ergab eine Aktivität von 0,2 mC/gK. Nach der Bestrahlung waren die Kristalle tiefviolett gefärbt. Die Verfärbung ging jedoch schon beim Erhitzen auf ca. 200°C innerhalb einiger Stunden fast ganz zurück.

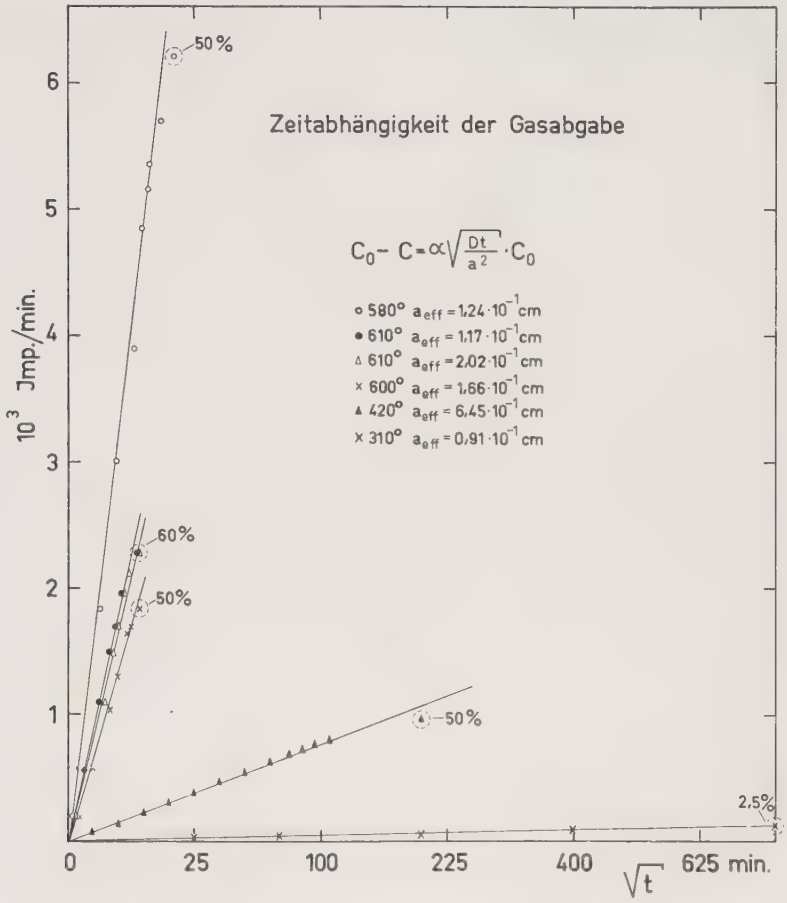

Abb. 3. Die Diffusionverluste des radioaktiven Ar^{39} in Abhängigkeit von $\sqrt{t}$.

Da die Proben zu Beginn der Messung noch auf Zimmertemperatur waren und sich dann innerhalb von ein bis zwei Minuten auf die Solltemperatur erwärmten, wurde jeweils für die einzelne Temperatur auf eine effektive Anfangszeit $t_0 = 0$ zurückextrapoliert. Die Ergebnisse zeigen, dass innerhalb der Messgenauigkeit die für Volumendiffusion zu fordernde $t^{1/2}$–Abhängigkeit der Gasabgabe erfüllt ist.

Die Abweichung der obersten Messwerte von den Geraden in Abb. 3 erklären sich dadurch, dass das negative lineare Glied in Gleichung (4) nicht berücksichtigt wurde, was wiederum notwendig was, um alle Messwerte auf einer Abbildung zu vereinigen. So erkären sich die scheinbaren Abweichungen der eingekreisten Messpunkte auf der Geraden. Bei unseren Messungen sind die Diffusionsverluste

meistens wesentlich kleiner als 10%, so kann das lineare Glied der Gleichung (4) ohne nennenswerten Fehler vernachlässigt werden.

Die Uebereinstimmung der Messkurven der Abbildung 3 mit den von der Theorie geforderten Werten ist somit befriedigend. Für das hier untersuchte Temperaturgebiet können wir daher die unter 1, 3 und 5 gemachten Voraussetzungen als zutreffend ansehen.

Zur Prüfung der Vorassetzungen 2 und 4 wurde einmal die Bestrahlungszeit

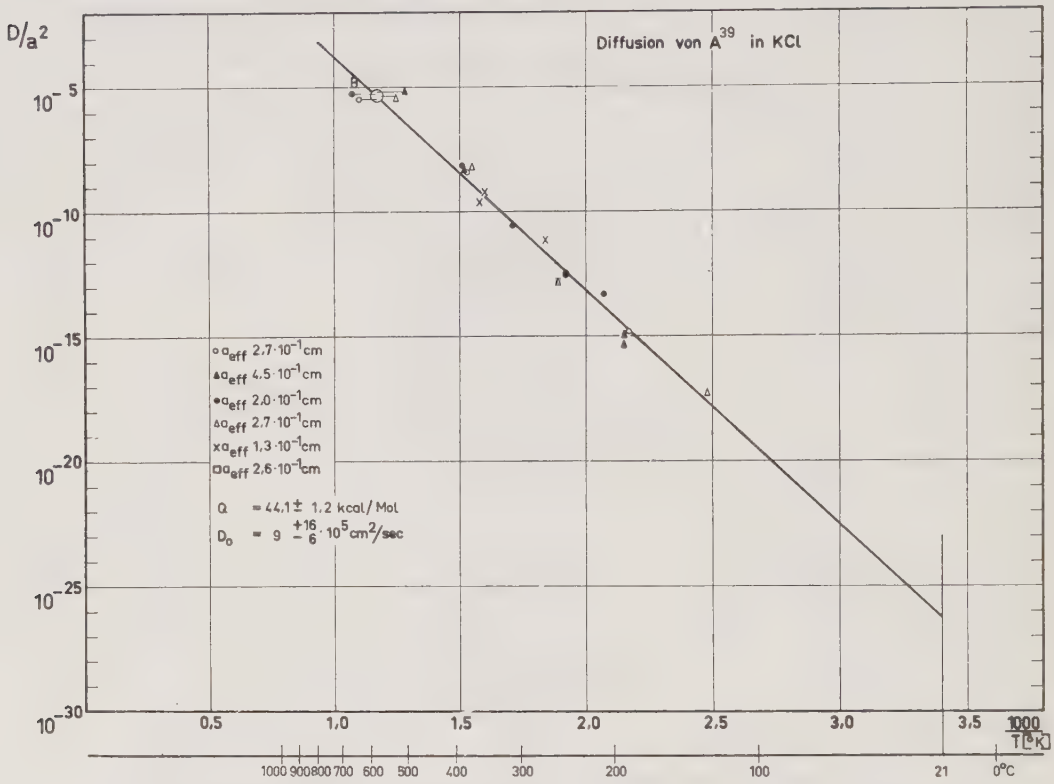

Abb. 4. Unabhängigkeit der Diffusionskonstanten von Korngrösse und Bestrahlungszeit.

verdoppelt und zum anderen die Korngrösse der Kristalle variiert. Da die Korngrösse quadratisch in die Formel zur Bestimmung der Diffusionskonstanten eingeht, entspricht einer Aenderung des Radius um den Faktor 5 eine Aenderung der Diffusionskonstanten um den Faktor 25 für den Fall, dass die Gasabgabe von der Korngrösse unabhängig ist. Die Ergebnisse der Abb. 4 zeigen, dass dei Diffusionskonstante D innerhalb der Messgenauigkeit eine Konstante ist. Damit bestehen die Voraussetzungen 2 und 4 zu Recht. Da mit der Bestrahlungsdauer auch die Anfangskonzentration C_0 des Argons variiert wird, wird auch hier nochmals die Voraussetzung 1 als richtig bestätigt.

An Feldspat haben Evernden *et al.* (1960) die Unabhängigkeit der Diffusionskonstanten von der Korngrösse nicht bestätigen können. Dies dürfte aber an den ganz anders gelagerten Versuchsbedingungen liegen. Die Autoren finden, dass die

Diffusionskonstante von Argon in Feldspat bei zunehmender Korngrösse anwächst.

Die Messergebnisse der Abb. 1 wurden so gewonnen, dass stets dieselbe Probe im angegebenen Temperaturintervall mehrere Male von tiefen zu hohen Temperaturen hin gemessen wurden. Wir müssen uns nun fragen, nachdem sich die Voraussetzungen 1 bis 5 als richtig erwiesen haben, ob bei dieser Versuchsreihe auch die oben zitierten mathematischen Bedingungen *a*, *b* und *c* erfüllt sind. Die Forderung *a* nach isotroper Diffusion dürfte mit der betreffenden mineralogischen Gitterstruktur beantwortet werden können. Da hier keine Schichtgitter vorliegen, dürfte diese Bedingung erfüllt sein.

Die Richtigkeit der Bedingung *b* ist zu überprüfen, da z.B. bei Beginn der 2. Messreihe sicher kein Rechteckprofil der Argonkonzentration mehr vorhanden ist. Wir wollen daher diese Bedingung als verletzt ansehen und annehmen, dass die gemessenen Argonverluste aus einer oberflächennahen Schicht stammen. Sollte sich diese Annahme als richtig erweisen, dann könnte eine Verletzung der Bedingung *c* (verschwindende Oberflächenbelegung mit Argon) nur noch den Charakter einer Korrektur tragen. Der Verdacht lag nahe, dass selbst bei sehr geringfügigen Argonverlusten (z.B. $< 1‰$) schon eine derartige Verarmung der oberflächennahen Schichten eintritt, dass die Voraussetzung *b* verletzt wird. Die Berücksichtigung dieses Effektes erfordert einigen mathematischen Aufwand. Daher hat Wrage (1961) unter Annahme der Verletzung der Bedingung *b* die Diffusionsgleichung näherungsweise dadurch gelöst, dass er ein in der Grenzschichttheorie erprobtes Verfahren von Kármán (1921) und Pohlhausen (1921) auf dieses Problem angewendet hat. Dabei ist δ_k ein Mass für diese oberflächennahe Schicht, wie sie sich nach der *k* ten Diffusionsmessung in einem Kristall ausgebildet hat.

Das allmähliche Anwachsen dieser Schichtdicke wird rekursiv verfolgt. Die Diffusionskonstante konnte dabei aus folgendem Formalismus gewonnen werden:

$$\delta_k = a \cdot \frac{(C_0 - C)_k}{C_0} + \delta_{k-1} \tag{5}$$

$$D_k = \frac{a}{6C_0} \cdot \frac{\delta_{k-1}(C_0 - C)_k}{t_k - t_{k-1}} \tag{6}$$

wobei a = Radius der Korngrösse;
$(C - C_0)_k$ = Argonabgabe bei der k ten Messung;
C_0 = Gesamtargongehalt;
$t_k - t_{k-1}$ = Messzeit bei der k ten Messung;
bedeutet

2.3. *Ergebnisse an Moldavit und Sanidin*

Mit Hilfe der Gleichungen (5) und (6) konnte man aus den gemessenen Argonverlusten für Moldavit und Sanidin D/a^2 in Abhängigkeit von $[1/T]$ dadurch bestimmen, dass man für den Gang der Messungen das Fortschreiten der Grenzschichtdicke δ berechnet hat. Die Ergebnisse sind in Abb. 5 dargestellt. Es fallen jetzt alle Werte mit der Geraden der jeweils ersten Messreihe der Abb. 1 zusammen.

Dieses Ergebnis bestätigt die Richtigkeit des verwendeten Modells. Die Zusammenstellung der Ergebnisse in Abb. 5 nach der Formel von Wrage (1961) zeigt

also, dass die Formel von Carslaw und Jaeger (1959) für unsere Versuchsbedingungen nur auf die jeweils erste Messreihe anwendbar ist. Wiederholt man die Messreihe, so ist die Voraussetzung des Rechteckprofils der Anfangskonzentration so stark verletzt, dass nach der Formel von Wrage (1961) gerechnet werden muss.

Die Gasabgabe für Sanidin von radiogenem Ar^{40} wurde im hiesigen Institut von Lippolt (1961) massenspektrometrisch gemessen. Er fand grössenordnungsmässige Uebereinstimmung der obigen Ergebnisse, woraus ebenfalls geschlossen

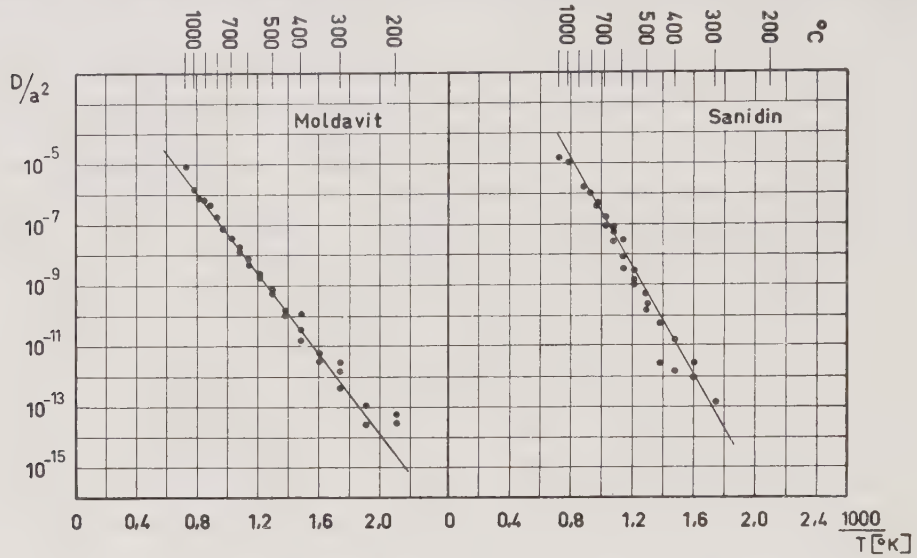

Abb. 5. D/a^2 in Abhängigkeit von $1/T$ für Moldavit und Sanidin.

werden kann, dass der Strahlenschaden sich nicht auf die Argon-Diffusion auswirkt.

Zusammenfassend lässt sich also sagen, dass:

(a) es sich bei diesen Messungen um reine Volumendiffusion handeln muss; und

(b) durch die Reaktorbestrahlung infolge der sehr befriedigenden Reproduzierbarkeit der Kurven des Vergleichs einer massenspektrometrisch gewonnenen Kurve kein nennenswerter Strahlenschaden auftritt, der die Argon-Diffusion merkbar zu beeinflussen vermag.

3. Diffusion durch andere Mechanismen

3.1. *Auswertung der Messergebnisse für Phonolith*

Es liegt nun nahe, den bisher im Hochtemperaturgebiet als gültig befundenen Rechenformalismus der Volumendiffusion auf den Niedertemperaturast einer Knickkurve zu übertragen.

In Abb. 6 wurde eine solche Kurve mit einem Knick bei etwa 350°C einmal nach der Beziehung (4) von Carslaw und Jaeger (1959) und einmal unter Berücksichtigung der fortschreitenden Grenzschichtdicke ausgewertet (Formel (5) und (6) von Wrage, 1961). Es handelt sich dabei um ein Phonolithgestein vom Kaiserstuhl. Hier liegen nun die Verhältnisse gegenüber den oben dargestellten Messungen (Abb. 1 und 5) gerade umgekehrt: bei Carslaw und Jaeger (1959) fallen die

beiden Messreihen zusammen, bei der Anwendung der Theorie von Wrage (1961) spalten sie auf und alle Messwerte verschieben sich dabei insgesamt zu höheren Messwerten hin. Daraus ist zu schliessen, dass es sich in diesem Fall nicht um Volumendiffusion handeln kann.

Das Modell des idealen, störungsfreien Festkörpers, aus dem das Argon nur durch Volumendiffusion entweichen kann, muss durch das Modell des realen Festkörpers mit seinen strukturellen Störungen, die wir allgemein Gefügefehlordnungen nennen wollen, ersetzt werden.

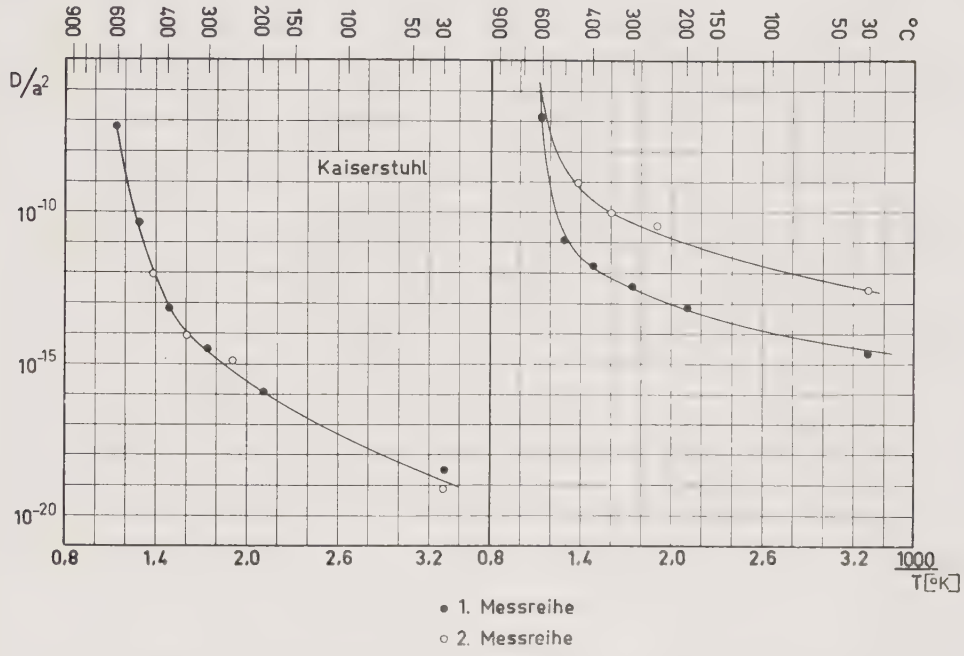

Abb. 6. Diffusionsverluste an einem Kaiserstühler Phonolith. (a) Nach Carslaw und Jaeger (1959) ohne Anknüpfung gerechnet (b) Unter Berücksichtigung der fortschreitenden Grenzschichtdicke gerechnet. (Formel von Wrage, 1961.)

Aus früheren Untersuchungen (Gentner und Kley, 1957) ist bereits bekannt, dass bei bestimmten natürlichen Substanzen durch mechanische Zerkleinerung das in grösseren Gefügestörungen gespeicherte radiogene Argon verloren geht. Wenn wir nun diesen Gefügefehlordnungen unsere proben einen bestimmten Argongehalt zuschreiben, der mit einen charakteristischen Diffusionsvorgang entweicht, so lässt sich die Kurve der Abb. 6(a) bzw. 6(b) als Ueberlagerung von mindestens zwei Diffusionsmechanismen, der Volumendiffusion und der Diffusion längs Gefügefehlordnungen, auffassen. Da die Aktivierungsenergien der beiden Prozesse sich erheblich unterscheiden (bis zu einem Faktor 10) ist zunächst schon ein weiterer Hinweis gegeben, dass hier ein von der Volumendiffusion grundlegend verschiedener Diffusionsprozess vorliegen muss. Diese Vorstellung hat folgende Konsequenzen:

(a) Bei hinreichend langen Messzeiten unterhalb der Knicktemperatur muss die in den Gefügefehlordnungen gespeicherte Gasmenge ausgetrieben werden

können, ohne dass durch die in diesem Temperaturgebiet um mehrere Grössenordnungen kleinere Volumendiffusion messbare Beträge nachgeliefert werden können.

(b) Durch Erhitzen der Probe über den Knickpunkt hinaus müssen sich diese Gefügefehlordnungen je nach thermischer Behandlung verschieden stark wieder auffüllen lassen, da in diesem Temperaturgebiet die Volumendiffusion um Grössenordnungen höher ist.

(c) Der Knickpunkt muss sich je nach Stärke der Auffüllung verschieben lassen. An Augit wurden Versuche in dieser Richtung ausgeführt.

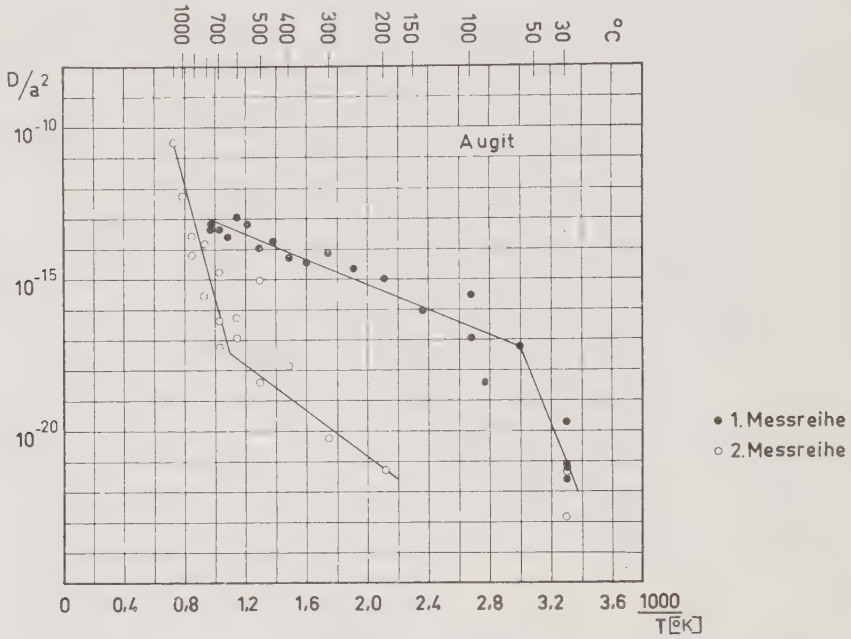

Abb. 7. D/a^2 in Abhängigkeit von $1/T$ für Augit. Die 2. Messreihe liegt bei Temperaturen $<700°C$ um 5 Grössenordnungen unter der ersten, das vermutlich die verstärkte Argonabgabe aus Gefügefehlordnungen demonstriert.

3.2. *Natürliche Mineral- und Gesteinsproben*

In Abb. 7 sind die Messergebnisse an Augit (chem. Summenformel (Ca, Fe) (Mg, Fe, Al) $[(SiAl)_2O_6]$) dargestellt. Die erste Messreihe unterscheidet sich wesentlich von der zweiten.

Offenbar ist das in den Gefügefehlordnungen nach der Bestrahlung vorhandene Argon bei der ersten Messeihe bevorzugt abgegeben worden; bei den nächsten Messreihen konnte dann durch Diffusion aus den Gefügefehlordnungen kein Argon mehr nachgeliefert werden.

Bei dem Ca-haltigen Glimmer Margarit (Fechtig *et al.*, 1960) wurde eine ähnliche starke Abweichung der ersten Messreihe von den folgenden gefunden. Nach den im vorigen Abschnitt erwähnten Beobachtungen können wir eine früher geäusserte Vermutung, dass die Ausheilung eines Strahlenschadens möglicherweise diesen Effekt verursache, nicht mehr in Betracht ziehen; inwieweit jedoch beim Glimmer die Austreibung des stets vorhandenen Wassers und beim

Augit die Austreibung anderer Gase bei diesen ungewöhnlich starken Effekten mitspielen, kann zur Zeit noch nicht beantwortet werden.

In neueren Messungen von HART (1960) an Feldspat, Glaukonit, Hornblende, Muskovit und Pyroxen wurden komplizierte Verhältnisse bei der Argonabgabe gefunden. Inwieweit man bei diesen Ergebnissen zwischen Volumen- und Nichtvolumendiffusion unterscheiden sollte, müsste überprüft werden.

4. Brauchbarkeit der erhaltenen Messwerte in Bezug auf Korrekturen von K–Ar-Altern

Es soll in diesem Abschnitt die Frage nach der Korrektur von K–Ar-Altern diskutiert werden, die an den untersuchten Materialien etwa ausgeführt werden. Gleichzeitig sollen die Ergebnisse hinweisend für eine generelle Möglichkeit der Alterskorrektur für K–Ar-Alter sein.

Da wir für die auf der Erde herrschenden Lagertemperaturen mit der Ueberlagerung mindestens zweier Diffusionsmechanismen, der Volumendiffusion und der Diffusion längs Gefügefehlordnungen, rechnen müssen, so müssen sich derartige Alterskorrekturen auf jeden einzelnen dieser Diffusionsmechanismen beziehen. In Tabelle 1 sind für die untersuchtne Substanzen die gewonnenen Diffusionsdaten bei Zimmertemperatur, getrennt für Volumendiffusion und Diffusion längs Gefügefehlordnungen, zusammengestellt.

Betrachten wir zuerst die Volumendiffusion. Die Werte für D und D/a^2 bei Zimmertemperatur wurden durch Extrapolation der Geraden in ln D–$1/T$-bzw. im ln D/a^2–$1/T$-Diagramm für hohe Temperaturen gewonnen. Für die Volumendiffusion sind in der Tabelle 1 auch die gemessenen Werte der Aktivierungsenergie Q in kcal/mol angegeben. Die Werte liegen zwischen 25 und 92 kcal/mol. Der Fehler dürfte i.a. kleiner als 10% bleiben. Es fällt dabei besonders die Diskrepanz der Werte für die beiden Augite auf. Diese grosse Abweichung erklärt sich dadurch, dass der Wert für Augit I von 26,9 kcal/mol sicher zu niedrig ist, da die damaligen Messungen (FECHTIG, *et al.*, 1960) nicht bis zu genügend hohen Temperaturen ausgeführt wurden. Der Wert für das synthetische KCl mit $Q = 44{,}1$ kcal/mol ist in guter Uebereinstimmung mit der von AMIRKHANOV *et al.*, (1959) für natürliches Sylvin gefundendenen Aktivierungsenergie von $Q = 47$ kcal/mol.

Massgebend für den Gasverlust ist die Grösse D/a^2, wie schon in unserer früheren Arbeit (FECHTIG *et al.*, 1960) eingehend auseinandergesetzt wurde. Aus der Tabelle 1 folgt, dass für alle untersuchten Substanzen dieser Wert $D/a^2 < 10^{-23}$ sec^{-1} bleibt. Der Korrekturparameter $d^2 = \lambda\, a^2/D$ bleibt daher für Zimmertemperatur in allen diesen Fällen bei den angegebenen Kristallgrössen $d^2 > 1000 \cdot \pi^2$. Mit diesen Werten ist daher, wie aus dem Diagramm der Abb. 5 unserer früheren Arbeit hervorgeht, keinerlei Argonverlust durch Volumendiffusion zu befürchten.

Es muss jedoch betont werden, dass dieses Ergebnise nur für den Fall gilt, dass die untersuchte Probe dauernd bei Zimmertemperaturg gelagert ist. Infolge der hohen Aktivierungsenergien können bei höheren Lagerungstemperaturen u.U. schon beträchtliche Diffusionsverluste entstehen. Es ist daher für eine zuverlässige Alterskorrektur eines K–Ar-Alters sehr wichtig, dass die Temperaturgeschichte

Tabelle 1. Diffusionsdaten der untersuchten Substanzen für Zimmertemperatur (20°C)

Material	Q (kcal/mol)	a (cm)	Volumendiffusion			Diffusion Längs Gefügestörungen		
			D (cm^2/sec)	D/a^2 (sec^{-1})	$d^2 = \lambda \cdot a^2/D$	D (cm^2/sec)	D/a^2 (sec^{-1})	$d^2 = \lambda . a^2/D$
Moldavit	29,5	$4 \cdot 10^{-2}$	$8 \cdot 10^{-27}$	$5 \cdot 10^{-24}$		$<8 \cdot 10^{-27}$	$<5 \cdot 10^{-24}$	$>1000 \cdot \pi^2$
Sanidin	39,8	$4 \cdot 10^{-2}$	$3 \cdot 10^{-31}$	$2 \cdot 10^{-28}$		$<3 \cdot 10^{-31}$	$<2 \cdot 10^{-28}$	$>1000 \cdot \pi^2$
syn. Sylvin	44,0	$4 \cdot 10^{-2}$	$5 \cdot 10^{-27}$	$3 \cdot 10^{-24}$		$<1 \cdot 10^{-20}$	$<6 \cdot 10^{-18}$	$>1 \cdot \pi^2$
Phonolith	91,5	$<5 \cdot 10^{-2}$	$<1 \cdot 10^{-30}$	$<1 \cdot 10^{-30}$		$2 \cdot 10^{-22}$	$1 \cdot 10^{-19}$	$17 \cdot \pi^2$
Augit II	83,2	$1 \cdot 10^{-1}$	$<1 \cdot 10^{-30}$	$<1 \cdot 10^{-30}$	$>1000 \times \pi^2$	$1 \cdot 10^{-23}$	$1 \cdot 10^{-21}$	$1700 \cdot \pi^2$
Augit I*	26,9	$4 \cdot 10^{-2}$	$1 \cdot 10^{-28}$	$6 \cdot 10^{-26}$		$1 \cdot 10^{-22}$	$6 \cdot 10^{-19}$	$50 \cdot \pi^2$
Flusspat*	43,5	$4 \cdot 10^{-2}$	$<1 \cdot 10^{-30}$	$<1 \cdot 10^{-30}$		$5 \cdot 10^{-23}$	$3 \cdot 10^{-20}$	$200 \cdot \pi^2$
Anorthit*	55,9	$4 \cdot 10^{-2}$	$<1 \cdot 10^{-30}$	$<1 \cdot 10^{-30}$		$2 \cdot 10^{-23}$	$1 \cdot 10^{-20}$	$50 \cdot \pi^2$
Margarit*	53,7	$5 \cdot 10^{-2}$	$<1 \cdot 10^{-30}$	$<1 \cdot 10^{-30}$		$3 \cdot 10^{-25}$	$1 \cdot 10^{-22}$	$>1000 \cdot \pi^2$

* Messungen siehe Fechtig *et al.* (1960).

der zu datierenden Probe bekannt ist. Als Beispiel hierzu seien die Ergebnisse der Datierung des Bugginger Kalisalzlagers (GENTNER *et al.*, 1954) betrachtet. Damals wurde aus den Ergebnissen derK–Ar-Altersbestimmungen geschlossen, dass bei 40°C, der heutigen Temperatur des Salzlagers, die Diffusionskonstante von Argon D (40°C) = (8 $\pm$7) 10^{-20} cm²/sec sei. Es musste weiter angenommen werden, dass das Lager sich bei 80°C gebildet hatte und bis heute sich auf 40°C abgekühlt hat. Unsere jetzigen Ergebnisse der Diffusionskonstanten von Ar in KCl liegen wesentlich tiefer. Doch ergibt sich für 80°C: $D = 10^{-22}$ cm²/sec. $D/a^2 = 10^{-19}$ sec^{-1} und $d^2 = 17 \cdot \pi^2$, was aber Verluste bis 15% allein durch die Volumendiffusion bewirken kann.

Wie gross ist nun der Einfluss der Diffusion längs Gefügefehlordnungen? Hier befinden wirs uns in einem Dilemma, weil wir einerseits zwar Diffusionskonstanten messen können, andererseits aber keine zuverlässige Korrekturformel kennen. Die Diffusion längs Gefügefehlordnungen kann nämlich nicht generell mathematisch erfasst werden. KALBITZER (1961) hat im hiesigen Institut nach noch unveröffentlichten Messungen im Falle des synthetischen KCl grundsätzlich gezeigt, dass man die Anteile des Argons in den Gefügestörungen messen kann, doch liegen bis jetzt noch keine diesbezüglichen Messungen an natürlichen Substanzen vor. Es ist jedoch zu vermuten, und unsere Ergebnisse an Augit scheinen das zu bestätigen, dass der Anteil des Argons, das in den Gefügestörungen sitzt, klein ist gegenüber dem Gesamtargongehalt der Kristalle. Diese Aussage wird sicherlich für Minerale richtig sein, die das Kalium nicht als blosse Verunreinigung, sondern als ordentliche Gitterbausteine enthalten. Zur Korrektur selbst lässt sich damit aus unseren Messergebnissen schliessen, dass bei niedrigen Temperaturen das Argon aus Gefügefehlordnungen stets schneller abgegeben wird als das Argon, das sich auf Gitterfehlplätzen oder auf Gitterzwischenplätzen befindet. Bei Anwendung der von WASSERBURG (1957) gegebenen Korrekturformel wird deshalb eine solche Korrektur stets zu hoch ausfallen. Der Korrekturparameter $d^2 = \lambda \cdot a^2/D$ für die Diffusion längs Gefügefehlordnungen liegen zum Teil so, dass das in solchen Gitterstörungen gebundene Argon merkbare Diffusions-verluste zeigt. Für Moldavit, Sanidin, Margarit und Augit II sind auch hierfür keine Verluste vorhanden. Dagegen müsste man ein K–Ar-Alter an Flussspat um höchstens 5% an Augit I und Anorthit um höchstens 10% und an Phonolith um höchstens 15% korrigieren. In Sylvin erleidet das so gebundene Argon dagegen grössere Verluste, die eine Alterskorrektur bis zu 100% bewirken können.

Diese Ergebnisse sind in recht guter Uebereinstimmung mit den K–Ar-Altersbestimmungen an den verschiedenen Mineraltypen. Während sich Sanidine und Glimmer sehr gut, viele Feldspäte und Gesteine weniger gut für die K–Ar-Altersbestimmungen eignen, sind Salze nur sehr bedingt verwendungsfähig. Diese Tatsache zeigte sich anhand unserer Diffusionsmessungen ebenfalls sehr deutlich.

An dieser Stelle sei noch eine Bemerkung gemacht über die Frage, ob Diffusionsmessungen zum Zwecke einer Alterskorrektur an n-aktiviertem Material oder solche an natürlichem Material mit radiogenem Argon sich besser eignen.

Der Hauptvorwurf gegen die Methode der n-Aktivierung richtet sich gegen einen möglicherweise auftretenden Strahlenschaden, der die Diffusionsphänomene in gröberen oder feineren Zügen verfälschen könnte. Nach unseren Messungen haben

wir bezüglich der Argondiffusion gröbere Effekte nicht feststellen können; die Frage nach geringeren Effekten muss noch offen bleiben.

Jedoch scheint uns der wesentliche Vorteil dieser Methode der zu sein, dass–ganz abgesehen von der um Grössenordnungen höheren Empfindlichkeit–ein bekanntes, in hoher Näherung rechteckiges Konzentrationsprofil vorliegt, wohingegen bei der Messung von radiogenem Ar^{40} in Gesteinen und Meteoriten von vornherein keine Angabe über schon vollzogene Diffusionsverluste vorliegt; das gerade kann in Temperaturgebieten, in denen die ausdiffundierenden Mengen den in der Lagerungszeit verlorenen gleichkommen, zu erheblichen Verfälschungen führen (vgl. Beispiel Moldavit, Sanidin). Die ermittelten Diffusionskonstanten können je nach Gasverlust viel zu niedrig, die Aktivierungsenergien zu hoch in der Auswertung erscheinen.

Zusammenfassend lässt sich folgendes zur Korrektur von K–Ar-Altern sagen: im allgemeinen setzt sich der Diffusionsverlust von Argon aus Mineralien aus mehreren Komponenten zusammen. Um eine zuverlässige Korrektur zu erhalten, muss man jede dieser Komponenten einzeln betrachten. Für die Volumendiffusion lässt sich ohne Schwierigkeiten eine Korrektur angeben. Die Korrektur, die man mit demselben Formalismus für die anderen Komponenten erhält, ist sicher zu gross, weil einerseits die derzeit zur Verfügung stehenden Korrekturformeln auf der Volumendiffusion basieren, die betreffenden Verluste aber andererseits aus Gefügestörungen stammen und mithin anderen Gesetzen gehorchen. Da bei niedrigen Temperaturen das Argon aus Gefügestörungen stets schneller abgegeben wird als solches, das durch Volumendiffusion nach aussen tritt, liefert eine solche Korrektur stets einen zu grossen Wert. Der richtige Alterswert liegt deshalb zwischen dem schon auf Volumendiffusion korrigierten Wert und dem zusätzlich nach der Diffusion längs Gefügefehlordnungen korrigierten Wert.

Anerkennungen—Herrn Professor Frechen vom Mineralogischen Institut der Universität Bonn danken wir für die Ueberlassung der Sanidin- und Augit II-Proben aus der Eifel. Herrn Professor Wimmenauer vom Geologischen Landesamt Baden-Württemberg, Freiburg i.Br., danken wir für die Ueberlassung der Kaiserstühler Phonolithe. Herrn Professor Maier-Leibnitz, München, und seinen Mitarbeitern danken wir für die Bestrahlung der Mineralproben im Forschungsreaktor Garching bei München.

Literatur

Amirkhanov K. I., Brandt S. B., Bartniski E. N. und Voronovskij S. M. (1959) Ueber die Diffusion radiogenen Argons in Sylvinen. *Dokl. Akad. Nauk. SSSR* **126,** 538.

Carslaw H. S. und Jaeger J. C. (1959) *Conduction of Heat in Solids* (2nd Ed.) S. 92. Clarendon Press, Oxford.

Cook L. G. (1939) Untersuchungen über Chrom- und Eisenhydroxyde und ihre Bedeutung für die Emaniermethode. *Z. phys. Chem.* B **42,** 221.

Evernden J. F., Curtis G. H., Kistler R. W. und Obradovich J. (1960) Argon Diffusion in Glauconite, Microcline, Sanidine, Leucite and Phlogopite. *Amer. J. Sci.* **258,** 583.

Fechtig H., Gentner W. und Zähringer J. (1960) Argonbestimmungen an Kalium-mineralien—VII. Diffusionsverluste von Argon in Mineralien und ihre Auswirkung auf die Kalium-Argon Altersbestimmung. *Geochim. et Cosmochim. Acta* **19,** 70.

Flügge S. und Ziemens K. E. (1939) Die Bestimmung von Korngrössen und Diffusionskonstanten aus dem Emaniervermögen. *Z. phys. Chem.* B **42,** 179.

Gentner W., Goebel K. und Präg R. (1954) Argonbestimmungen an Kalium-mineralien—III. Vergleichende Messungen nach der Kalium-Argon -und Uran-Helium-Methode. *Geochim. et Cosmochim. Acta* **5,** 124.

Gentner W. und Kley W. (1957) Argonbestimmungen an Kalium-mineralien—IV. Die Frage der Arvonverluste in Kalifeld-späten und Glimmermineralien. *Geochim. et Cosmochim. Acta* **12,** 323.

Hart S. R. (1960) *Some Diffusion Measurements Relating to the K–A Dating Method.* Eighth Annual Progress Report for 1960 US-Atomic Energy Commission Contract at (30–1)–1381.

Jost B. (1952) *Diffusion in Solids, Liquids and Gases* p. 45. Academic Press, New York.

Kalbitzer S. (1961) Private Mitteilung.

von Kármán Th. (1921) Ueber laminare und turbulente Reibung. *Z. angew Math. Mech.* **1,** 233.

Lippolt H. J. (1961) Dissertation, Heidelberg.

Pohlhausen K. (1921) Zur näherungsweisen Integration der Differentialgleichung der laminaren Reibungsschicht. *Z. angew. Math. Mech.* **1,** 235.

Reichenberg D. (1953) Properties of ion-exchange resins in relation to their structure—III. Kinetics of exchange. *J. Amer. Chem. Soc.* **75,** 589.

Wasserburg G. J. (1957) Argon-40: potassium-40 dating. *Nuclear Geology* (Edited by Faul H.) New York.

Wrage E. G. (1962) Argonbestimmungen an Kaliummineralien—VIII. Ein Näherungsverfahren zur Lösung von Diffusionsproblemen. *Geochim. et Cosmochim. Acta.* **26,** im Druck.

Geochimica et Cosmochimica Acta, 1961, Vol. 25, pp. 312 to 314. Pergamon Press Ltd. Printed in Northern Ireland

BOOK REVIEW

R. E. Stevens, Michael Fleischer, W. W. Niles, A. A. Chodos, R. H. Filby, R. K. Leininger, L. H. Ahrens, and F. J. Flanagan: **Second report on a cooperative investigation of the composition of two silicate rocks.** United States Geological Survey Bulletin 1113. U.S. Government Printing Office, Washington 25, D.C. (1960). pp. iv + 126, 40 cents.

In 1951 the writer had the privilege of preparing for this Journal a review of the first Report dealing with the analysis of the two international standard rock samples, G–1 and W–1, the famous—or notorious—Bulletin 980 published by the United States Geological Survey. Nine years later, this second Report appeared, and it is of great interest to see the directions in which most progress has been made during the interval.

It is now clearly possible, in the light of the new results reported, to assign preferred values to the major constituents of the Westerly granite and Centerville diabase samples which must lie very close to the truth. Judging from the present Bulletin, it does not perhaps seem as if the two samples have altogether fulfilled their original purpose of providing internationally accepted standards for the spectrographic analysis of major constituents in igneous rocks. Some new work along these lines is indeed reported, but it is the wealth of new data for the minor and trace elements which will be of the greatest interest to most spectrographically inclined geochemists. Continued progress in developing rapid methods of silicate analysis, leaning heavily upon spectrophotometric measurements, flame photometry, and complexometric titrations, has probably to some extent discouraged attempts to achieve comparable accuracy for major elements using the optical spectrograph.

Part I of Bulletin 1113, pp. 3–43, by R. E. Stevens and W. W. Niles, lists the results of about a further 30 analyses each of G–1 and W–1 for major constituents, which have been made in laboratories all over the world since the appearance of Bulletin 980. Both conventional and rapid analyses are represented. The corresponding norms are not listed. The new analyses do not fundamentally alter the picture of the state of silicate rock analysis as it was ten years ago, although there seems little doubt that the more recent analyses are, on the whole, better. The samples are, of course, no longer to be described as unknowns, despite the apparent variability in their composition revealed by Bulletin 980.

In discussing the variations in the results for the two rocks, Stevens and Niles have replaced the histograms of Bulletin 980 by **S**-curves in the present Report, and these portray the situation more clearly.

More is said about the procedures used in classical analysis, and the pitfalls associated with them, than in Bulletin 980, and the reviewer particularly welcomes the clear expression of the opinion that the conventional methods of analysis are sound in themselves, and it is the skill and competence of the individual analyst in carrying them out that vary. The second batch of results now available enables Stevens and Niles to come down unhesitatingly on the right side of the fence; Bulletin 980 left one with the impression that with regard to this question of the inherent reliability of methods on the one hand and the skill of the individual analyst on the other, the compilers were leaning over backwards to preserve scientific objectivity. One of the most significant findings in the whole of the present Report seems to the reviewer to be the extremely close agreement between the medians of the preferred values for the various major constituents in G–1 and W–1, derived from statistical treatment of all the results (p. 38), and the averages of the highly precise analyses made in the Rock Analysis Laboratory of the University of Minnesota, reported by Goldich and Oslund (1956) and quoted on p. 37. Although, as the Bulletin points out, an investigation of this kind can never yield a final and entirely definitive result, petrologists and geochemists now know the major element composition of these standard samples within sufficiently narrow limits for practically every purpose.

The test organised by FAIRBAIRN and SCHAIRER (1952) subsequent to the publication of Bulletin 980, in which samples of a synthetic granite glass were analysed by chemists of recognised competence, revealed a tendency towards systematic errors in the determination of SiO_2 (low) and Al_2O_3 (high), as a result of which FAIRBAIRN (1953) applied corrections for these constituents in his recommended values for G–1 and W–1. This matter is taken further in the present Bulletin, where in Part 2, R. E. STEVENS and A. A. CHODOS (pp. 45–56) have made careful determinations of the SiO_2 contents of the test rocks by combined wet chemical and spectrographic methods. They find, among other things, that surprisingly little SiO_2 escapes into the filtrate if the dehydration is carefully done, and that the impurities in the separated silica itself comprise a good deal that does not belong to the R_2O_3 group (such as NaCl and a good selection of trace elements). Errors of several tenths per cent in the Al_2O_3 figure could arise from this latter cause.

Although STEVENS and CHODOS state that the precision of their special SiO_2 determinations was somewhat disappointing, they confirm FAIRBAIRN's findings that SiO_2 determinations are generally low, although a smaller correction than that applied by FAIRBAIRN seems to be indicated. Even the values reported by GOLDICH and OSLUND may be one or two tenths per cent low.

In Part 3 (pp. 57–82) R. H. FILBY and R. K. LEININGER have collected together and discussed all available spectrographic analyses of G–1 and W–1 for major constituents. During the past ten years, spectrographers must have consumed quite large quantities of these samples as standards in the course of their researches; it is perhaps a little disappointing that even after all this time, FILBY and LEININGER are only able to list half a dozen attempts to determine the major element compositions of these rocks *ab initio* using the spectrograph. It emphasises the dependent nature of this method of analysis. This section of the Report presents a useful and lucid account of the principles and pitfalls of spectrographic analysis (pp. 62–3), and discusses again the vexed questions of precision and accuracy. Many analysts will concede that spectrographic methods may be precise, but systematic errors of one kind and another are often encountered, and some may take exception to the remark (p. 58) that "..... spectrographic methods are as precise (*and therefore probably as accurate*) as chemical methods for several constituents", (my italics).

FILBY and LEININGER give their own recommended values for the major constituents of G–1 and W–1 (Table 17, p. 78), in part independently of the statistically derived values in Part 1 of the Report. Spectrographic figures for MgO in G–1, and for TiO_2 and MnO in both rocks are preferred; chemical figures for the remainder. Part 3 ends with an interesting couple of pages on some analyses made with a direct-reading spectrometer ("quantometer"), which generally yielded better precision than the ordinary spectrographic methods.

For the pure geochemist, as distinct from the petrologist, Part 4 of the Report is probably the most useful. It lists determinations for 39 trace elements, which represents a tremendous step forward since Bulletin 980, where only a handful of such determinations could be reported. L. H. AHRENS and MICHAEL FLEISCHER have assembled all the data available up to the time the Bulletin went to press. More analyses are constantly being made and published, and it is in this field of trace analysis that G–1 and W–1 really come into their own as standard samples.

The majority of analyses listed are, of course, spectrographic, but there is a sprinkling of results obtained by other methods. It is particularly gratifying to see already values reported for eleven elements derived from neutron activation analysis, and for four elements by stable isotope dilution (mass spectrometric) analysis. These elegant methods are inherently much more accurate than spectrographic analysis, and generally more precise, so that they can be treated to some extent as referee methods. The neutron activation method has the almost overriding advantage of freedom from reagent blanks. The results obtained from these methods should probably, therefore, be given more weight than the corresponding spectrographic figures, and this has generally been done by AHRENS and FLEISCHER in arriving at a recommended value for a particular element. In the case of Cu in G–1 however, where the spectrographic values range from 5 to 25 p.p.m., averaging 14 p.p.m., a value of 13 p.p.m. has been recommended rather than the average of 9·5 p.p.m. obtained from 6 analyses by neutron activation. In the case of W–1, the recommended average of 110 p.p.m. (mostly spectrochemical) happens to agree closely with the neutron activation figure of 112 p.p.m.

It seems to be the case that some laboratories are not entirely satisfied that the available samples of G–1 and W–1 are absolutely homogeneous as regards the content of some trace elements present in minute amounts (e.g. fractions of a part per million), and this tends somewhat to reduce the usefulness of the samples. The powders supplied—particularly G–1—are on the coarse side, so that a sample weighing, say, 10–100 mg removed for analysis may not be as representative of the contents of the bottle as would a sample weighing a gram. If, on the other hand, a larger sample is removed from the bottle and further mixed and ground before use, contamination is easily introduced, especially at the fractional part per million level.

More investigations of the trace element variation from bottle to bottle of the samples should probably be carried out. In the case of Pb in G–1, however (Part 5 of the Bulletin, pp. 113–121, by F. J. Flanagan), such an investigation has proved the samples to be homogeneous as far as this element is concerned, the true value being about 50 p.p.m., whereas previous analyses had shown a curious bimodal distribution centred about 27 and about 50 p.p.m. Flanagan's description of the experiments planned to resolve the problem of the Pb content of G–1 provides an object lesson in such matters.

To conclude, it is apparent that rather better rock analyses are probably being made now than 10 years ago—even if only because G–1 and W–1 are being used to calibrate rapid methods and check conventional ones—but the position is still far from comforting. What is much more satisfactory is the widespread cooperation among geochemists interested in trace elements in providing good figures for the two standard rocks, which perhaps find their greatest usefulness in this field. But what happens when the samples are exhausted?

E. A. Vincent

NOTICE

The Record in the Meteorites—IV

Origin of Diamonds in Iron Meteorites

Michael E. Lipschutz and Edward Anders

(*Geochim. et Cosmochim. Acta* **24**, 83–105)

This manuscript was mailed to Professor Wahl on June 28th, 1960, who was Editor for Cosmochemistry at that time. We are advised that due to serious illness he was unable to process the manuscript; and that it was not received by an active member of the Board of Editors until September 13, which is the date of receipt recorded in the Journal. We are anxious to have the point of earlier submission established, since the first independent evidence in support of our ideas, the discovery of coesite, was reported on July 20th, 1960 (Chao, Shoemaker and Madsen, *Science* **132**, 220–2) and our paper was completed before we learned of this discovery.

Enrico Fermi Institute for Nuclear Studies and
Department of Chemistry, University of Chicago
Chicago, Illinois

Michael E. Lipschutz
Edward Anders

INFORMATION FOR CONTRIBUTORS

I. GENERAL

1. Papers on *geochemistry* should be submitted to the appropriate Executive Editor—Prof. L. R. WAGER for papers from the United Kingdom and British Commonwealth and for papers in English from Europe; PROF. C. W. CORRENS for papers in German or French; Prof. J. A. S. ADAMS for papers from the American continents. Papers submitted for publication will naturally be judged from the standpoint of scientific originality and novelty. Technical details of apparatus used in scientific investigation can, however, be presented in brief notes. Critical comments or preliminary results requiring early publication should be submitted as letters to the editors. Where possible, letters should be confined to 500 words. The preparation of progress reports and review articles will be invited by the editors from time to time. The journal appears as independent and complete numbers, which are combined into volumes of about 300 pages.

2. Only papers which have not been previously published can be accepted. Authors must agree not to publish elsewhere a paper submitted to and accepted by *Geochimica et Cosmochimica Acta*.

3. Fifty reprints of each paper are provided free. Additional copies can be purchased if ordered at the time the first proofs are returned. A reprint order form will accompany first proofs.

II. SCRIPT REQUIREMENTS

1. Scripts must be written in one of the three official languages—English, French or German.

2. The script should be typed (not a carbon copy). The text must be ready for printing and should be carefully checked for errors. Authors will receive proofs for correction. The original script plus two copies will assist in expediting publication.

3. Illustrations should accompany the script mounted on separate sheets. Line diagrams that require to be redrawn should include all relevant details. Half-tone illustrations should be restricted to the minimum necessary. Photographs should be enlarged sufficiently to permit their clear reproduction and if words or numbers appear on them, two copies should be sent, one clearly printed and the other without inscription. All illustrations should be provided with descriptive legends, which should be given on a separate sheet. Any lettering on diagrams—other than Greek letters, symbols, etc.—should be stencilled and should be sufficiently large and bold to permit reproduction when the diagram has been reduced to a size suitable for inclusion in the journal.

4. References in the text should be given by quoting the author's name and year of publication, i.e. AHRENS (1952). *Full references should be listed at the end of each paper, in alphabetical order, in the following manner*

AHRENS, L. H. (1952). The use of ionization potentials—I. Ionic radii of the elements. *Geochim. et Cosmochim. Acta* **2**, 155–169.

and should include the full title of the article, standard abbreviated title of the journal, year, volume number and inclusive page numbers.

5. The text of articles submitted should be concise and in a readily understandable style. The technical description of the methods used should only be given in detail when such methods are new. The essential contents of each paper should be briefly recapitulated in an abstract in English. Such an abstract may, however, be submitted by the author in the language of the original typescript for translation into English by the editorial staff.

6. To conserve space, authors are requested to mark less important portions of the paper (such as description of methods, record of experimental results, etc.) for printing in smaller type.

7. Indices of refraction should be denoted by the symbols α, β, γ, ω, ε, n, and vibration directions by X, Y, Z, O and E.

Pergamon Press are also publishers of the following Journals.

JOURNAL OF NUCLEAR ENERGY:
PARTS A/B: REACTOR SCIENCE AND TECHNOLOGY;
PART C: PLASMA PHYSICS—ACCELERATORS—THERMONUCLEAR RESEARCH
HEALTH PHYSICS (*The Official Journal of the Health Physics Society*)
JOURNAL OF INORGANIC AND NUCLEAR CHEMISTRY
TETRAHEDRON (*The International Journal of Organic Chemistry*)
TALANTA (*An International Journal of Analytical Chemistry*)
INTERNATIONAL JOURNAL OF APPLIED RADIATION AND ISOTOPES
BIOCHEMICAL PHARMACOLOGY
ARCHIVES OF ORAL BIOLOGY
* BIOPHYSICS
* JOURNAL OF MICROBIOLOGY, EPIDEMIOLOGY AND IMMUNOBIOLOGY
* PROBLEMS OF HEMATOLOGY AND BLOOD TRANSFUSION
* PROBLEMS OF VIROLOGY
* PROBLEMS OF ONCOLOGY
* SECHENOV PHYSIOLOGICAL JOURNAL OF THE U.S.S.R.
* PAVLOV JOURNAL OF HIGHER NERVOUS ACTIVITY
* ELECTRIC TECHNOLOGY, U.S.S.R.
* RADIO ENGINEERING
* RADIO ENGINEERING AND ELECTRONICS
* TELECOMMUNICATIONS
* PHYSICS OF METALS AND METALLOGRAPHY
* THE ABSTRACTS JOURNAL OF METALLURGY
* APPLIED MATHEMATICS AND MECHANICS
CHEMICAL ENGINEERING SCIENCE
JOURNAL OF ATMOSPHERIC AND TERRESTRIAL PHYSICS
PLANETARY AND SPACE SCIENCE
ANNALS OF THE INTERNATIONAL GEOPHYSICAL YEAR
SPECTROCHIMICA ACTA
JOURNAL OF THE MECHANICS AND PHYSICS OF SOLIDS
ACTA METALLURGICA
(*for the Board of Governors of Acta Metallurgica*)
INTERNATIONAL JOURNAL OF THE PHYSICS AND CHEMISTRY OF SOLIDS
DEEP-SEA RESEARCH
JOURNAL OF NEUROCHEMISTRY
JOURNAL OF PSYCHOSOMATIC RESEARCH
JOURNAL OF INSECT PHYSIOLOGY
INTERNATIONAL JOURNAL OF AIR AND WATER POLLUTION
INTERNATIONAL ABSTRACTS OF BIOLOGICAL SCIENCES
(*for Biological and Medical Abstracts Ltd.*)
RHEOLOGY ABSTRACTS
VACUUM
OPERATIONAL RESEARCH QUARTERLY
ANNALS OF OCCUPATIONAL HYGIENE
ELECTROCHIMICA ACTA
JOURNAL OF CHILD PSYCHOLOGY AND PSYCHIATRY
JOURNAL OF SMALL ANIMAL PRACTICE
SOLID-STATE ELECTRONICS
INTERNATIONAL JOURNAL OF MECHANICAL SCIENCES

* *Translations of Russian journals published on behalf of the Pergamon Institute, a division of Pergamon International Corporation*

Leaflets giving further details and subscription rates of each of these journals are available on request

THE GEOCHEMICAL SOCIETY

OFFICERS

HAROLD C. UREY, President
ROBERT M. GARRELS, Vice-President
FRANCIS R. BOYD, JR., Secretary
GEORGE T. FAUST, Treasurer

COUNCILLORS

FRANS E. WICKMAN, 1961–1963
O. FRANK TUTTLE, 1961–1963
ALBERT E. J. ENGEL, 1959–1961
FRIEDRICH G. HOUTERMANS, 1959–1961
RALPH CANNON, 1960–1962
TH. G. SAHAMA, 1960–1962

REGIONAL VICE-PRESIDENTS

LOUIS H. AHRENS
RUI RIBEIRO FRANCO
ING. GEORGES ORDOÑEZ
C. W. CORRENS
J. F. LOVERING
KEN SUGAWARA

COMMITTEES

Auditing Committee

WILLIAM L. HILL, Chairman
JOSEPH J. TREGONING
C. R. NASSER

Constitution and By-Laws

BRIAN J. SKINNER, Chairman
BRIAN H. MASON
WILLIAM S. FYFE

Education Committee

KURT E. LOWE, Chairman
JOHN G. WOODRUFF
PAUL L. CLOKE
J. LAWRENCE KULP
D. M. HENDERSON

Membership Committee

RICHARD H. JAHNS, Chairman
HARVEY C. DIEHL
CHESTER B. SLAWSON
JAMES E. SLOSSON
WALLACE A. BROECKER

Nominating Committee

RUSTUM ROY, Chairman
HAROLD M. SMITH
PAUL B. BARTON, JR.
ROBERT M. GROGAN
GEORGE W. WETHERILL

Programme Committee

REYNOLDS DENNING, Chairman
HAROLD M. SMITH

Publications Committee

E. WM. HEINRICH

Research Committee

CLIFFORD A. HOPSON, Chairman
EWART A. VINCENT
KEN SUGAWARA
KARL H. WEDEPOHL
KALERVO RANKAMA

Russian Translations Committee

EARL INGERSON, Chairman
JOHN M. HUNT
THURE G. SAHAMA
CHARLES F. DAVIDSON
ZDENEK PÁCAL
RAYMOND SIEVER
SOL R. SILVERMAN

Standards Committee

ALVIN VAN VALKENBURG, Chairman
FELIX CHAYES
GEORGE S. SWITZER
JOHN A. MAXWELL
LORIN R. STIEFF
MICHAEL FLEISCHER
GUNNAR KULLERUD
J. FRANK SCHAIRER
THOMAS C. HOERING

Tellers Committee

JOSEPH J. FAHEY, Chairman
CHARLES R. NASSER
HUGH GREENWOOD